Functional validation of cancer stem cell markers in primary human colorectal cancer and established cell lines

Inauguraldissertation

zur
Erlangung der Würde eines Doktors der Philosophie
vorgelegt der
Philosophisch-Naturwissenschaftlichen Fakultät
Der Universität Basel

von

Manuele Giuseppe Muraro

aus **Italien**

Basel, 2014

Genehmigt von der Philosophisch-Naturwissenschaftlichen Fakultät
auf Antrag von

Members of the dissertation committee:

Faculty Responsible: Prof. Alex N. Eberle

Dissertation Supervisor: Prof. Giulio C. Spagnoli

Co-examiner: Prof. Gerhard Christofori

Basel, 13 November 2012

Prof. Dr. J. Schibler
The Dean of Faculty

Namensnennung-Keine kommerzielle Nutzung-Keine Bearbeitung 3.0 Schweiz
(CC BY-NC-ND 3.0 CH)

Sie dürfen: **Teilen** — den Inhalt kopieren, verbreiten und zugänglich machen

Unter den folgenden Bedingungen:

Namensnennung — Sie müssen den Namen des Autors/Rechteinhabers in der von ihm festgelegten Weise nennen.

Keine kommerzielle Nutzung — Sie dürfen diesen Inhalt nicht für kommerzielle Zwecke nutzen.

Keine Bearbeitung erlaubt — Sie dürfen diesen Inhalt nicht bearbeiten, abwandeln oder in anderer Weise verändern.

Wobei gilt:

- **Verzichtserklärung** — Jede der vorgenannten Bedingungen kann **aufgehoben** werden, sofern Sie die ausdrückliche Einwilligung des Rechteinhabers dazu erhalten.
- **Public Domain (gemeinfreie oder nicht-schützbare Inhalte)** — Soweit das Werk, der Inhalt oder irgendein Teil davon zur Public Domain der jeweiligen Rechtsordnung gehört, wird dieser Status von der Lizenz in keiner Weise berührt.
- **Sonstige Rechte** — Die Lizenz hat keinerlei Einfluss auf die folgenden Rechte:
    - Die Rechte, die jedermann wegen der Schranken des Urheberrechts oder aufgrund gesetzlicher Erlaubnisse zustehen (in einigen Ländern als grundsätzliche Doktrin des **fair use** bekannt);
    - Die **Persönlichkeitsrechte** des Urhebers;
    - Rechte anderer Personen, entweder am Lizenzgegenstand selber oder bezüglich seiner Verwendung, zum Beispiel für **Werbung** oder Privatsphärenschutz.
- **Hinweis** — Bei jeder Nutzung oder Verbreitung müssen Sie anderen alle Lizenzbedingungen mitteilen, die für diesen Inhalt gelten. Am einfachsten ist es, an entsprechender Stelle einen Link auf diese Seite einzubinden.

Quelle: http://creativecommons.org/licenses/by-nc-nd/3.0/ch/ Datum: 12.11.2013

the statistician George Box once wrote:

“ALL MODELS ARE WRONG BUT SOME ARE USEFUL”.

Contents

1. INTRODUCTION ..... - 1 -

1.1 Colorectal Cancer ..... - 6 -

1.1.1 Anatomy ..... - 6 -

1.1.2 Risk factors for colorectal cancer ..... - 9 -

1.1.3 Prognostic factors ..... - 11 -

1.1.4 Therapy ..... - 16 -

1.2 The Cancer Stem Cell Model ..... - 17 -

1.2.1 A paradigm shift ..... - 17 -

1.2.2 Cancer Stem Cells in CRC ..... - 20 -

1.2.3 Colorectal Cancer Stem Cell Markers ..... - 22 -

CD133 (Prominin-1) ..... - 22 -

CD44 ..... - 23 -

CD166 ..... - 23 -

CD24 ..... - 24 -

Lgr5 ..... - 25 -

1.2.4 Clinical implications of the CRC CSC model ..... - 26 -

1.3 Development of CSC specific treatments ..... - 28 -

2. AIMS OF THE STUDY ..... - 29 -

3. RESULTS ..... - 31 -

3.1 Prognostic impact of the expression of putative cancer stem cell markers CD133, CD166, and CD44s in colorectal cancer ..... - 33 -

Introduction ..... - 33 -

Materials and Methods ..... - 34 -

Patients and clinico-pathological data ..... - 34 -

Tissue microarray and Immunohistochemistry ..... - 37 -

Evaluation of immunohistochemistry ..... - 37 -

Tumor invasion assay ..... - 39 -

Statistical Analysis ..... - 39 -

Results ..... - 40 -

Tissue microarray analysis: Normal mucosa versus colorectal cancer ..... - 40 -

Invasiveness of tumor cells differing in CD44 and CD166 expression ..... - 43 -

Discussion ..... - 44 -

3.2 Higher percentage of CRC-SCs in primary CRC does not correlate with higher engraftment rates in immunodeficient mice ..... - 47 -

Introduction ..... - 47 -

Materials and Methods ..... - 48 -

Digestion of human tumor specimens ..... - 48 -

Tumor transplantation ..... - 49 -

Flow cytometric analysis ..... - 49 -

Statistical Analysis ..... - 50 -

Results..... - 50 -

CRC samples phenotype..... - 50 -

Tumorigenic potential of CRC-derived cell suspension..... - 53 -

Discussion..... - 53 -

3.3 CRC CSC Markers in human established CRC Cell Lines..... - 56 -

3.4 Differential gene expression patterns in 3D cultures of human colon cancer cells in the presence of hypoxic and/or necrotic cores..... - 73 -

Introduction..... - 74 -

Material and Methods..... - 76 -

Cell cultures..... - 76 -

Generation of MCTS..... - 77 -

Growth kinetics analysis..... - 77 -

Xenograft cultures..... - 77 -

Spheroid fixation, cryosection and H&E staining..... - 78 -

Immunostaining..... - 79 -

Real-time RT-PCR..... - 80 -

Results..... - 81 -

MCTS formation and growth kinetics..... - 81 -

Definition of MCTS maturation stages..... - 81 -

Differential gene expression patterns..... - 83 -

Discussion..... - 86 -

4. CONCLUSIONS & OUTLOOK..... - 93 -

Reference List.....a

-1-

INTRODUCTION

Cancer is a leading cause of death in economically developed countries and its incidence is continuously increasing mainly because of the aging and growth of the world population alongside cancer-causing behaviors and environmental pollution.

Cancer is a multifactorial disease caused by combinations of genetic, behavioral, and environmental factors. It is characterized by disruptive cell division, a changes in cell morphology, and the ability of cancer cells to develop an invasive phenotype (1).

Colorectal cancer (CRC) is a public health priority given the high incidence and mortality associated with this disease. It is the third most common cancer in men and

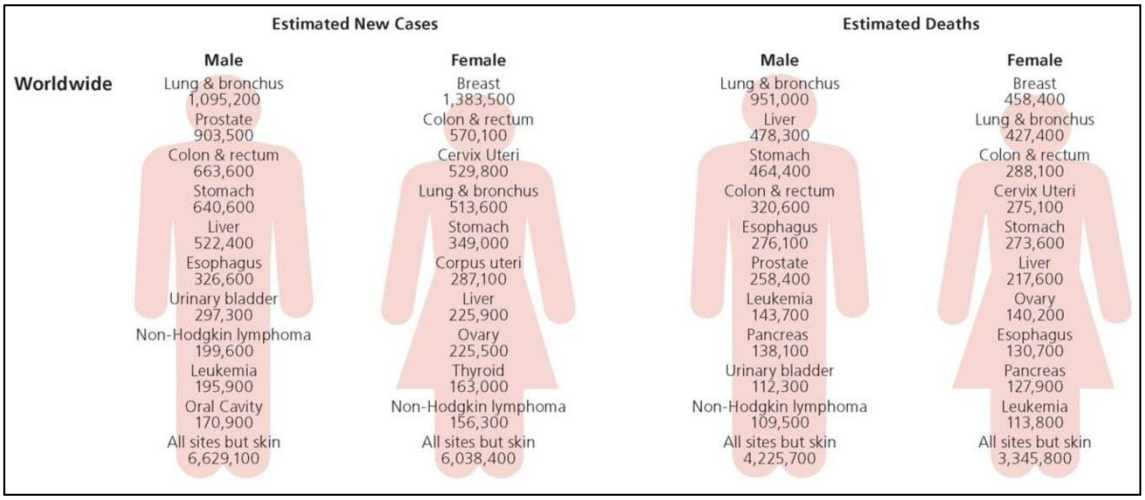

Figure 1 Estimated new cancer cases and deaths worldwide for leading cancer sites. Source: GLOBOCAN 2008 (modified from: Jemal et al. CA: a cancer journal for clinicians, 2011)

the second in women worldwide, the second most common cause of death from cancer in Europe and the fourth worldwide with over 1.2 million new cancer cases and 608,700 deaths estimated to have occurred in 2008 (Figure 1) (2-4). Although, it is among the most preventable cancers, it is frequently diagnosed only when symptoms become apparent or troublesome. By that time, CRC may be in an advanced stage.

Surgery continues to be the mainstay of treatment, with the greatest influence on survival. However, while surgery excises detectable tumor tissues, occult metastases frequently produce disease recurrences (5). Recurrence rates range between 10% for tumors confined to mucosa (stage I) and more than 50% for tumors with metastases to regional lymph nodes (stage III) (6).

According to the model developed by Vogelstein and colleagues (Figure 2), CRC arises through a series of genetic alterations of the gastrointestinal epithelial cells that disrupt normal mechanisms of proliferation and self-renewal (7). Such mutations drive the transition from healthy colonic epithelia to increasingly dysplastic adenoma and finally to cancer.

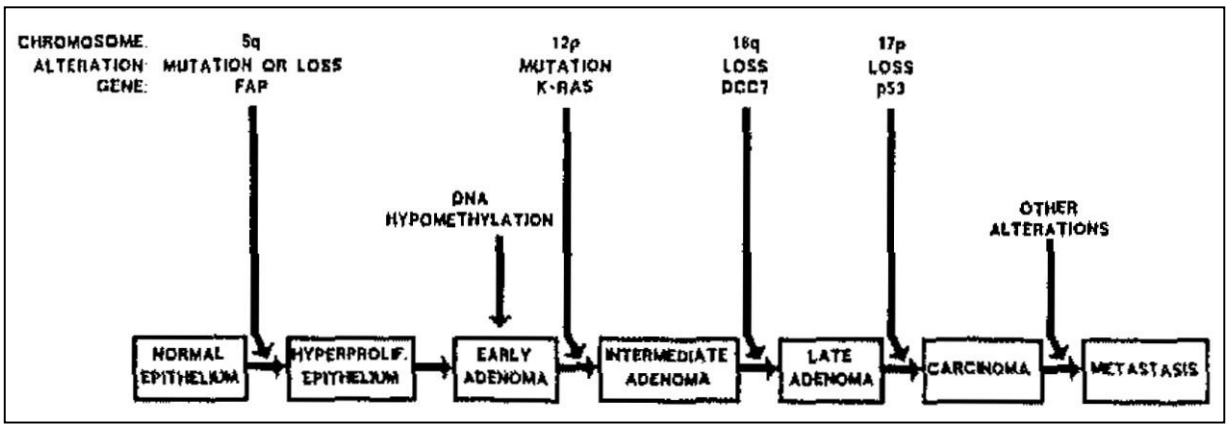

Figure 2 A genetic model for colorectal tumorigenesis.
(from: Fearon E. and Vogelstein B., Cell, 1990)

Stem cells of the gastrointestinal tract may represent a natural target of tumorigenic mutations, due to both their long life span and to their capacity for self-renewal. The so-called “cancer stem cell model” proposes that, similar to normal tissues, cancers are also hierarchically organized (8). Only rare tumor cells, endowed with self-renewal and differentiation capacity, defined as “cancer stem cells” (CSCs), are postulated to be capable of tumor initiation and maintenance (Figure 3). In contrast, the majority of cells representing the tumor bulk do not possess the capacity to transplant cancers in immunodeficient hosts.

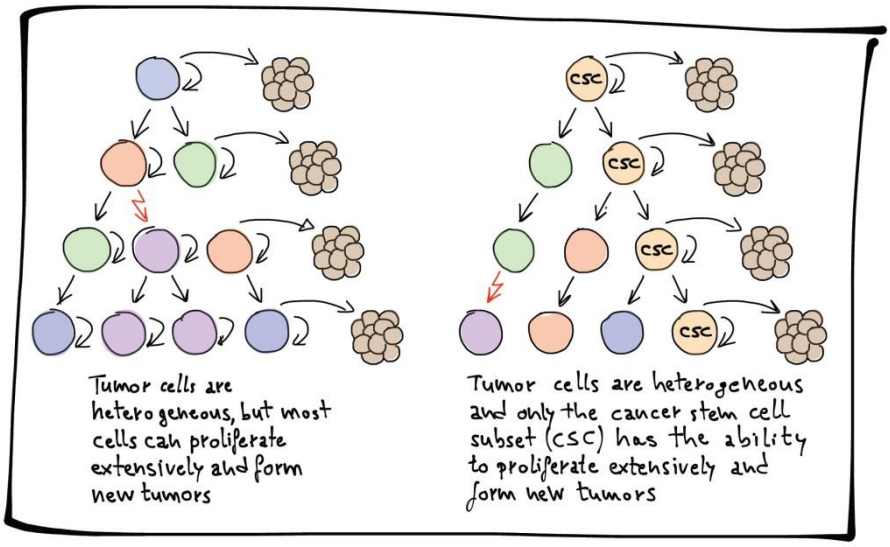

Figure 3 Two alternative models have been put forward to explain how tumours initiate and develop. The stochastic model (a) proposes that tumour cells are heterogeneous, but that virtually all of them can function as a tumour-founding cell, although this might happen only rarely. Conversely, the hierarchical model (b) implies that only a small subpopulation of tumour stem cells can proliferate extensively and sustain the growth and progression of a neoplastic clone. (modified from Reya T., Nature 2001)

Conventional cancer therapies rely on the eradication of all tumor cells, but if the putative CSCs may be less sensitive to these therapies, then they will remain viable after therapy. The CSC hypothesis implies that to achieve a complete and durable remission the therapy has to eradicate the CSCs (Figure 4).

The development of novel compounds able to specifically target CSC populations currently represents a major challenge in anti-cancer drug discovery. An absolute prerequisite for the achievement of this goal is represented by the establishment of reliable CSC models in vitro. Established cell lines are largely used for screening of novel anti-cancer compounds. However, whether they do comprise CSC populations resembling those of primary tumors, remains highly debated.

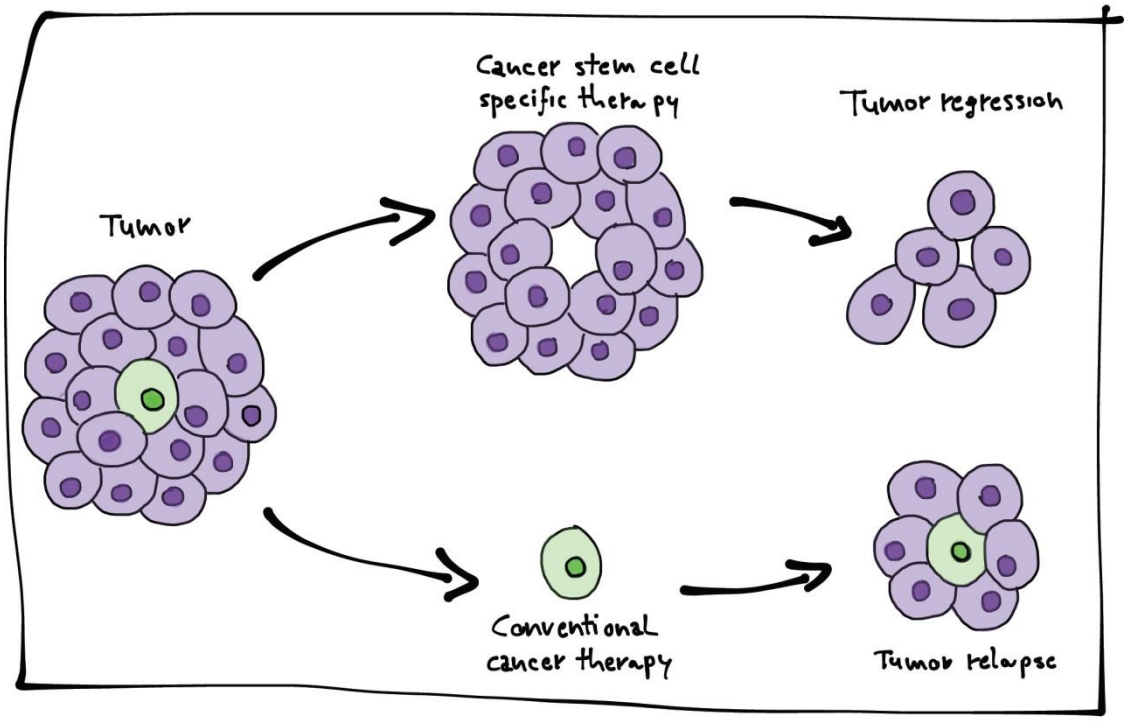

Figure 4 A new treatment strategy that specifically targets cancer stem cells, when combined with current treatments, may lead to a more complete and durable regression of malignant cancers. (modified from Reya T., Nature 2001)

1.1 Colorectal Cancer

1.1.1 Anatomy

The colon consists of five distinct anatomical sections. Starting from the ileum, the final section of the small intestine, the colon, may be divided in cecum, ascending colon, transverse colon, descending colon, and sigmoid colon (9).

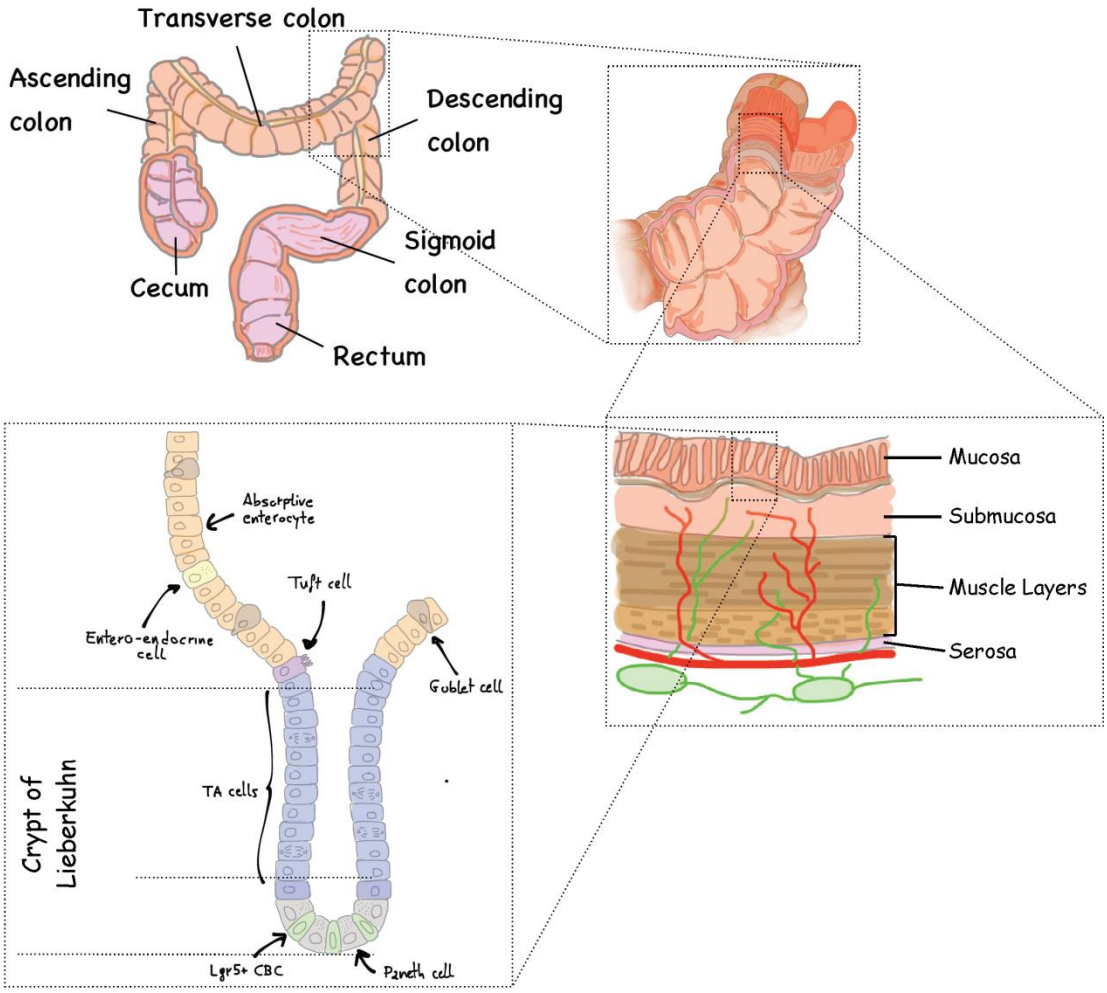

Figure 5 Structure of the colon – (Upper Left) Different segment of the colon. (Lower right) Structure of the colon wall. (Lower Left) Structure of the crypt of Lieberkühn. (modified from: Adams Atlas Anatomy; Rizk and Barker, WIRE 2012)

Unlike other parts of the gastrointestinal system (GI), the colon is not primarily responsible for the absorption of food and nutrients. Instead, its main function is to extract water and salt from solid waste before it arrives, through the rectum, to the anus and is then excreted. A minor role in the absorption of specific nutrients, including vitamins, and, more specifically, vitamin K, has also been reported (9).

Colon is organized into four histologically distinct layers. The epithelial layer is made up of a single sheet of columnar epithelial cells, which form finger-like invaginations into the underlying connective tissue of the lamina propria to form the basic functional unit of the intestine, the crypt, also called gland of Lieberkuhn (Figure 5) (10). Each crypt contains around 2000 cells and approximately 14,000 crypts per square centimeter are located in the adult human colon with a total renewal turnover rate of five days.

This process is fuelled by adult multipotent stem cells placed at the bottom of each crypt and engaged in a crosstalk with perycryptal myofibroblasts, closely adherent to the basal lamina surrounding the crypt (11). During asymmetric division, these cells undergo self-renewal and generate a population of transit-amplifying cells that occupy the lower two thirds of the crypt. Upon migration upward from the crypt, these cells proliferate and differentiate into one of the epithelial cell types of the intestinal wall that constitute the top third of the crypt. The terminally differentiated cells are continually extruded into the lumen (12).

There are three major terminally differentiated epithelial lineages in the colon: the colonocytes, also termed absorptive enterocytes; the mucus-secreting goblet cells; and the less abundant enteroendocrine cells (Figure 5, lower left panel). Finally, Paneth cells, functionally similar to neutrophils, are scattered at the bottom of the

crypt only in the small intestine epithelium and do not follow the upward migratory pathway (12).

1.1.2 Risk factors for colorectal cancer

Primary predisposition to CRC is usually genetic but other conditions and factors that could lead to increased risk of CRC are:

- **Age:** CRC incidence increases with age. CRC rarely affects people younger than 50. CRC in young adults is usually associated with conditions of familial predisposition.
- **Familial clustering:** subjects with relatives that have been affected by familial adenomatous polyposis (FAP) or by hereditary nonpolyposis CRC (HNPCC) have an increased risk of developing CRC.
- **Smoke:** long-term smoking increases CRC incidence (13).
- **Lifestyle:** Current dietary recommendations to prevent colorectal cancer include increasing the consumption of whole grains, fruits and vegetables, and reducing the intake of red meat(14, 15).The evidence for a preventive role of fibers fruits and vegetables however, is poor (15). Physical activity can moderately reduce the risk of colorectal cancer (16).
- **Environmental factors:** People living in industrialized areas have a higher risk of developing CRC(17).
- **Presence of chronic inflammatory** processes of the intestine, such as Crohn's disease and ulcerative colitis is associated with CRC development. About 1% of patients with CRC have a history of ulcerative colitis. The risk of developing CRC is directly related to the severity of intestinal mucosal damage and the extent of inflammation. The risk of developing CRC in subjects with Crohn's disease is lower than patients with ulcerative colitis (18, 19).

- **Polyps of the colon:** Polyps are a risk factor for CRC, particularly if they are adenomatous. Siblings and parents of patients with adenomatous colorectal polyps have a 1.78 relative risk for developing CRC. The age at the time of polyp diagnosis is an important prognostic factor for the risk of cancer development. Siblings of patients with adenomatous polyps diagnosed before age 60 have a 2.59 relative risk for developing CRC. Polyp size and histology are directly related to the risk of CRC, with villous polyps larger than 2 cm having a 50% greater chance of containing cancer cells than smaller or nonvillous polyps (20, 21).

1.1.3 Prognostic factors

Outcome prediction in CRC usually relies on histopathological evaluation of tissue samples obtained during surgical removal of the primary tumor. Currently, the most important conventional prognostic factors are histological tumor grade and tumor stage of disease at the time of diagnosis (pTNM -UICC-, Astler-Coller, or Dukes's), including depth of tumor invasion, involvement of regional lymph nodes, and metastatic spread to distant organs. Such approaches have been shown to be prognostically valuable (22).

In addition to these classic clinicopathological parameters, molecular markers of prognostic and predictive relevance are continuously being proposed for a wide variety of tumors including CRC (23).

Staging reflects the extent or severity of cancerous disease based on the extension of the tumor and its spread in the body. Establishing the stage of the disease helps to plan treatments and to predict the likely outcome or course of the disease.

Different staging systems have been developed. The Dukes' classification, proposed by Dr. Cuthbert E. Dukes in 1932, focuses on tissue infiltration and presence of lymph node involvement and distant metastases (24). The original Dukes classification of 1932 described the staging of rectal carcinoma only but is also usually applied to carcinomas of the colon. It originally included three simple stages, A to C. Stage D was added later. Dukes' stages of cancer are the following:

Dukes' A: Invasion into but not through the bowel wall (90% 5-y survival)

Dukes' B: Invasion through the bowel wall but not involving lymph nodes (70% 5-y survival)

Dukes' C: Involvement of lymph nodes (30% 5-y survival)

Dukes' D: Widespread metastases

The TNM classification is the most widely used. The TNM staging system for all solid tumors was devised by Pierre Denoix between 1943 and 1952, considering size and extension of the primary tumor, lymphatic involvement, and the presence of metastases to classify cancer progression. Degree of tissue infiltration, discriminating between the invasion of the mucosa only, muscle layer or sierosa is accurately analyzed.

While “T” stands for the size of the tumor and whether it has invaded nearby tissues, “N” refers to regional lymph node invasion, and “M” to distant metastases (following table, Figure 6, and Panel 1) (25).

The American Joint Committee on Cancer and the International Union Against Cancer (AJCC/IUAC) has developed an additional staging system partially using TNM scoring system to describe the extent of disease progression in cancer patients:

AJCC/IUAC stage	TNM stage	TNM stage criteria for colorectal cancer
Stage 0	Tis N0 M0	Tis: Tumor confined to mucosa; cancer-*in-situ*
Stage I	T1 N0 M0	T1: Tumor invades submucosa
Stage II-B	T2 N0 M0	T2: Tumor invades muscularis propria
Stage II-A	T3 N0 M0	T3: Tumor invades subserosa or beyond (without other organs involved)
Stage II-B	T4 N0 M0	T4: Tumor invades adjacent organs or perforates the visceral peritoneum
Stage III-A	T1-2 N1 M0	N1: Metastasis to 1 to 3 regional lymph nodes. T1 or T2.
Stage III-B	T3-4 N1 M0	N1: Metastasis to 1 to 3 regional lymph nodes. T3 or T4.
Stage III-C	any T, N2 M0	N2: Metastasis to 4 or more regional lymph nodes. Any T.
Stage IV	any T, any N, M1	M1: Distant metastases present. Any T, any N.

Panel 1 – Colon and rectal cancer staging by AJCC

American Joint Committee on Cancer

Colon and Rectum Cancer Staging

7th EDITION

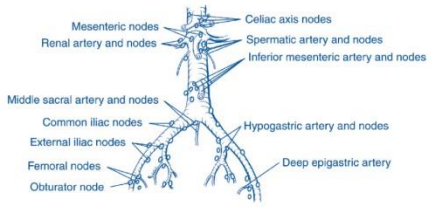

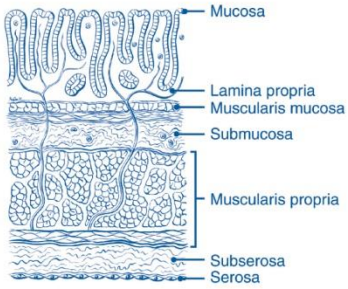

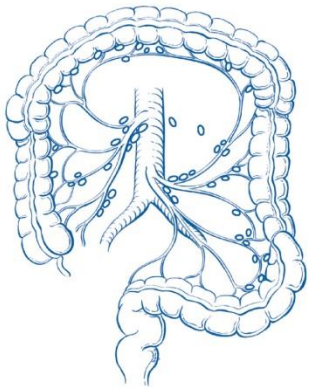

Definitions

Primary Tumor (T)

- **TX** Primary tumor cannot be assessed
- **T0** No evidence of primary tumor
- **Tis** Carcinoma in situ: intraepithelial or invasion of lamina propria[1]
- **T1** Tumor invades submucosa
- **T2** Tumor invades muscularis propria
- **T3** Tumor invades through the muscularis propria into pericolorectal tissues
- **T4a** Tumor penetrates to the surface of the visceral peritoneum[2]
- **T4b** Tumor directly invades or is adherent to other organs or structures[2,3]

Regional Lymph Nodes (N)[4]

- **NX** Regional lymph nodes cannot be assessed
- **N0** No regional lymph node metastasis
- **N1** Metastasis in 1–3 regional lymph nodes
- **N1a** Metastasis in one regional lymph node
- **N1b** Metastasis in 2–3 regional lymph nodes
- **N1c** Tumor deposit(s) in the subserosa, mesentery, or nonperitonealized pericolic or perirectal tissues without regional nodal metastasis
- **N2** Metastasis in 4 or more regional lymph nodes
- **N2a** Metastasis in 4–6 regional lymph nodes
- **N2b** Metastasis in 7 or more regional lymph nodes

Distant Metastasis (M)

- **M0** No distant metastasis
- **M1** Distant metastasis
- **M1a** Metastasis confined to one organ or site (for example, liver, lung, ovary, nonregional node)
- **M1b** Metastases in more than one organ/site or the peritoneum

ANATOMIC STAGE/PROGNOSTIC GROUPS

Stage	T	N	M	Dukes*	MAC*
0	Tis	N0	M0	–	–
I	T1	N0	M0	A	A
	T2	N0	M0	A	B1
IIA	T3	N0	M0	B	B2
IIB	T4a	N0	M0	B	B2
IIC	T4b	N0	M0	B	B3
IIIA	T1–T2	N1/N1c	M0	C	C1
	T1	N2a	M0	C	C1
IIIB	T3–T4a	N1/N1c	M0	C	C2
	T2–T3	N2a	M0	C	C1/C2
	T1–T2	N2b	M0	C	C1
IIIC	T4a	N2a	M0	C	C2
	T3–T4a	N2b	M0	C	C2
	T4b	N1–N2	M0	C	C3
IVA	Any T	Any N	M1a	–	–
IVB	Any T	Any N	M1b	–	–

NOTE: cTNM is the clinical classification, pTNM is the pathologic classification. The y prefix is used for those cancers that are classified after neoadjuvant pretreatment (for example, ypTNM). Patients who have a complete pathologic response are ypT0N0cM0 that may be similar to Stage Group 0 or I. The r prefix is to be used for those cancers that have recurred after a disease-free interval (rTNM).
* Dukes B is a composite of better (T3 N0 M0) and worse (T4 N0 M0) prognostic groups, as is Dukes C (any TN1 M0 and Any T N2 M0). MAC is the modified Astler-Coller classification.

ajcc®

American Cancer Society®

Financial support for AJCC
7th Edition Staging Posters
provided by the American Cancer Society

Notes

[1] Tis includes cancer cells confined within the glandular basement membrane (intraepithelial) or mucosal lamina propria (intramucosal) with no extension through the muscularis mucosae into the submucosa.

[2] Direct invasion in T4 includes invasion of other organs or other segments of the colorectum as a result of direct extension through the serosa, as confirmed on microscopic examination (for example, invasion of the sigmoid colon by a carcinoma of the cecum) or, for cancers in a retroperitoneal or subperitoneal location, direct invasion of other organs or structures by virtue of extension beyond the muscularis propria (that is, a tumor on the posterior wall of the descending colon invading the left kidney or lateral abdominal wall; or a mid or distal rectal cancer with invasion of prostate, seminal vesicles, cervix, or vagina).

[3] Tumor that is adherent to other organs or structures, grossly, is classified cT4b. However, if no tumor is present in the adhesion, microscopically, the classification should be pT1-4a depending on the anatomical depth of wall invasion. The V and L classifications should be used to identify the presence or absence of vascular or lymphatic invasion, whereas the PN site-specific factor should be used for perineural invasion.

[4] A satellite peritumoral nodule in the pericolorectal adipose tissue of a primary carcinoma without histologic evidence of residual lymph node in the nodule may represent discontinuous spread, venous invasion with extravascular spread (V1/2), or a totally replaced lymph node (N1/2). Replaced nodes should be counted separately as positive nodes in the N category, whereas discontinuous spread or venous invasion should be classified and counted in the Site-Specific Factor category Tumor Deposits (TD).

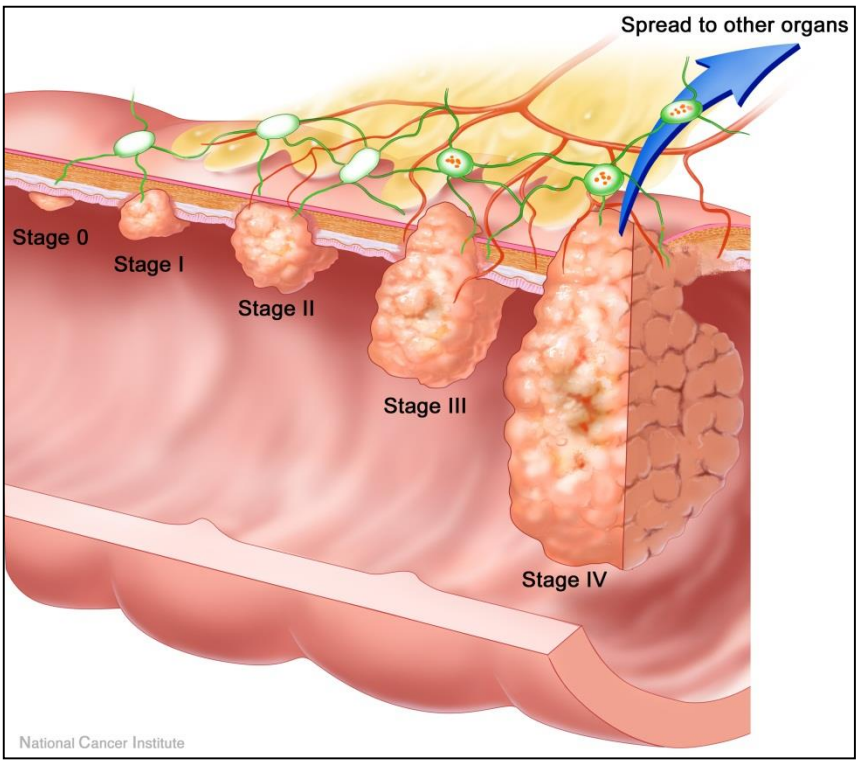

Figure 6 Stages of Colon Cancer: Stage I. The cancer is contained only in the inner layers of the colon wall. There is no spread to adjacent lymph nodes or other organs; Stage II. The cancer has grown through all the layers of the bowel wall, but not to lymph nodes or other organs; Stage III. The cancer has spread to adjacent lymph nodes, but not to other organs; Stage IV. The cancer has spread to other organs such as the liver or the lungs. (modified from: National Cancer Institute)

In recent years, several studies have shed light on the importance of the tumor-infiltrating immune cells as an essential prognostic factor for patients' disease-free, overall survival, and clinical response to adjuvant therapies (22, 26, 27). Importantly, tumor cells can express tumor associated antigens and become targets for T cell-mediated adaptive immune response (28). In particular, Galon and colleagues (22, 29) found that the analysis of CRC immune infiltrate represented a better predictor of patient survival than histopathological methods currently used to stage CRC.

First, they showed that a strong in situ immune reaction in the tumor correlated with a favorable prognosis regardless of the local extent of the tumor and of invasion of regional lymph nodes (Stage I, II, and III). Second, they defined an

“immune-score” reflecting the CD8+/CD45RO+ T cell density in the center of the tumor and at the invasive margin. They found that the immune-scoring was significantly superior to the TNM staging. Indeed, patients with low immune-score had severe prognosis, while patient with high immune-score experienced low recurrence rates (22). Finally, they hypothesized a central role of memory T cells in the control of tumor recurrence.

1.1.4 Therapy

Surgery is the mainstay of treatment of localized disease with the greatest influence on survival. Over 70% of patients with stages I–III CC can be cured by surgery alone. On the other hand, the use of adjuvant chemotherapy at different stages of the disease is debated.

Over 20 years of clinical trials have led to the acceptance of 5-fluorouracil/leucovorin (5FU/LV) as the standard of care for patients with node-positive CRC. A number of clinical trials were conducted in the 80s and 90s to address the schedule-dependent mode of action of 5FU in order to increase efficacy while reducing toxicity. At present time, adjuvant chemotherapy is recommended for stage III and high-risk stage II cancers.

All in all, in stage II CRC, 60% to 70% of patients are cured with surgery alone, and 15 to 20% relapse despite adjuvant chemotherapy. In stage III CRC, 40 to 50% of patients are cured by surgery, while approximately 35% of patients will relapse, despite adjuvant chemotherapy (30).

In the metastatic setting, patients are treated with standard first- and second-line chemotherapy regimens, 5-FU/LV with oxaliplatin (FOLFOX) and 5-FU/LV with irinotecan (FOLFIRI), eventually in combination with the anti–vascular endothelial growth factor (anti-VEGF) monoclonal antibody bevacizumab, and/or the anti–epidermal growth factor (anti-EGFR) antibodies, cetuximab or panitumumab. Frequently, patients are sequentially administered all these treatments due to the inability to predict responsiveness, except for EGFR inhibitors, which are usually omitted in patients with tumors harboring KRAS mutations. (30).

1.2 The Cancer Stem Cell Model

1.2.1 A paradigm shift

Most tumors appear to contain morphological and functionally heterogeneous populations of cancer cells (31). This observation is traditionally explained by postulating variations in tumor microenvironment and coexistence of multiple genetic subclones created by progressive and divergent accumulation of independent somatic mutations (32). This implies that tumor tissue grew from the expansion of heterogeneous clonal populations and, also, that virtually all cells within the tumor have the capacity to regenerate and propagate cancer.

Since last decade two models for the development of solid tumors have been proposed: the “conventional” stochastic model suggests an accumulation of successive mutations and the clonal selection of tumorigenic cells, whereas a second model can be referred to as the hierarchical model, which postulates cancer stem cells as the origin of cancer.

In 1997, Dick and colleagues (33), studying human acute myeloid leukemia (AML), discovered that only a small subset of cells is capable of to transfering AML from patients to immunodeficient mice regenerating all types of cells that characterize AML. Stem cells are defined as cells that have the ability to perpetuate themselves through self-renewal and to generate mature cells of a particular tissue through differentiation (8). Because stem cells are the only long-lived cells in many tissues, especially in renewing systems such as human gut epithelia, they persist long enough in the tissue to undergo a prolonged sequence of successive mutation and selection

cycles inherent with the concept of multistage carcinogenesis (32). These are the bases of the original concept of “cancer stem cells” (CSC).

CSCs do not necessarily originate from the transformation of normal stem cells but they may arise from a restricted number of progenitors or more differentiated cells that have acquired self-renewing capacity. The original rigid interpretation of the model presents malignancy as a hierarchically organized tissue with a CSC population at the top that generates the more differentiated bulk of the tumor cells. In this model, the differentiated tumor cells have lost their clonogenic ability and their capacity to drive long-term progression of the malignancy (34).

CSCs were described having three common characteristics: i) they are the only cells in the tumor endowed with tumorigenic potential when xeno-transplanted into immunodeficient mice, ii) they are capable to recreate the full phenotypic heterogeneity of the original tumor, and iii) they are characterized by the expression of a distinctive surface markers profile that allows to isolate them from the non-tumorigenic tumor cells.

Stem cell biology could provide new insights into cancer biology due to the analogies existing between normal stem cells and tumorigenic cells. In fact, a growing body of evidence is increasingly supporting the idea that at least some human cancers may be considered as a stem cell disease (12).

An important reason for the widespread interest in the CSC model is that it can comprehensibly explain essential, poorly understood clinical events, such as therapy resistance, minimal residual disease, and tumor recurrence (34). The observation that cancer growth can be sustained by a minor subpopulation of tumor cells with unique functional properties could also assist in the design of new and more effective

antitumor treatments. According to the CSC model, therapeutic approaches that do not eradicate the CSC compartment are likely to achieve little success. Indeed, they might kill the majority of tumor cells, resulting in tumor shrinkage, but ultimately fail to prevent disease relapse and metastatic dissemination (8). Furthermore, antitumor treatments are generally screened based on their capacity to induce a clinical response (i.e., a dramatic regression, either complete or partial, of the tumor lesion). This approach, however, tends to select for treatments that are active on the bulk of tumor cell population but not necessarily on CSCs. New approaches for the preclinical evaluation of treatment efficacy will then need to be devised (32).

1.2.2 Cancer Stem Cells in CRC

The observation that the accumulation of mutations involving oncogenes and tumor suppressor genes accompanies the progression of the disease along the adenoma– carcinoma sequence induced Fearon and Vogelstein to formulate in the 1990s the “adenoma–carcinoma model”. They postulated that the neoplastic process, initiated by APC or β-catenin mutations and tumor progression, results from the sequential mutation of other genes, such as K-Ras and p53, in the context of a growing genomic instability. This model has been further refined and the studies performed on relatively rare inherited cases led to the identification of genetic alterations that play a major role in the development of sporadic CRC. Recent studies have shown that the mutations that were found in human colorectal cancer generate intestinal carcinomas in mice only when forced to occur in stem cells (35). According to the cancer stem cell hypothesis, it can be assumed that the first mutational hit occurs in a colonic SC located at the crypt bottom that, being long-lived, can accumulate oncogenic mutations over years or decades. Eventually, the entire niche will be colonized by mutant stem cells, and the crypt will be filled with their progeny (36). The proliferating cancer cells will be subjected to further changes that may result in cancer progression.

A number of studies have been conducted that provide evidence for the existence of colon CSCs and demonstrate that the CRC tumorigenic cell population can be FACS-purified by virtue of their cell surface phenotype. In particular, CSC populations have been identified in primary tumors either by CD133 expression (37, 38), or by co-expression of CD166/CD44 (39). More recently, normal and malignant

colonic cells with a higher activity of the detoxifying enzyme aldehyde dehydrogenase 1 (ALDH1) have showed stem cell properties. The isolation of CRC cells with higher ALDH1 activity was associated with higher tumorigenic capacity after xenografting in immunodeficient mice (40).

Recently, Clevers and colleagues demonstrate that Lgr5+ cells are the crypt stem cells, and also that deletion of APC in these cells leads to neoplastic transformation generating adenoma structures (35, 41). At the same time, Zhu et al. showed that CD133+Lgr5+ co-expressing cells are responsible for the formation of the entire intestinal epithelium, and are susceptible to transformation (42).

Therefore, identification of biomarkers for human CRC-SCs has the potential to improve the understanding of the mechanism underlying tumor growth and progression.

1.2.3 Colorectal Cancer Stem Cell Markers

Colon CSCs were originally identified through the expression of the CD133 glycoprotein using an antibody directed to its epitope AC133. Other cell surface markers, such as CD44, CD166, Musashi-1, CD29, CD24, leucine-rich repeat-containing G-protein-coupled receptor 5 (Lgr5), and aldehyde dehydrogenase 1 (ALDH1), have been proposed since (43).

CD133 (Prominin-1)

CD133 (prominin-1) is a glycoprotein with an N-terminal extracellular domain, two large extracellular loops, which are strongly N-glycosylated, and an intracellular C-terminus (44). The AC133 antigen, which represents a hyper-glycosylated version of CD133, is primarily expressed in stem and progenitor cells such as embryonic epithelium, brain stem cells, hematopoietic stem cells, and in cancers such as leukemia and retinoblastomas. (45)

CD133 was first reported as a putative CRC-SC marker in the studies conducted by O'Brien et al. (37) and Ricci-Vitiani et al. (38) by evaluating the tumorigenic potential of freshly isolated CD133 expressing cells from human CRC specimens and injecting them into immunodeficient mice. Cells bearing the glycosylated epitope AC133 were the only able to generate tumors in mice, whereas their negative counterparts were not. More importantly, tumor xenografts generated by CD133+ CRC-SCs displayed the same morphologic features of the parental tumor reproducibly maintained upon serial transplantation, suggesting that the molecular heterogeneity of the original tumor was effectively recapitulated.

Subsequent studies, however, have shown that in both mouse and human colorectal cancers, CD133 expression is not restricted to rare cell subsets, but it is detectable in relatively large numbers of tumor cells, irrespective of their tumorigenicity. Furthermore, Shmelkov et al. demonstrated that both, CD133+ and CD133- cells have tumor seeding capacity in metastatic colon cancers, thus questioning the validity of CD133 as a marker (46).

CD44

Proteins encoded by the CD44 gene constitute a large family of at least 20 isotypic variants, based on differential splicing and post-translational glycosylation. CD44 is a single transmembrane protein with a short intracellular domain, whose expression is regulated by the Wnt signaling pathway via β-catenin. CD44 has been described as part of the CSCs signature for colon carcinomas (39), head and neck carcinomas, non-small cell lung cancer, hepatocellular carcinoma, and breast cancer (45).

CD44 is one of the best described markers of CSCs in numerous different malignancies, raising the question as to whether this abundant protein fulfills essential tasks in CSCs (45).

CD166

CD166 (also called activated leukocyte cell adhesion molecule ALCAM) is a highly conserved multidomain transmembrane glycoprotein of the immunoglobulin superfamily and is widely expressed in a variety of normal tissues. This molecule mediates homotypic and heterotypic interactions between cells. It plays a role in the

development of different tissues, for example in neurogenesis and haemotopoiesis, and it participates in the mechanisms of the immune response (47). It is also expressed in various malignant lesions, such as melanoma and esophageal, gynecologic, prostate, and pancreatic cancers, and its expression is associated with diverse outcomes in different tumors (47). CD166 expression is reported to be significantly elevated in CRC as compared with normal mucosa. However, inconsistent data exist regarding the prognostic significance of CD166 expression in CRC (23, 48, 49).

CD24

CD24 is a glycosylated adhesion molecule that was first described in normal B and T cells. It is a protein anchored into the plasma membrane via glycosyl-phosphatidyl-inositol and interacts with P-selectin. CD24 is implicated in T cell costimulation, regulation of T cell homeostatic proliferation, growth and metastatisation of cancer cells, and apoptosis. CD24 ligands are organ-specific and could include CD24 itself, P-selectin, and fibronectin. The lack or low cell surface expression of CD24, concomitant with high expression of CD44 has been associated with a CSC phenotype in breast cancer. Pancreatic CSCs, instead, are defined by the expression of both CD24 and CD44. CD24 expression is a prognostic marker for ovarian, breast, prostate, and non-small cell lung carcinomas (45). Expression of CD24 in mammary carcinoma cell lines resulted in an enhancement of tumorigenic and metastatic potentials of the cells (50). Furthermore, Yeung and colleagues, studying human CRC cell lines, proposed the co-expression of CD44 and CD24 as an additional CSC phenotype (51).

Lgr5

The Wnt signaling pathway regulates the proliferative activity of intestinal crypt cells. Mutations of the Wnt negative regulator adenomatous polyposis coli (APC) activate the Wnt pathway that induces transcription of genes via transcription factors of the T-cell factor (Tcf) family. Lgr5/Gpr49 is one of the Tcf4 target genes that appears to be specifically active in the small cycling cells that are interspersed between the Paneth cells of the small intestine. In studies of genetic mouse models, Lgr5-positive cells were found to represent the long-lived stem cells of the small intestine and colon (41, 52). Deletion of the APC gene, a central regulator of β-catenin stability, in Lgr5-positive cells results in fast and progressive transformation (45). Therefore, it has been suggested that Lgr5 might represent good marker for the characterization and the isolation of human CRC-SC (53, 54).

While phenotypic characterization of CSCs derived from colorectal cancers is still debated, still unclear is whether these surface proteins represent mere surrogate markers or play specific roles in the regulation of CSC functions.

1.2.4 Clinical implications of the CRC CSC model

The term CSC refers to cancer cells sharing discrete properties with normal stem cells including self-renewal and the ability to initiate a hierarchy of more differentiated cells unable to self-renew. Based on these properties, the CSC hypothesis makes two important predictions: (i) CSCs are required for tumor growth and metastasis; and, (ii) elimination of CSCs is required for cure (8).

One of the major concerns in the use of cytotoxic agents is that they are designed to kill actively proliferating cells, which represent the bulk of the tumor cell population. Thus, even if antitumor strategies lead to shrinkage in tumor size and disease remission, they fail to prevent relapse due to CSCs survival. According to the CSC model, tumor growth is sustained by a small population of cells that current therapeutic measures fail to eradicate. A CSC-specific therapy will not cause tumor-size reduction in short term, but it will prevent successive regrowth. In order to successfully eradicate tumors, anti-cancer treatments should primarily target CSC subsets. (55)

Experimental data provide evidence that failure of chemo- and radiotherapy might be due to CSCs resistance to treatment (56-58). Indeeed, CSCs have been found to express high levels of DNA repair mechanisms (59, 60), detoxifying enzymes, such as aldehyde dehydrogenase-1 (ALDH1) (61), and molecular pumps (62-64). Furthermore, due to their relatively quiescent state they represent unlikely targets for anti-proliferative treatments. The designs of new therapeutic approaches specific for CSCs are therefore needed.

In support of this hypothesis, Todaro et al. recently demonstrated that CD133+ CRC-SCs produce interleukin-4 (IL4), an autocrine growth factor that promotes tumor resistance to the chemotherapeutic agents 5FU and oxaliplatin. On the basis of this finding, they devised a strategy to sensitize the CRC-SCs to chemotherapy through the targeting of IL-4 (65). The ‘‘malignant’’ microenvironment has proven essential for the maintenance and development of CSCs. Interruption of the crosstalk network between the elements of the niche and CSCs will dramatically affect their capacity to support tumor growth and metastatic potential.

However, although CSCs have been postulated to be responsible for decisive pathophysiological steps, directly affecting clinical behavior of cancers, limited data unequivocally support this concept. Most recently, a number of studies have begun to evaluate the role of CSCs in determining patients’ prognosis (31).

In breast cancer, immunohistochemical quantification of CD44+/CD24−/low CSC phenotype did not correlate with tumor progression or overall survival, but a higher percentage of CSCs was found in primary tumors with distant metastases (66).

1.3 Development of CSC specific treatments

The potential goal of a CSC-specific therapy is the eradication of all CSCs irrespective of their phenotypic heterogeneity.

Remarkably defined signaling pathways, e.g. self-renewal regulation by Wnt in CRC might be shared by normal SCs and CSC (67). Therefore significant toxicity of specific treatments might be expectable (31). In addition, treatments directly affecting CSC might provide selective pressure, resulting in the emergence of resistant clones (31).

Tumor microenvironment is a key factor modulating metabolism, tumor growth, progression and metastasis to distant sites, and ultimately poor prognosis (67-69). Thus, the development of novel therapies targeting CSC might require an improved knowledge of mechanisms regulating SC and CSC interaction. Different approaches are currently being considered for the development of CSC-specific treatments. Surface markers representing potential targets for monoclonal antibodies are currently being evaluated. Alternatively the use of compounds inhibiting possibly with differential effectiveness, signaling pathways in common between SC and CSC, including Wnt/β-catenin, Hedgehog, Notch, Bmi-1, PTEN, telomerase, and efflux transporters, are also being investigated.

-2-

AIMS OF THE STUDY

The identification of markers identifying CSC is fundamental for the validation of the CSC paradigm and for the development of new CSC-specific drugs and novel therapeutic approach.

Here we addressed:

1) The prognostic relevance of the expression of CSC surface markers in CRC clinical specimens.
2) The “in vivo” tumorigenicity of primary CRC derived cells, as related to their expression of putative CSC surface markers.
3) The possibility of using cells derived from established CRC cell lines expressing CSC surface markers as CSC cellular model.
4) The development of innovative culture models of potential relevance for the screening of anti CRC compounds.

-3-

RESULTS

During my doctoral studies I first addressed, in collaboration with the Institute of Pathology of Basel, we evaluated the prognostic significance of the expression of putative cancer stem cells markers on a large cohort of CRC. Then I evaluated the tumorigenicity of primary CRC specimens in immunodeficient mice based on the percentages of cells expressing putative CSCs markers in order to evaluate if a correlation engraftment potential could be postulated.

Following these studies, I addressed the suitability of human established CRC cell lines for CSC specific drug testing. I established the expression of the putative CSC markers on the cell lines and then I compared the putative cancer stem cells isolated based on the expression of CSC markers with well-known stem cells and cancer stem cells features namely: spheroid formation ability, clonogenicity, enzyme and pump activity related to drug resistance, tumorigenicity, and drug resistance to drugs commonly used in CRC chemotherapy.

Finally, considering the potential relevance of growth in spheroid architectures in CSC biology, I developed a three-dimensional culture system for established CRC cell lines.

3.1 Prognostic impact of the expression of putative cancer stem cell markers CD133, CD166, and CD44s in colorectal cancer

Based on the original paper:

Prognostic impact of the expression of putative cancer stem cell markers CD133, CD166, CD44s, EpCAM, and ALDH1 in colorectal cancer.

Lugli A, Iezzi G, Hostettler I, Muraro MG, Mele V, Tornillo L, Carafa V, Spagnoli G, Terracciano L, Zlobec I.

Br J Cancer. 2010

Introduction

Putative CSC populations have been identified in several types of solid tumors, on the basis of the expression of specific markers and of functional stem cell-like properties, including high clonogenicity, differentiation capacity, spheroid formation, and, critically, the ability to reproduce the original tumor on transplantation in immunodeficient mice (37-39, 70).

Phenotypic characterization of CSC derived from colorectal cancers is still debated. Initial works indicated CD133 molecule as a reliable CSC marker in primary human colorectal cancers. Instead, Dalerba and colleagues identified CRC-SC in a subset of EpCAM positive cells co-expressing CD44 and CD166 (37-39). Subsequent studies have shown that in both mouse and human colorectal cancers the proposed markers are not restricted to rare cell subsets, but their expression can be detected in relatively large populations of tumor cells, irrespective of their tumorigenicity ((46) and Muraro et al, unpublished).

CSCs have been suggested as the driving force behind tumor initiation, growth, and metastasis, with a potentially high clinical relevance. However, little and contradictory information is available in literature about the prognostic relevance

associated with the expression of putative CSC markers in CRC. Choi et al. reported no correlation between survival and high expression of CD133 and CD24 studying 523 cases (71). Instead, Horst et al., Kojima et al., and Li et al. reported low to poor survival associated with high expression of CD133 in a cohort of 77, 189, and 104 cases, respectively (72-74). Contradictory findings have been reported about the association between the expression of CD44 and tumor progression, and, in particular, with the expression of its isoform CD44v6 (75-77). Membranous but not cytoplasmic expression of CD166 has been found to correlate with a shortened survival, in a study based on 111 cases (23). A comprehensive analysis of the expression of multiple putative CSC markers in large groups of patients with detailed statistical analysis of the prognostic significance of the co-expression of multiple CSC markers within the same tumor is still missing.

By using a tissue micro-array including 1420 primary colorectal cancers with full clinico-pathological data and follow-up we addressed expression and the prognostic significance of CD133, CD166, CD44s, and EpCAM expression in colorectal cancer.

Materials and Methods

Patients and clinico-pathological data

Archival paraffin-embedded material from 1420 patients with primary, pre-operatively untreated colorectal cancer were retrieved from multiple centers including the Institute of Pathology, University Hospital of Basel, Switzerland, the Institute of Clinical Pathology, Basel Switzerland and the Institute of Pathology, Stadtspital Triemli, Zürich, Switzerland. All histopathological information was systematically re-reviewed from the corresponding H&E slides including pT classification, pN classification, tumor

grade, histologic subtype, and the presence of vascular invasion. Tumor border configuration was diagnosed according to Jass et al. as “pushing /expanding” when there was a reasonably well-circumscribed margin at the invasive front and as “infiltrating” when no recognizable margin of growth and a streaming dissection between normal structures of the bowel wall was present (78). Clinical information was retrieved from patient records and included age, gender, tumor location, and disease-specific survival time. For patients diagnosed at the Institute for Pathology, Stadtspital Triemli, Zürich, information on local recurrence, (n=476), distant metastasis (n=489) and adjuvant therapy (n=478) was available. Patient characteristics are summarized in Table 2. The use of these materials in this study was approved by the local ethics committee.

Table 1 Summary of patient characteristics (n = 1420)

Clinicopathological feature	Outcome	Frequency *N* (%)
Age (years; $n = 1420$)	Mean (range)	69.9 (30–96)
Gender ($n = 1414$)	Female	741 (52.4)
	Male	673 (47.6)
Histological subtype ($n = 1420$)	Mucinous	119 (8.4)
	Other	1301 (91.6)
Tumour location ($n = 1400$)	Right sided	488 (34.9)
	Left sided	430 (30.7)
	Rectum	482 (34.4)
T classification ($n = 1387$)	pT1	62 (4.5)
	pT2	203 (14.6)
	pT3	899 (64.8)
	pT4	223 (16.1)
N classification ($n = 1363$)	N0	711 (52.2)
	N1	358 (26.3)
	N2	294 (21.6)
Tumour grade ($n = 1385$)	G1	31 (2.2)
	G2	1177 (85.0)
	G3	177 (12.8)
Vascular invasion ($n = 1385$)	Absent	1002 (72.4)
	Present	383 (27.7)
Tumour border configuration ($n = 1384$)	Infiltrating	871 (62.9)
	Pushing	513 (37.1)
Local recurrence ($n = 476$)	Absent	276 (58.0)
	Present	200 (42.0)
Distant metastasis ($n = 489$)	Absent	401 (82.0)
	Present	88 (18.0)
Post-operative therapy ($n = 478$)	No	377 (78.9)
	Yes	101 (21.1)
Survival time (months) ($n = 1379$)	5-year survival rate	56.4 (54–59)

Tissue microarray and Immunohistochemistry

Tumor specimens from all 1420 patients as well as 57 samples of normal colonic mucosa were included on a previously described tissue microarray (79). Tissue cylinders with a 0.6 mm diameter were punched from morphologically representative tissue areas of each “donor” tissue block and brought into one recipient paraffin block (3x2.5 cm) using a homemade semi-automated tissue arrayer. Immunohistochemistry was performed for protein markers CD133, CD44s, CD166. Detailed staining procedures have been described elsewhere (80). The following primary antibodies were used: anti-human CD133 (clone C24B9; 1:100; Cell Signaling), anti-human CD166 (clone M0G/07; 1:200; Novocastra), and anti-human CD44s (clone DF1485; 1:50; Dako). Negative controls underwent the same protocol with the primary antibody omitted. Primary antibodies were omitted in slides serving as negative controls

Evaluation of immunohistochemistry

For CD133, CD166, and CD44s, only membranous staining was considered (Figure 7). Tissues were scored semi-quantitatively by evaluating the proportion of positive tumor cells over the total number of tumor cells (percentage of positive tumor cells per tissue microarray punch). Then, using receiver operating characteristic (ROC) curve analysis (81), appropriate cut-off scores for each marker were obtained. Positive staining in percentages of cells above or below the cut-off scores was classified as “overexpression” or “loss”, respectively. The reliability of the cut-off score was confirmed by 200 bootstrapped replications, a method which re-samples the data with replacement.

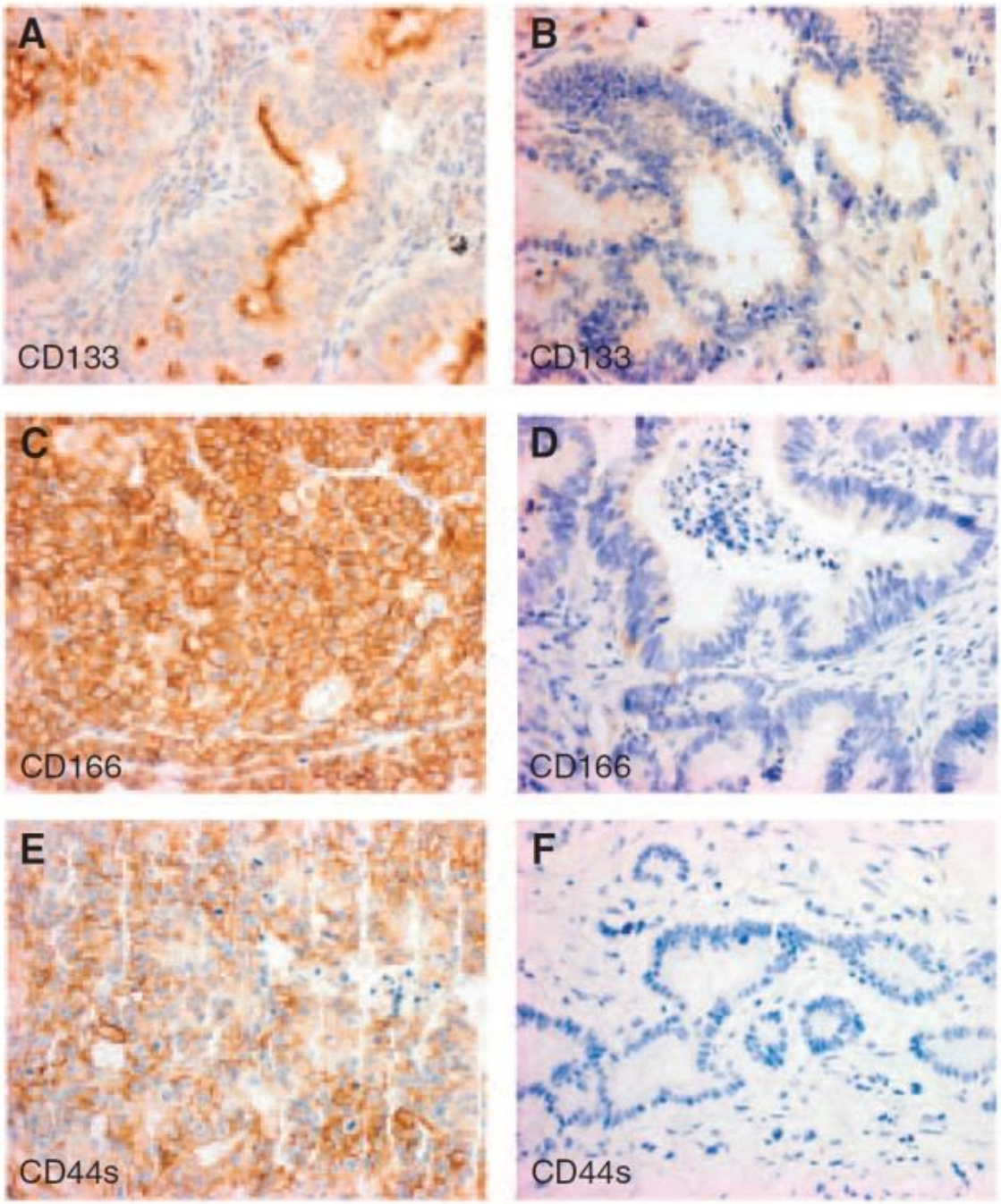

Figure 7 Colorectal cancer samples with membranous positivity and corresponding negative staining for CD133 (A and B), CD166 (C and D), and CD44s (E and F).

Tumor invasion assay

The colorectal cancer cell lines LS180, SW480, and COLO205 were cultured in RPMI 1640 medium supplemented, with GlutaMAX, MEM NEAA, 10mM HEPES, 1mM sodium pyruvate, kanamycin sulphate, and 10% FCS (all the reagents were from Gibco, Paisley, UK). For invasion assays, cells were stained with APC-conjugated anti-CD44s and PE-conjugated anti-CD166 antibodies (BD Pharmingen, San Jose, CA, USA), and CD44+/CD166+ or CD44-/CD166- cell subsets were sorted by flow cytometry. Dead cells were excluded by DAPI staining. Purity of sorted cells was >97%. Unsorted tumor cells or sorted subsets were tested for invasiveness in a chemoinvasion assay (82). Briefly, tumor cells re-suspended in serum-free medium were seeded in transwell plates on uncoated or matrigel-coated membranes (8 mm pore size, BD Biocoat Tumor invasion assay, BD Biosciences, San Jose, CA, USA). Medium containing 5% FCS was seeded in the lower chambers and the cells were incubated at 371C for 20 h. Inserts were then removed and numbers of cells migrated into the lower chambers were quantified by CyQUANT Cell Proliferation Assay Kit (Invitrogen, Paisley, UK). Percentages of cell invasion were calculated according to the following formula: (relative fluorescent units (RFU) of cells invaded through matrigel-coated membranes/mean RFU of cells migrated through uncoated membranes) x100.

Statistical Analysis

Chi-Square tests were carried out for categorical endpoints. The product-limit method and log-rank or Wilcoxon tests were used to assess differences in survival time. The 5-year survival rates and 95% confidence intervals (CI) were obtained. For Cox multiple regression analysis, the assumption of proportional hazards was verified

prior to each analysis. Patient with missing clinico-pathological data or with non-evaluable immunohistochemistry were excluded from the analysis. Hazard ratios (HR) and 95%CI were obtained to assess the prognostic effect of each protein marker on outcome. All tests were two-sided and p-values were considered statistically significant with $p<0.05$.

Results

Tissue microarray analysis: Normal mucosa versus colorectal cancer

Mean percentage of cells expressing CD133 was <1% in normal mucosa and 24.7% in CRC ($p<0.001$). CD44 and CD166, expression in normal tissue was detectable on average in 4.3% and 41.3% of cells, respectively, and in 33.1% and 64.4% of cancer cells ($p<0.001$).

In order to evaluate the prognostic significance of the expression of these markers receiver-operating curves (ROC) (81) were calculated.

Based on the analysis of 1245 cases, a 5% cut-off score was defined for CD133 expression. With this setting 616 cases (49.5%) displayed overexpression and 629 cases (50.5%) loss of expression. Neither condition showed a significant correlation with overall survival.

Regarding CD166, cut-off score was established at 65%, based on the ROC analysis of 1274 cases. In 775 (60.8%) and 499 cases (39.2%), respectively, overexpression or loss of expression were detected.

Interestingly, CD166 loss was associated to advanced pT ($p=0.002$), lymphatic metastases ($p=0.004$), and worse overall survival ($p=0.015$; Figure 3A). However, CD166 loss was not an independent prognostic factor in multivariable analysis

including age, T classification, N classification, vascular invasion, tumor border configuration and metastasis.

Regarding CD44s (Table 2), the relevant cut-off score was set at 5% based on the analysis of 1261 individual specimens. In 607 cases (48.1%) we observed loss and in 654 (51.9%) CD44 overexpression. Similarly to CD166, CD44 loss was associated with higher T stage (p=0.014) and lymphatic metastases (p=0.002). Most importantly survival rate was significantly lower (p=0.019) for patients bearing tumors with loss as compared to those bearing cancers overexpressing (Figure 8B). Again, however, the

	CD166, *N* (%)			CD44s, *N* (%)		
Clinicopathological feature	**Loss**	**Overexpression**	***P*-value**	**Loss**	**Overexpression**	***P*-value**
T classification						
pT1–2	72 (14.7)	165 (21.7)	0.002	96 (16.0)	137 (21.5)	0.014
pT3–4	417 (85.3)	594 (78.3)		503 (84.0)	500 (78.5)	
N classification						
pN0	228 (47.4)	417 (55.9)	0.004	275 (47.2)	353 (56.0)	0.002
pN1–2	253 (52.6)	329 (44.1)		308 (52.8)	277 (44.0)	
Tumour grade						
G1–2	438 (89.9)	658 (86.8)	0.097	611 (88.7)	474 (87.0)	0.361
G3	49 (10.1)	100 (13.2)		78 (11.3)	71 (11.0)	
Vascular invasion						
Absent	340 (69.8)	564 (74.4)	0.076	418 (69.6)	473 (74.6)	0.048
Present	147 (30.2)	194 (25.6)		183 (30.4)	161 (25.4)	
Tumour border configuration						
Pushing	140 (28.8)	323 (42.6)	<0.001	197 (32.8)	261 (41.3)	0.002
Infiltrating	346 (71.2)	435 (57.4)		404 (67.2)	371 (58.7)	
Tumour location						
Left sided	328 (66.1)	492 (64.4)	0.529	476 (68.7)	341 (61.4)	0.008
Right sided	168 (33.9)	272 (35.6)		217 (31.3)	214 (38.6)	
Local recurrence						
Absent	43 (50.6)	201 (60.2)	0.109	133 (54.7)	121 (64.0)	0.052
Present	42 (49.4)	133 (39.8)		110 (45.3)	68 (36.0)	
Metastasis						
Absent	70 (79.6)	275 (81.4)	0.699	202 (82.5)	159 (82.0)	0.894
Present	18 (20.5)	63 (18.6)		43 (17.6)	35 (18.0)	
Survival rate (95% CI)						
5 year	52.9 (48-57)	59.0 (55-63)	0.015	53.4 (49-58)	59.3 (55-63)	0.019

Table 2 Association of membranous CD166, and CD44s with clinico-pathological features in colorectal cancer patients. Abbreviation: CI = confidence interval; ROC = reveiver-operating characteristic. Cut off scores for overexpression derived from ROC curve analysis were 65% for CD166, and 5% for CD44s.

prognostic effect of CD44 loss was not independent, as shown by multivariable analysis taking into account age, TNM status, vascular invasion and tumor border configuration.

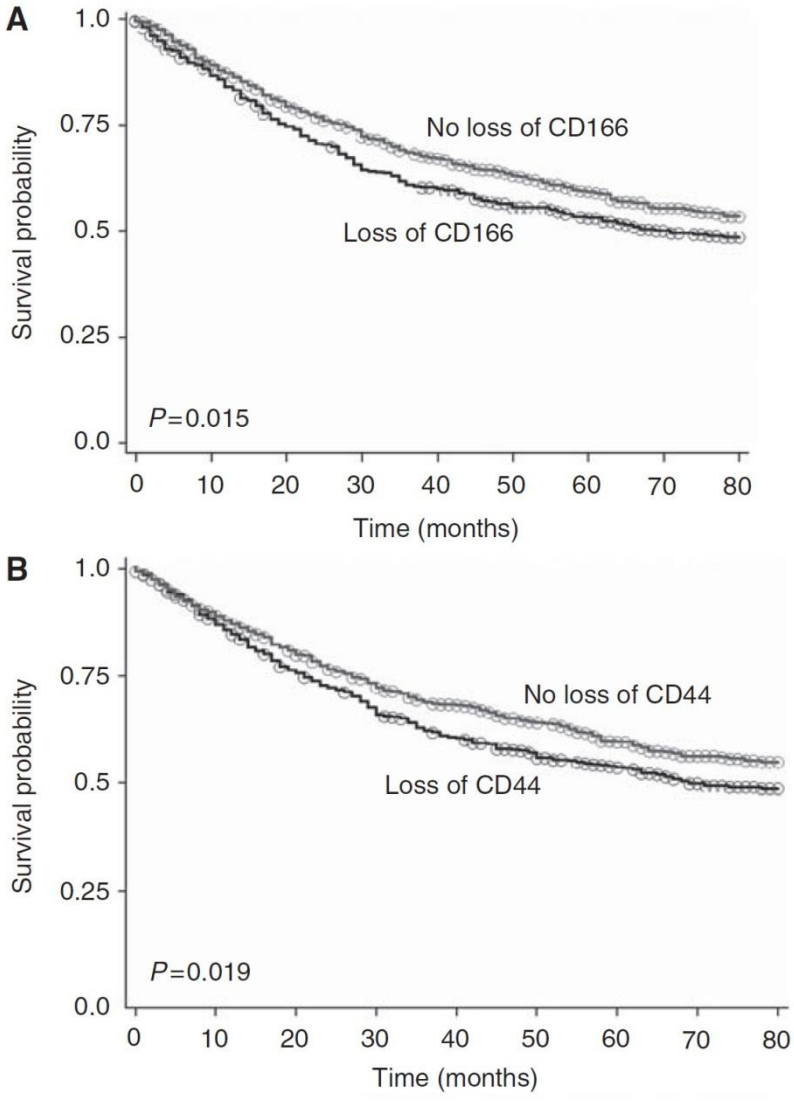

Figure 8 Kaplan–Meier survival curves illustrating survival time differences in patients with (A) loss vs overexpression of membranous CD166, (B) loss vs overexpression of CD44s

Invasiveness of tumor cells differing in CD44 and CD166 expression

Since CD44 and CD166 are adhesion molecules, we hypothesized that their loss might directly favor the invasiveness of tumor cells, possibly as a consequence of reduced adhesion. To address this issue in a controlled in vitro model, we investigated the invasive potential of CD44+/CD166+ or CD44-/CD166- cells derived from the human colorectal cancer cell lines, LS180, SW480 and COLO205. All three cell lines displayed a heterogeneous surface expression of CD44 and CD166 (Figure 9, left panels). However when CD44+/ CD166+ and CD44-/ CD166- cell subsets were sorted and evaluated for their invasive capacity, in all cases the double negative fractions exhibited significantly higher invasive potential than their positive counterparts (Figure 9, right panels). These results suggest that absence of CD44 and CD166 molecules is directly associated to higher invasive capacity of tumor cells.

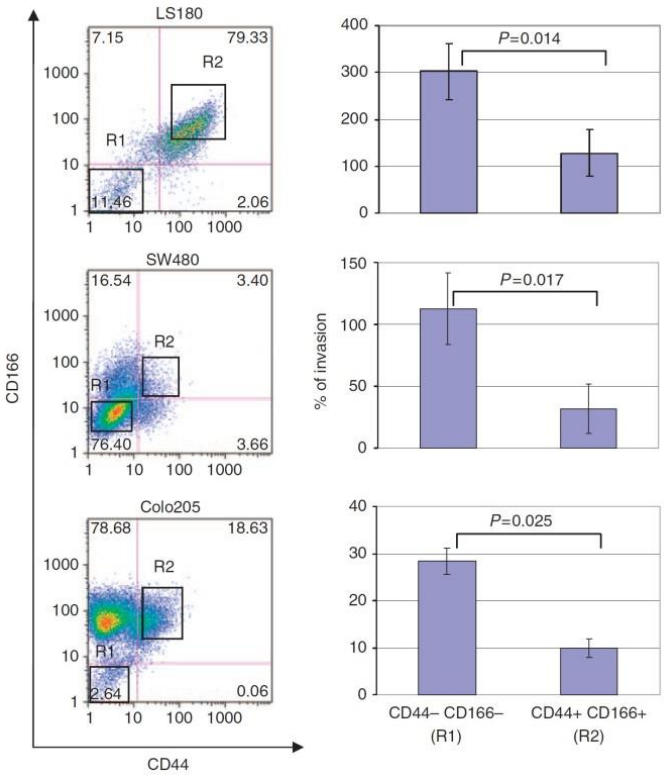

Figure 9 The CD44-/CD166- tumor cells display higher invasive potential than CD44+/CD166+ cells. The CD44-/CD166- and CD44+/CD166+ cell subsets were sorted by flow cytometry, according to the gates depicted, from LS180, SW480, and COLO205 cell lines. Sorted subsets were tested in invasion assays. Percentages of cell invasion (mean values ± SD) are shown. Data are representative of six independent experiments.

Discussion

We have evaluated the relationship between expression of proposed putative CSC markers and most clinically relevant features of colorectal cancer. Our findings suggest that, despite the increased expression of CD133, CD166, and CD44s, from normal to early colorectal cancer, their expression is not “per se” associated with unfavorable prognosis. In contrast, it is the overall decreased membranous expression of CD166, and CD44s, which is linked to tumor progression and an aggressive tumor phenotype, a result confirmed for CD44s and CD166, using three established colorectal cancer cell lines.

CD44 has long been thought of as a marker of tumor invasiveness and metastasis and has also recently been described as a putative colorectal CSC marker (39). Early works investigating the CD44s gene reported a poorer survival in patients with increased expression levels of the specific gene or protein (76). However, more recent results suggest either no role for CD44s or a worse clinical outcome associated with loss of protein expression (71, 83). As already shown by others (77), we also observed an increasing expression of CD44s from normal to tumor tissue. Notably, loss of membranous CD44v6 expression has been shown to be linked to a highly aggressive tumor phenotype (79). In this study, we found that loss of CD44s expression is linked to a significantly worse clinical outcome in univariate but not in multivariable analysis suggesting that the findings concerning survival time may be confounded by other relevant prognostic factors.

Regarding the prognostic impact of CD166 in colorectal cancer an increasing expression of CD166 from normal to tumor tissue (23), and also an age-dependent correlation between the increase of CD44 and CD166 expression and the numbers of

polyps has been reported (84). We confirmed the previous findings but, in contrast, we observed a significant adverse effect of loss, rather than increase, of membranous CD166 expression on clinical outcome. A similar association between decreased membranous CD166 staining and poorer prognosis was previously reported in other tumor types, including ovarian and prostate cancer (85, 86).

The prognostic significance of CD133 expression in primary CRC has been previously evaluated in a few studies. Either no correlation (73) or a significant negative association (49, 71-74) between increased CD133 expression and clinical outcome has been found in studies including limited numbers of cases (77 (72), 189 (73), and 104 (74) cases). However, recent study, including a larger group of cases (n=523), reported lack of correlation between CD133 expression and patient survival (71). In line with the latter findings, we also did not observe any significant correlation between CD133 and clinical outcome. Thus, CD133 expression does not appear to be per se predictive of unfavorable clinical outcome.

Several reasons for these discrepancies can be hypothesized including differences in sample size (power for detecting prognostic differences), methodology (tissue microarray versus whole tissue sections) and certainly the choice of cut-off scores for the definition of positive staining or staining intensity.

Since loss of expression of CD44 and CD166 by immunohistochemistry correlated with worse prognosis, we further evaluated the in vitro the invasive capacity of CD44-/CD166- and CD44+/CD166+ cells sorted from three established human CRC cell lines. Indeed, in all cases a highly significant increase of the invasive potential was noted for the CD44-/CD166- fraction. Our in vitro findings strongly suggest that CD44 and CD166 expression may limit tumor cell spreading in surrounding

tissues, thus underlining the hypothesis that loss of expression of these markers, rather than their over-expression, is associated with a more aggressive tumor phenotype.

To our knowledge, this is the first systematic assessment of the prognostic value of CD133, CD166, and CD44 in colorectal tumors evaluated on a large number of cases. Our findings indicate that expression of CSC markers is not per se predictive of poor clinical outcome. Loss of expression of CD166, and CD44s is rather linked to an aggressive tumor phenotype, and, particularly, to the presence of an infiltrating tumor margin which may implicate these proteins in events occurring at the invasive tumor front.

3.2 Higher percentage of CRC-SCs in primary CRC does not correlate with higher engraftment rates in immunodeficient mice

Introduction

Human tumor biology has long been studied in experimental xenogeneic colon cancer models, by injecting cell lines, or cell suspensions or fragments of primary tumors into immunocompromised mice.

The emerging concept of CSCs represents an innovative model with the potential to unravel new approaches for both drug discovery and preclinical screening. The gold standard for the identification of CSCs is represented by their in-vivo tumor formation capacity in immunodeficient mice recapitulating all the more differentiated cell populations detectable in primary tumors. Furthermore CSC should be serially re-transplantable consistent with a self-renewal potential (87).

Xenografts are usually implanted into subcutaneous tissue, a site easily accessible for both graft procedure and observation of tumor growth. Despite their ectopic location, CSCs have been shown to display a distinctive ability to generate heterogeneous tumors with histological patterns similar to those detectable in clinical specimens.

The study of CSCs in solid cancers presents technical hurdles related to tissue dissociation, separation of cellular subpopulations, and a poor knowledge of membrane markers. The extensive manipulation required by the isolation of cells

expressing CSC markers from primary tumors could affect their tumorigenic potential. Our approach was to evaluate the tumorigenic potential of CRC cells expressing putative CSC markers without sorting them from the original primary tumor derived cell suspensions but inoculating the entire heterogeneous population subcutaneously into the mouse flank, in order to investigate if samples with different expression of putative CSC markers may have different capacity to engraft in mice. Our data indicate that there is no correlation between percentages of cells expressing of CSC markers in tumor cell suspensions and their tumorigenic capacity in different immunodeficient recipient models.

Materials and Methods

Digestion of human tumor specimens

Tumor cells suspension were derived from freshly excised CRC samples, obtained from consenting patients undergoing surgical treatment at Basel University Hospital, Kantosspital St.Gallen and Ospedale Civico di Lugano. Tissues were enzymatically digested in serum-free DMEM (GIBCO), supplemented with Collagenase IV (1mg/ml) and DNAse I (50 mg/ml, both from Sigma-Aldrich), and a cocktail of antibiotics, including Kanamycin (GIBCO), Amphotericin B (Sigma-Aldrich), Metronidazol (200mg/ml, Sigma-Aldrich) and Cefuroxim (6mg/ml, Sigma-Aldrich). After digestion, tissue explants were ground inside a 100 µm sterile cell filter with the blunt end of a Luer syringe while continually rinsing with cell medium. Once most of the cells were collected, the mixture was filtered again through a 70 µm sterile cell filter and centrifuged for 5 min at 1500 rpm. The supernatant was removed and cells were resuspended in 1 mL of medium and counted.

Tumor transplantation

In vivo experiments were approved by the Basel Cantonal Veterinary Office. Eight–ten week old NOD/SCID (NS) and NOD/SCID IL-2 receptor γ chain (NSG) deficient mice, initially obtained from Charles River Laboratories (Germany), were bred and maintained under specific pathogen free conditions in the animal facility of the Department of Biomedicine of the University of Basel. Eight to ten week old mice were used for xenografting experiments.

Freshly isolated primary tumor cells (500.000) prepared in a 1:1 mixture of PBS and Growth Factor Reduced BD Matrigel Matrix (BD Biosciences) were injected in the left flank of recipient mice. Tumor development was monitored by palpation. Time to onset of a palpable tumor was recorded and the tumor size was measured weekly by a dial caliper. Tumor volumes were calculated according to the formula (length x width2)/2. Mice were sacrificed when tumors reached a maximum diameter of 10 mm.

Flow cytometric analysis

Surface phenotype of freshly isolated primary tumor cells was determined by flow cytometry. The following antibodies were used: phycoerythrin- (PE) or allophycocyanin- (APC) labeled anti-CD133 (clone AC133/1, Miltenyi Biotec, Bergish, Gladbach, Germany), PE-labeled anti-CD166 (clone 3A6, BD Biosciences, San Josè, CA), fluorescein isothiocyanate- (FITC) , APC- or APC-H7-labeled anti-CD44 (clone G44-26, BD Biosciences), FITC- or PE-labeled anti-CD24 (clone ML5, BD Biosciences). Propidium iodide (PI, 0.5 µg/ml) was added to the samples prior to analysis. Relative fluorescence intensities were measured using a BD FACS Calibur flow cytometer (BD Biosciences), or a CyAn ADP Analyzer (Beckman Coulter, Krefeld, Germany) following exclusion of dead

cells based on PI incorporation. Analysis was performed using FlowJo software (Tree Star, Portland, OR).

Statistical Analysis

Statistical analysis was performed by 2-tailed Student's t-test using the GraphPad Prism 5 software (GraphPad Software, Inc., La Jolla, CA). P-values ≤0.05 were considered significant.

Results

CRC samples phenotype

We analyzed the expression of putative CRC-SC markers CD133, CD44, CD166, and CD24, and their combinations within EpCAM positive population in all human CRC samples processed and also in the corresponding healthy mucosa (n = 51). We found that expression was significantly higher in the tumor as compared to the autologous corresponding healthy mucosa for all markers alone (CD133 $p<0.0001$; CD44=0.0004; CD166 p=0.0015; CD24 p=0.004) and in combination (CD166/CD44 p=0.0212; CD133/CD44 p=0.0121) (Figure 10a). Notably, we observed that several tumor samples expressed the putative CSC markers at high extents and, in general a high heterogeneity was observed among the specimens analyzed (CD133 range 0.12-77.12%; CD44 range 0,48-70.64%; CD166 range 0.18-41.12%; CD24 range 7.66-98.58%) (Figure 10A and Table 3A and 3B).

Table 3A Summary of phenotypical characterization of tumorigenic CRC samples analyzed.

Sample	Strain	Tumorigenic	EpCAM		CD133		CD44		CD166		CD166/CD44		CD133/CD44		CD24	
			Mucosa	Tumor	Mucosa	Tumor	Mucosa	Tumor	Mucosa	Tumor	Mucosa	Tumor	Mucosa	Tumor	Mucosa	Tumor
1	NS	yes		66,65		32,26		0,48		13,04		0,15		0,39		
2	NS	yes	76,43	24,34	0,06	3,06			0,16	16,43						
3	NS	yes	38,23	41,73	0,28	2,66	3,50	2,83	0,52	0,18	0,36	0,01				
4	NS	yes	78,37	78,23	0,34	45,10	4,36	6,06	0,46	0,89	0,10	0,38				
5	NS	yes	32,41	45,40	0,46	48,40	1,82	5,31	13,41	34,32	0,94	4,16				
6	NS	yes	43,84	72,38	1,61	5,96	1,51	1,90	23,16	3,12	1,30	0,25	0,37	0,21		
7	NS	yes	53,22	58,77	2,09	53,54	1,68	5,45	2,51	20,76						
8	NS	yes	66,70	5,18	4,99	14,96	3,79	63,51	0,34	12,69	0,13	12,10				
9	NS	yes	57,09	46,34	16,57	15,71	5,97	16,62	6,48	16,37	4,29	2,84	2,24	3,34		
10	NS	yes		39,86		0,76		6,26		11,48		3,97		0,68		
11	NS	yes		76,24		8,47				5,24						
12	NS	yes		60,54		34,66		32,49		22,60						
13	NS	yes		20,70		48,07		14,10		18,28		6,31		12,96		
14	NS	yes		51,82		34,38		33,71		13,06						
15	NSG	yes	62,05		3,53		5,36		9,55		4,24		0,54		46,94	
16	NSG	yes	66,80	56,38	9,05	12,64	5,66	5,67	3,45	5,08	1,39	1,85	2,62	2,50	75,88	81,55
17	NSG	yes	46,53	88,13	4,62	34,31	6,71	42,09	8,26	29,03	4,60	24,00	1,26	24,17	67,72	80,33
18	NSG	yes	52,06	72,25	5,49	21,58	0,91	12,93	5,36	5,32	0,28	1,10	0,37	1,67	55,13	71,10
19	NSG	yes	30,34	33,98	0,88	19,50	0,97	1,33	4,28	8,92	0,66	0,52	0,39	1,29	2,96	10,32
20	NSG	yes				13,87		13,09		12,67		7,15		4,97		
21	NSG	yes	15,03	15,11	14,27	9,81	6,99	13,07	2,24	12,68	1,18	5,90	2,80	3,07	44,11	29,98
22	NSG	yes			2,70	49,13	2,05	2,30	3,66	5,83						
23	NSG	yes	58,57	46,22	0,84	2,68	2,32	2,40	2,23	1,06	0,49	0,38	0,32	0,21		
24	NSG	yes	67,53	87,53	2,02	2,73	1,31	12,13	1,38	1,72	0,55	1,71	0,53	1,70	1,90	71,71

Tumorigenic

Table 3B Summary of phenotypical characterization of non tumorigenic CRC samples analyzed.

				EpCAM		CD133		CD44		CD166		CD166/CD44		CD133/CD44		CD24	
	Sample	Strain	Tumorigenic	Mucosa	Tumor	Mucosa	Tumor	Mucosa	Tumor	Mucosa	Tumor	Mucosa	Tumor	Mucosa	Tumor	Mucosa	Tumor
Non Tumorigenic	1	NS	no				2,53		22,59		1,18		0,41		0,97		
	2	NS	no	59,69	45,56	6,92	14,73	4,60	3,14	8,84	41,12	3,52	2,46	2,84	2,20		
	3	NS	no	46,74	58,83	1,39	7,45	1,45	1,16	0,74	0,59	0,29	0,24	0,05	0,84		
	4	NS	no	28,50	50,24	0,92	14,20	5,96	3,10	2,78	3,02	0,29	0,22	0,03	0,47		
	5	NS	no		76,23		3,29		1,69		1,19		0,21		0,76		
	6	NS	no		36,93		11,33		15,18		20,58		9,78				
	7	NS	no		76,28		46,68		11,25		3,84		3,89		5,48		
	8	NS	no		56,24		35,53		22,10		0,00		0,33		20,91		
	9	NS	no		40,96		64,09		46,62		17,59		15,96		35,78		
	10	NS	no	32,12	79,36	13,55	0,12	7,52	60,48	3,55	8,86	1,80	5,86	1,06	0,50		
	11	NS	no	2,49	59,70	6,25	16,53		8,51		16,83		3,69		6,54		
	12	NS	no		7,80		24,54		70,64		5,14		4,23		20,56		
	13	NS	no	53,85	11,54	10,32	43,28	7,68	33,51	4,75	12,49	2,88	10,17			25,78	62,90
	14	NS	no	56,25	61,47	6,97	66,93	13,64	21,66	10,52	8,15	6,80	7,25			37,76	59,65
	15	NSG	no		52,75		19,27		8,79		0,64		0,94		3,82		22,26
	16	NSG	no		44,48		1,71		8,39		2,23		2,52		1,43		54,39
	17	NSG	no		88,77		11,23		16,19		9,04		5,33		4,29		48,07
	18	NSG	no	88,61	80,18	9,30	77,12	6,32	38,29	2,81	16,21	1,68	12,30	3,99	38,75	83,79	98,58
	19	NSG	no		84,10		42,07		12,77		4,05		2,37		13,83		63,90
	20	NSG	no	73,17	86,25	2,10	2,53	4,36	3,36	4,34	1,50					12,96	29,74
	21	NSG	no	92,40	88,05	1,19	32,78	0,83	3,29	2,15	19,67	0,21	0,49	0,15	2,07	23,98	42,09
	22	NSG	no	0,33	57,16	3,20	13,02	1,55	11,39	0,88	10,74		1,99			53,76	54,50
	23	NSG	no		68,64		21,18		2,68		13,84				2,13		
	24	NSG	no	37,97	14,30	1,86	16,28	9,64	26,12	6,19	10,06		2,65		5,58	26,45	38,89
	25	NSG	no		76,22		8,13		10,74		3,44		1,96		0,90		
	26	NSG	no				6,59		5,41		9,68						
	27	NSG	no	57,09	33,48	0,14	75,30	66,81	96,69	0,70	1,30	1,73	2,89	1,72	74,17	8,92	7,66

Tumorigenic potential of CRC-derived cell suspension

We then analyzed the correlation occuring between percentages of cells expressing CSC markers within the primary tumor derived cell suspensions and their relative tumorigenic capacity in two immunodeficient mouse models (NS and NSG) which were previously suggested to be characterized by differential "tumor take" capacity (37-39). Mouse engraftment was successful for 24 out of 51 human tumor specimens tested. Their capacity to engraft did not correlate with the percentages of cells bearing CSC markers within the epithelial fraction of the injected CRC derived cell suspensions tested (Figure 10B). Importantly, even tumor specimens highly expressing CSCs markers failed to efficiently engraft.

Furthermore, comparing the tumorigenic potential in two differentially immunodeficient mouse strains we did not observe significantly different engraftment capacity (NS 14/28; NSG 10/23) (table 3).

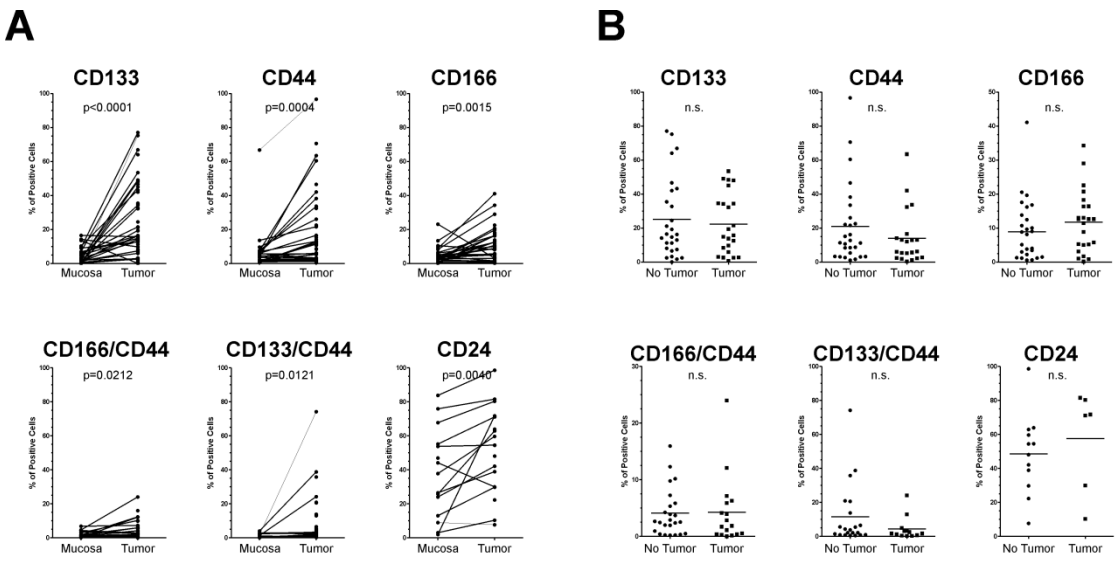

Figure 10 (A) Putative CSC marker expression in healthy mucosa as compared with corresponding tumor tissues. Percentage are related to the EpCAM positive cell fraction. (B) Engraftment capacity in relation to the expression of CSC markers in tumor tissue.

Discussion

Subcutaneous engraftment in immunodeficient mice is a widely used technic for the expansion of primary tumor cells possibly maintaining biological and histopathological features of original tissues (88).

According to the CSC model, only a subset of tumor cells has the capacity to sustain tumor growth and to reproduce the cellular heterogeneity typically characterizing clinical cancer specimens. It has been demonstrated that only the cells expressing CSC surface markers are able, once isolated and subcutaneously injected into immunodeficient recipient, to recapitulate the original heterogeneity of cancer cells of the tissue of origin.

In CRC it has been suggested that cells expressing CD133 (37, 38), or both CD166 and CD44 (39), sorted from digested primary tumor tissue, are capable to serially engraft in immunodeficient mice.

Our results show that all putative CSC markers are expressed to significantly higher extents in the tumor tissue as compare to the corresponding, autologous healthy mucosa. Most importantly, there is no correlation between percentages of EpCAM positive expressing defined CSC markers in primary tumor derived cell suspensions and their engraftment capacity. For CD44 and CD166 only 4/21 and 4/23 specimens, respectively, with more than 10% positive cells developed tumors. For CD133 and CD24 only 9/23 and 4/6 samples expressing markers in more than 10% of cells successfully engrafted.

Thus, CSC marker expression is not restricted to a small subset of cells within the tumor mass but it might rather be patient dependent.

Furthermore, samples characterized by high percentages of CSC markers expressing cells (CD133 range 0.12-77.12%; CD44 range 1.16-70.64%; CD166 range 0.59-41.12%; CD24 range 7.66-98.58%) (Figure 10A and Table 3) were unable to generate detectable tumor mass. These results contrast with the previously reported by Ricci-Vitiani, O'Brien, and Dalerba (37-39).

Our findings question the consistency of xenografting as "gold standard" assay for the identification and phenotypic characterization of CSCs or the validity of the proposed markers for the isolation of CRC-SCs.

3.3 CRC CSC Markers in human established CRC Cell Lines

STEM CELLS TRANSLATIONAL MEDICINE®

CANCER STEM CELLS

CD133+, CD166+CD44+, and CD24+CD44+ Phenotypes Fail to Reliably Identify Cell Populations with Cancer Stem Cell Functional Features in Established Human Colorectal Cancer Cell Lines

MANUELE GIUSEPPE MURARO,[a,b] VALENTINA MELE,[a,b,c] SILVIO DÄSTER,[a,b,d] JUNYI HAN,[a,b,e] MICHAEL HEBERER,[a,b] GIULIO CESARE SPAGNOLI,[a,b] GIANDOMENICA IEZZI[a,b]

Key Words. Cancer • Cell surface markers • Chemotherapy • Cancer stem cells • Colorectal cancer • Cancer cell lines

[a]Institute of Surgical Research and Hospital Management, [b]Department of Biomedicine, and [c]Institute of Pathology, University of Basel, Basel, Switzerland; [d]Department of Surgery, Basel University Hospital, Basel, Switzerland; [e]Department of Gastroenterology, Shanghai East Hospital, Tongji University, Shanghai, China

Correspondence: Manuele Giuseppe Muraro, M.Sc., Institute of Surgical Research and Hospital Management, Hebelstrasse 20, 4031 Basel, Switzerland. Telephone: 41-61-265-2376; Fax: 41-61-265-3990; e-mail: murarom@uhbs.ch; or Giandomenica Iezzi, M.D., Institute of Surgical Research and Hospital Management, Hebelstrasse 20, 4031 Basel, Switzerland. Telephone: 41-61-265-2376; Fax: 41-61-265-3990; e-mail: giezzi@uhbs.ch

Received January 5, 2012; accepted for publication July 3, 2012; first published online in SCTM *EXPRESS* August 6, 2012.

1066-5099/2012/$20.00/0

http://dx.doi.org/10.5966/sctm.2012-0003

ABSTRACT

Increasing evidence that cancers originate from small populations of so-called cancer stem cells (CSCs), capable of surviving conventional chemotherapies and regenerating the original tumor, urges the development of novel CSC-targeted treatments. Screening of new anticancer compounds is conventionally conducted on established tumor cell lines, providing sufficient material for high-throughput studies. Whether tumor cell lines might comprise CSC populations resembling those of primary tumors, however, remains highly debated. We have analyzed the expression of defined phenotypic profiles, including CD133+, CD166+CD44+, and CD24+CD44+, reported as CSC-specific in human primary colorectal cancer (CRC), on a panel of 10 established CRC cell lines and evaluated their correlation with CSC properties. None of the putative CSC phenotypes consistently correlated with stem cell-like features, including spheroid formation ability, clonogenicity, aldehyde dehydrogenase-1 activity, and side population phenotype. Importantly, CRC cells expressing putative CSC markers did not exhibit increased survival when treated with chemotherapeutic drugs in vitro or display higher tumorigenicity in vivo. Thus, the expression of CD133 or the coexpression of CD166/CD44 or CD24/CD44 did not appear to reliably identify CSC populations in established CRC cell lines. Our findings question the suitability of cell lines for the screening of CSC-specific therapies and underline the urgency of developing novel platforms for anticancer drug discovery. STEM CELLS TRANSLATIONAL MEDICINE *2012;1:592–603*

INTRODUCTION

The cancer stem cell model proposes that, similar to normal tissues, cancers are also hierarchically organized. Only rare tumor cells, endowed with self-renewal and differentiation capacity, called cancer initiating cells or cancer stem cells (CSCs), are capable of tumor initiation and maintenance. In contrast, the majority of cells constituting the tumor bulk do not possess the capacity for regeneration [1, 2].

Putative CSC populations have been identified in several solid malignancies based on the expression of specific surface markers together with functional stem cell-like features, including high clonogenicity, differentiation capacity, spheroid formation, expression of stemness-related genes, and, critically, the ability to reproduce the original tumor upon transplantation in immunodeficient mice [3–5]. In human colorectal cancer (CRC), in particular, CSC populations have been identified in primary tumors either by CD133 expression [6, 7] or by coexpression of CD166/CD44 [8]. Furthermore, coexpression of CD44 and CD24 has been proposed as an additional CSC phenotype in established CRC cell lines [9].

The existence of CSCs has important implications for anticancer therapy. Indeed, in order to successfully eradicate tumors, anticancer treatments should primarily target CSC subsets [2, 4, 10]. Notably, similar to normal stem cells, CSCs have been found to express high levels of DNA repair mechanisms [11, 12]; detoxifying enzymes, such as aldehyde dehydrogenase-1 (ALDH-1) [13]; and molecular pumps [14–16], accounting for their resistance to radio- and chemotherapies. The development of novel, more effective treatments would therefore be desirable.

Primary screening of novel anticancer compounds is conventionally conducted on monolayers of established tumor cell lines, typically on the National Cancer Institute 60 (NCI60) panel, a collection of 60 tumor cell lines representing

nine distinct human tumor types [17]. Established cell lines are easy to propagate in vitro, thus providing sufficient material for extensive molecular and signaling characterization, as well as for high-throughput studies [18]. However, whether they do actually comprise CSC populations resembling those of primary tumors remains unclear. A hierarchical organization, based on the expression of CSC markers reported in primary tumors, has been observed in established cell lines of several tumor types, including breast cancer [19, 20], glioblastoma [21], pancreatic cancer [22], and CRC [9, 23]. On the other hand, established cell lines have been recognized to only partially reproduce phenotypes and gene expression profiles of the tumors they are derived from [24, 25]. Whether putative CSC populations derived from tumor cell lines may serve as a model for CSCs of primary tumors therefore remains to be assessed. Importantly, the use of cell line-derived CSCs for the screening of anticancer compounds specifically targeting CSC populations has recently been proposed [26]. The sensitivity of cell line-derived CSCs to current or novel chemotherapies, however, has not been thoroughly investigated so far.

We have analyzed the expression of putative CRC-derived CSC phenotypic profiles, including CD133+, CD166+CD44+, and CD24+CD44+, in a panel of 10 human established CRC cell lines and evaluated their correlation with several CSC functional properties, including spheroid formation ability, clonogenicity, ALDH-1 activity, side population (SP) phenotype, tumorigenicity, and sensitivity to anticancer compounds currently in use for CRC treatment.

Materials and Methods

Cell Lines and Culture Reagents

Authenticated human established CRC cell lines (CACO2, COLO201, COLO205, DLD1, HCT15, HCT116, HT29, LS180, SW480, and SW620) were purchased from American Type Culture Collection (Manassas, VA, http://www.atcc.org). After one to two passages, cells were frozen and stored in aliquots. When needed for experiments, early-passage cells were thawed and maintained in culture for less than 2 months. COLO201, COLO205, DLD1, LS180, HCT15, and HCT116 were maintained in RPMI-1640 medium supplemented with 10% fetal bovine serum (FBS), GlutaMAX-I, nonessential amino acids (NEAA), 100 mM sodium pyruvate, 10 mM HEPES (all from Gibco, Grand Island, NY, http://www.invitrogen.com), and 50 μM 2-mercaptoethanol (Sigma-Aldrich, St. Louis, MO, http://www.sigmaaldrich.com). HT29 was maintained in McCoy's 5A medium (Sigma-Aldrich) supplemented with 10% FBS and GlutaMAX-I. CACO2 was cultured in Minimum Essential Medium (Sigma-Aldrich) supplemented with 10% FBS, GlutaMAX-I, NEAA, and sodium pyruvate. SW480 and SW620 were cultured in L-15 medium (Leibovitz) (Sigma-Aldrich) with 10% FBS and GlutaMAX-I. All media were also supplemented with kanamycin sulfate (Gibco). For specific experiments cell lines were cultured in serum-free (SF) medium for CSC derived from human primary CRCs, as previously described [6, 27]. Cells were cultured at 37°C with 5% CO_2. All cultures were tested by polymerase chain reaction and proven to be mycoplasma-free prior to experimental investigations.

Flow Cytometric Analysis and Cell Sorting

The surface phenotype of cultured cells was determined by flow cytometry. Tumor cells were harvested upon incubation with TrypLE Express (Gibco). The following antibodies were used: phycoerythrin (PE)- or allophycocyanin (APC)-labeled anti-CD133 (clone AC133/1; Miltenyi Biotec, Bergisch Gladbach, Germany, http://www.miltenyibiotec.com); PE-labeled anti-CD166 (clone 3A6; BD Biosciences, San Diego, CA, http://www.bdbiosciences.com); fluorescein isothiocyanate (FITC)-, APC-, or APC-H7-labeled anti-CD44 (clone G44–26; BD Biosciences); and FITC- or PE-labeled anti-CD24 (clone ML5, BD Biosciences). Propidium iodide (PI) (0.5 μg/ml) was added to the samples prior to analysis. Relative fluorescence intensities were measured using a BD FACSCalibur flow cytometer (BD Biosciences) or a CyAn ADP analyzer (Beckman Coulter, Fullerton, CA, http://www.beckmancoulter.com) following exclusion of dead cells on the basis of PI incorporation. Cell sorting was performed using a BD Influx cell sorter (BD Biosciences). Analysis was performed using FlowJo software (Tree Star, Ashland, OR, http://www.treestar.com).

Spheroid Formation Assay

Multicellular tumor spheroids were generated as previously described [28]. Briefly, single-cell suspensions were seeded in six-well culture plates (1,000 cells per well in 2 ml), precoated with a 50 μg/ml poly-2-hydroxyethyl methacrylate (polyHEMA) solution (Sigma-Aldrich). Spheroid formation was assessed by light microscopy after 4–7 days of culture.

Limiting Dilution Analysis

Titrated numbers (from 300 cells per well to 1 cell per well) of unsorted tumor cells or sorted cell subsets were seeded in 96-well flat-bottomed plates and cultured for 10 days. Colony formation was then assessed by light microscopy. Clonal frequencies and statistical significance were evaluated by extreme limiting dilution analysis (ELDA) [29].

Evaluation of ALDH-1 Activity

ALDH-1 activity was assessed by staining with the Aldefluor reagent system (StemCell Technologies, Vancouver, BC, Canada, http://www.stemcell.com) according to the manufacturer's specifications. Briefly, cells were incubated in Aldefluor assay buffer containing ALDH substrate (BODIPY [Invitrogen, Carlsbad, CA, http://www.invitrogen.com]-aminoacetaldehyde, 1 μM) for 30 minutes at 37°C, to allow the conversion of Aldefluor substrate. As a negative control, an aliquot of each sample was treated with the ALDH inhibitor diethylaminobenzaldehyde (DEAB) (15 μM). Cells were then counterstained with PE-labeled anti-CD133, anti-CD166, or anti-CD24 and APC-labeled anti-CD44 antibodies. PI (0.5 μg/ml) was added to the samples prior to analysis. Flow cytometric analysis was performed by using a dual laser BD FACSCalibur (BD Biosciences). Dead cells were excluded on the basis of PI incorporation.

Side Population Analysis

SP analysis was performed as described in [30]. Briefly, tumor cell suspensions were incubated in prewarmed culture medium containing Hoechst 33342 (5 μg/ml; Invitrogen) for 2 hours at 37°C. An aliquot of each sample was treated with verapamil (50 μM) (Sigma-Aldrich) for 10 minutes at room temperature, prior to the addition of Hoechst 33342. After incubation, tumor cells were

washed and counterstained with FITC-labeled CD24-specific antibodies, PE-labeled CD166- or CD133-specific antibodies, and APC-labeled CD44-specific antibodies. Prior to analysis, 7-aminoactinomycin D (7-AAD) (4 μg/ml; Invitrogen) was added. Samples were analyzed by using a BD Influx (BD Biosciences). Dead cells were excluded on the basis of 7-AAD incorporation. Verapamil-treated samples were used as negative controls.

Chemosensitivity Assay

Dose-response curves were initially defined on parental cell lines. CRC cells (5×10^3 well) were plated in 96-well plates and after 2 days of culture were exposed to titrated concentrations of 5-fluorouracil (5-FU) (Teva Pharma AG, Aesch, Switzerland, http://www.tevapharma.ch), oxaliplatin, or irinotecan (both from Sigma-Aldrich). After 3 days, percentages of viable cells were determined by the 3-(4,5-dimethylthiazol-2-yl)-2,5-diphenyltetrazolium (MTT) assay [31]. Low, intermediate, and high drug concentrations for each cell line were selected and used to assess the chemosensitivity of sorted cell subsets in comparison with parental cell lines, as described above.

Transplantation of Tumor Cells in Mice

In vivo experiments were approved by the Basel Cantonal Veterinary Office. NOD/SCID mice, initially obtained from Charles River Laboratories (Sulzfeld, Germany, http://www.criver.com), were bred and maintained under specific pathogen-free conditions in the animal facility of the Department of Biomedicine of the University of Basel. Eight- to 10-week-old mice were used for experiments.

Unsorted cells or sorted cell subsets were resuspended in a 1:1 mixture of phosphate-buffered saline and growth factor-reduced Matrigel matrix (BD Biosciences) and inoculated subcutaneously into the flank of recipient mice. Tumor development was monitored by palpation. Time to onset of a palpable tumor was recorded, and the tumor size was measured weekly by a dial caliper. Tumor volumes were calculated according to the formula (length $\times$ width^2)/2. Mice were sacrificed when tumors reached a maximum diameter of 10 mm.

Statistical Analysis

Statistical analysis was performed by one-way analysis of variance and two-tailed Student's *t* test as appropriate, using the GraphPad Prism 5 software (GraphPad Software, Inc., San Diego, CA, http://www.graphpad.com). *p* values $\leq$ .05 were considered significant.

Results

Expression of CSC Markers on CRC Cell Lines

A panel of 10 well-characterized human CRC cell lines, including 6 cell lines included in the NCI60 panel, was used for this study (supplemental online Table 1). In order to identify putative CSC populations, the expression of surface molecules previously reported as CSC markers in human primary CRCs, including CD133, CD44, CD166, and CD24 [6–9], was analyzed by flow cytometry. All the markers were found to be heterogeneously expressed in different cell lines (Fig. 1). CD133 was expressed at very high levels and on virtually all cells (>99%) of the CACO2 cell line,

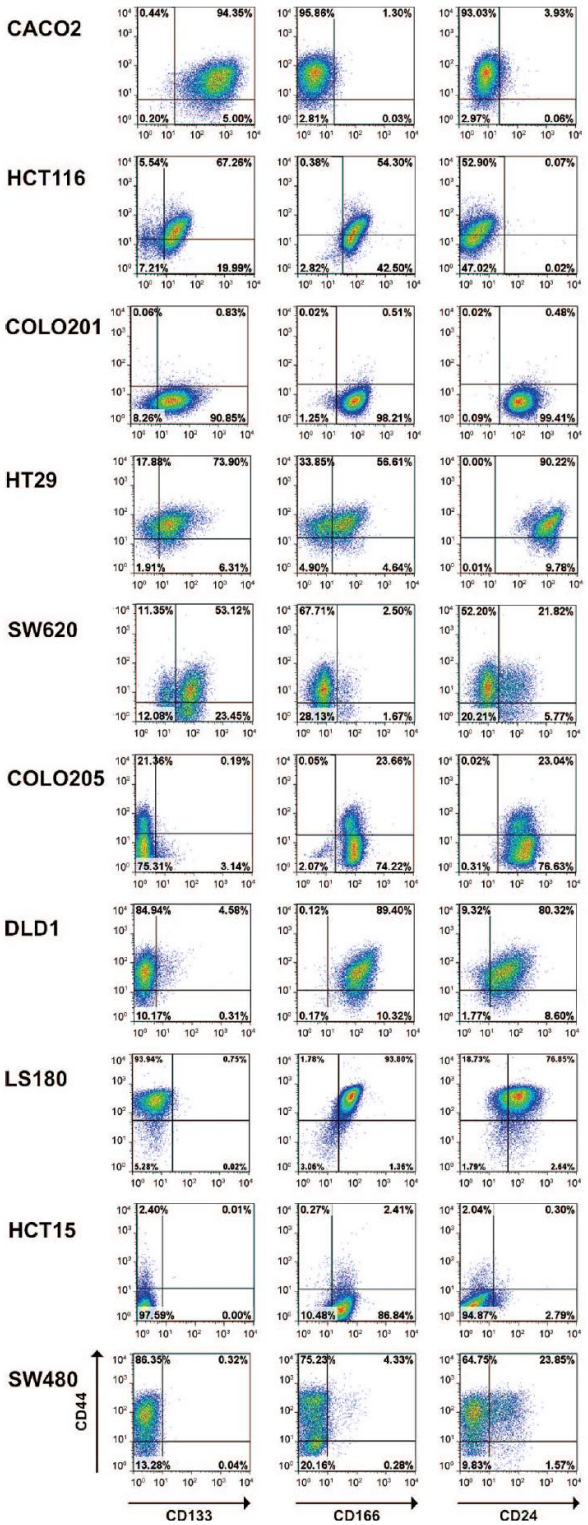

Figure 1. Cancer stem cell marker expression in human established colorectal cancer (CRC) cell lines. CRC cell lines were stained with fluorescein isothiocyanate-labeled anti-CD44, phycoerythrin-labeled anti-CD166 or anti-CD24, and allophycocyanin-labeled anti-CD133 antibodies and analyzed by flow cytometry. Dead cells were excluded on the basis of propidium iodide incorporation. Representative dot plots are shown.

whereas in the remaining cell lines it was expressed either by a majority of tumor cells (as on the HCT116, COLO201, HT29, and SW620 lines) or by a restricted cell subset (as on COLO205 and DLD1 cells). Finally, on three cell lines (LS180, HCT15, and SW480), it was not expressed at all. CD166 was expressed by a majority of cells in all cell lines, except for SW620 and SW480, where its expression was limited to a restricted cell subset, and CACO2 cells, which were completely negative. Most cell lines also expressed CD44 on a majority of cells. On the COLO205 and HCT15 cell lines, however, CD44 expression was present only on a minor cell fraction, and on COLO201 cells it was completely negative. Notably, in most cell lines (i.e., HCT116, HT29, COLO205, DLD1, LS180, and HCT15) CD166 and CD44 were coexpressed. Also, in the HCT116 and HT29 cell lines, coexpression of CD166, CD44, and CD133 molecules was detected in a majority of cells (data not shown).

Finally, CD24 was expressed on all cells in the COLO201, HT29, COLO205, DLD1, and LS180 cell lines, whereas it was only present on cell subsets in SW620, SW480, and HCT15. In contrast, CACO2 and HCT116 cells were completely negative. When present, CD24 was generally coexpressed with CD44, except for COLO201 cells.

Upon culture of cell lines in SF medium, a condition favoring preferential expansion of CSC subsets [7, 27] a slight increase in CD133 expression was detected on HT29 cells only, whereas no significant changes in CD166 expression were observed in any cell line (supplemental online Fig. 1). In contrast, CD44 expression was increased on COLO205, DLD1, and HCT15 cells, but it was decreased on SW620 and SW480 cells. Finally, CD24 was upregulated on SW620 and LS180 cells (supplemental online Fig. 1). In summary, all CRC cell lines analyzed included cells expressing putative CSC markers, although to different extents.

Correlation Between CSC Marker Expression and Spheroid Formation Ability

Next, we evaluated the correlation between CSC marker expression on CRC cell lines and functional CSC features. CSCs have been shown to display the ability to grow in spheroids, when cultured under low-adherence conditions [10, 32]. When spheroid formation ability was evaluated upon culture on polyHEMA-coated plasticware, no significant correlation with the expression of putative CSC markers was observed (Fig. 2). Indeed, spheroids were detected in cultures of CD133+ (HCT116 and HT29) as well as CD133− (DLD1 and HCT15) cell lines (Fig. 2A). LS180 cells, despite expressing both CD166 and CD44 markers at high levels, did not form spheroids, yet conversely, HCT15 cells, characterized by a limited expression of these markers, did. Spheroid formation also appeared to be independent from CD24 expression since cell lines largely positive for CD24 (e.g., COLO205) were not able to grow in spheroids, whereas cell lines negative for CD24 expression (i.e., HCT15 and HCT116) did grow in these conditions. Thus, expression of CD133, CD166/CD44, and CD24/CD44 does not correlate with spheroid formation ability. Moreover, the spheroid formation capacity of individual cell lines was not significantly modified upon culture of tumor cells in SF medium, except for COLO205 cells, which in SF medium were able to form aggregates (Fig. 2B).

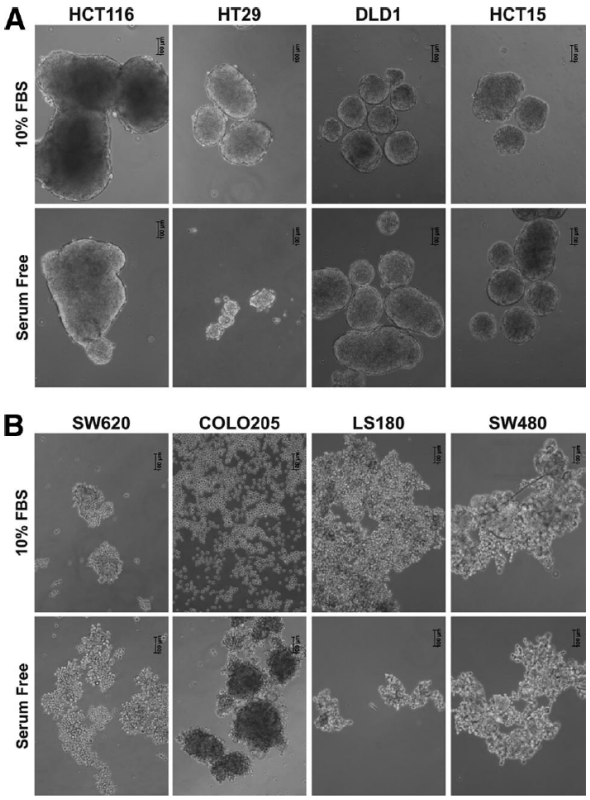

Figure 2. Spheroid formation ability of colorectal cancer (CRC) cell lines. CRC cell lines maintained in serum-containing or serum-free medium were cultured on poly-2-hydroxyethyl methacrylate-coated plates, and spheroid formation was evaluated after 7 days by microscopy. Pictures show one representative experiment out of five performed with similar results. Scale bars = 100 μm. Abbreviation: FBS, fetal bovine serum.

Clonogenicity of Tumor Cells Expressing Putative CSC Markers

We then analyzed the clonogenic potential of putative CSC populations derived from cell lines. CD133+, CD166+CD44+, or CD24+CD44+ cells were sorted by flow cytometry from individual cell lines (as depicted in supplemental online Fig. 2), and the frequencies of clonogenic cells within each subset were evaluated by limiting dilution analysis (Table 1). CD133+ cells isolated from HCT116 displayed in two of four experiments a slightly higher clonogenicity (up to twofold) as compared with their negative counterparts. When cultured in SF medium, CD133+ and CD133− HCT116 cells also exhibited comparable clonogenic capacity. Similarly, CD133+ cells from CACO2 and COLO205 exhibited equal or lower clonogenic capacity compared with CD133− cells.

When CD166+CD44+ and CD166−CD44− cells were compared, CD166+CD44+ cells from LS180 and COLO205, but not those from SW480, exhibited a higher frequency of clonogenic cells (an increase of greater than or equal to sevenfold) as compared with their negative counterparts. Higher clonogenicity of the CD166+CD44+ subset, as compared with its negative counterpart, was also observed upon culture of COLO205 cells in SF medium, although in the latter case frequencies of clonogenic cells were overall reduced in comparison with cultures performed in serum-containing medium. Finally, CD24+CD44+ and CD24−CD44+ cell subsets isolated from the LS180, SW620, and

Table 1. Clonogenicity of putative cancer stem cell (CSC) subsets sorted from colorectal cancer cell lines

Cell lines	CD133+	CD133−	Ratio
CACO-2			
Exp 1	1/64.5	1/69.8	1.01
Exp 2	1/87	1/113	1.29
Exp 3	1/53.9	1/23.1	0.43
HCT116			
Exp 1	1/7.58	1/11.71	1.54
Exp 2	1/5.46	1/5.23	0.95
Exp 3	1/3.17	1/6.58	2.07
Exp 4	1/3.83	1/3.84	1.00
Serum-free	1/5.81	1/5.64	0.97
COLO205			
Exp 1	1/3.06	1/3.96	1.29
Exp 2	1/2.12	1/2.96	1.39
Cell lines	**CD166+/CD44+**	**CD166−/CD44−**	**Ratio**
LS180			
Exp 1	1/61.1	1/866.4	14.2
Exp 2	1/39.7	1/595.3	15
Exp 3	1/54.6	1/517.7	9.5
SW480			
Exp 1	1/22.7	1/19	0.83
Exp 2	1/13	1/8.23	0.63
COLO205			
Exp 1	1/3.85	1/28.7	7.45
Serum-free	1/14.3	1/133.2	9.31
Cell lines	**CD24+/CD44+**	**CD24−/CD44+**	**Ratio**
LS180			
Exp 1	1/63.5	1/55	0.87
Exp 2	1/48.2	1/41.8	0.87
Serum-free	1/176	1/157	0.89
SW620			
Exp 1	1/2.6	1/1.9	0.73
Exp 2	1/2.41	1/3.02	1.25
Serum-free	1/3.59	1/2.06	0.57
DLD1			
Exp 1	1/58.3	1/35.1	0.60
Serum-free	1/19.3	1/9.46	0.49

CSC subsets were sorted from the indicated cell lines, and frequencies of clonogenic cells were estimated by limiting dilution assay.
Abbreviation: Exp, experiment.

DLD1 cell lines showed comparable clonogenicity in serum-containing medium and in SF medium. Therefore, expression of CSC markers does not appear to be strictly associated with a high clonogenicity of tumor cells.

ALDH-1 Activity of Putative CSC Populations in CRC Cell Lines

Normal stem cells, as well as CSCs, have been reported to express high levels of ALDH-1 enzyme [13, 33]. ALDH-1 activity was therefore evaluated on CRC cell lines in combination with the expression of putative CSC markers. Following Aldefluor staining, in all cell lines a large fraction of Aldefluor+ cells was detected (Fig. 3A), whose specificity was confirmed by treatment with the ALDH-1 inhibitor DEAB (supplemental online Fig. 3A). Overall, the percentages of Aldefluor+ cells did not correlate with the frequencies of tumor cells expressing CSC markers (data not shown). We then evaluated ALDH-1 activity within specific CSC subsets. Frequencies of Aldefluor+ cells within CD133+ or CD24+CD44+ cells were found to be comparable to those observed within their negative counterparts or parental cell lines (Fig. 3B; data not shown). In contrast, in the LS180 cell line, CD166+CD44+ cells were found to preferentially include Aldefluor+ cells as compared with the CD166−CD44− subset. The association between ALDH-1 activity and CD166/CD44 coexpression, however, was not present in other cell lines, including SW480, SW620, and COLO205 (Fig. 3B; data not shown). We also conversely evaluated the expression of CSC markers within Aldefluor+ fractions, as compared with Aldefluor− or unsorted cells, and we did not observe major differences (supplemental online Fig. 3B; data not shown). These findings indicate that in established CRC cell lines ALDH-1 activity is not limited to cells expressing putative CSC markers but is detectable throughout the entire tumor cell population.

SP Phenotype in CRC Cells Expressing CSC Markers

An additional feature of CSCs is represented by their ability to actively extrude the DNA-binding dye Hoechst 33342 through specific drug transporters, thus acquiring the so-called SP phenotype [14–16]. We tested whether putative CSC subsets preferentially display an SP phenotype. Upon incubation with Hoechst 33342, an SP was detected in all CRC cell lines, with the exception of SW620 (Fig. 4A). However, no significant correlation with the CSC marker expression was observed. Indeed, percentages of SP fractions were not increased within CD133+ or CD166+CD44+ cells as compared with their negative counterparts or with their parental cell lines (Fig. 4B). Accordingly, no preferential expression of CD133 or coexpression of CD166 and CD44 was found within SP as compared with non-side population (non-SP) subsets or with parental cell lines (supplemental online Fig. 4B). In contrast, CD24+CD44+ cells from the SW480 cell line, but not those from the LS180 or DLD1 cell line, displayed higher frequencies of SP cells as compared with CD24−CD44+ cells and with the unsorted SW480 cell line. Consistently, enriched expression of CD24/CD44 molecules was detected in SP in comparison with non-SP SW480 cells (supplemental online Fig. 4B).

Chemosensitivity of Putative CSC Populations in CRC Cell Lines

CSCs from primary tumors have been shown to display a high resistance to chemotherapeutic treatments [34–36]. We evaluated the sensitivity of putative CSC populations, derived from CRC cell lines, to chemotherapeutic drugs currently in use for CRC treatment, including 5-FU, oxaliplatin, and irinotecan. Different cell subsets sorted from individual cell lines were exposed to low, intermediate, and high drug concentrations, selected on the basis of dose-response curves of parental cell lines (see Materials and Methods). CD133+ cells from the HCT116 cell line displayed a significantly increased survival upon treatment with irinotecan, but not with 5-FU or oxaliplatin, in comparison with both CD133− and parental cells ($p < .05$; Fig. 5A). Instead, CD133+ cells sorted from the HT29 line exhibited slightly higher survival than CD133− cells in response to oxaliplatin ($p < .05$), whereas their sensitivity to 5-FU and irinotecan was comparable to that of their negative counterpart or the parental cell line (Fig. 5B).

CD166+CD44+ cells from the LS180 cell line displayed comparable sensitivity to 5-FU but reduced survival in response to both oxaliplatin and irinotecan as compared with CD166−CD44− cells and with parental cells ($p \leq .05$; Fig. 5C). CD166+CD44+ cells from the SW620 cell line showed slightly higher resistance to oxaliplatin as compared with parental cells ($p = .05$) but not with their negative counterpart, whereas in response to 5-FU and irinotecan they showed comparable or lower survival compared with the other populations tested (Fig. 5D).

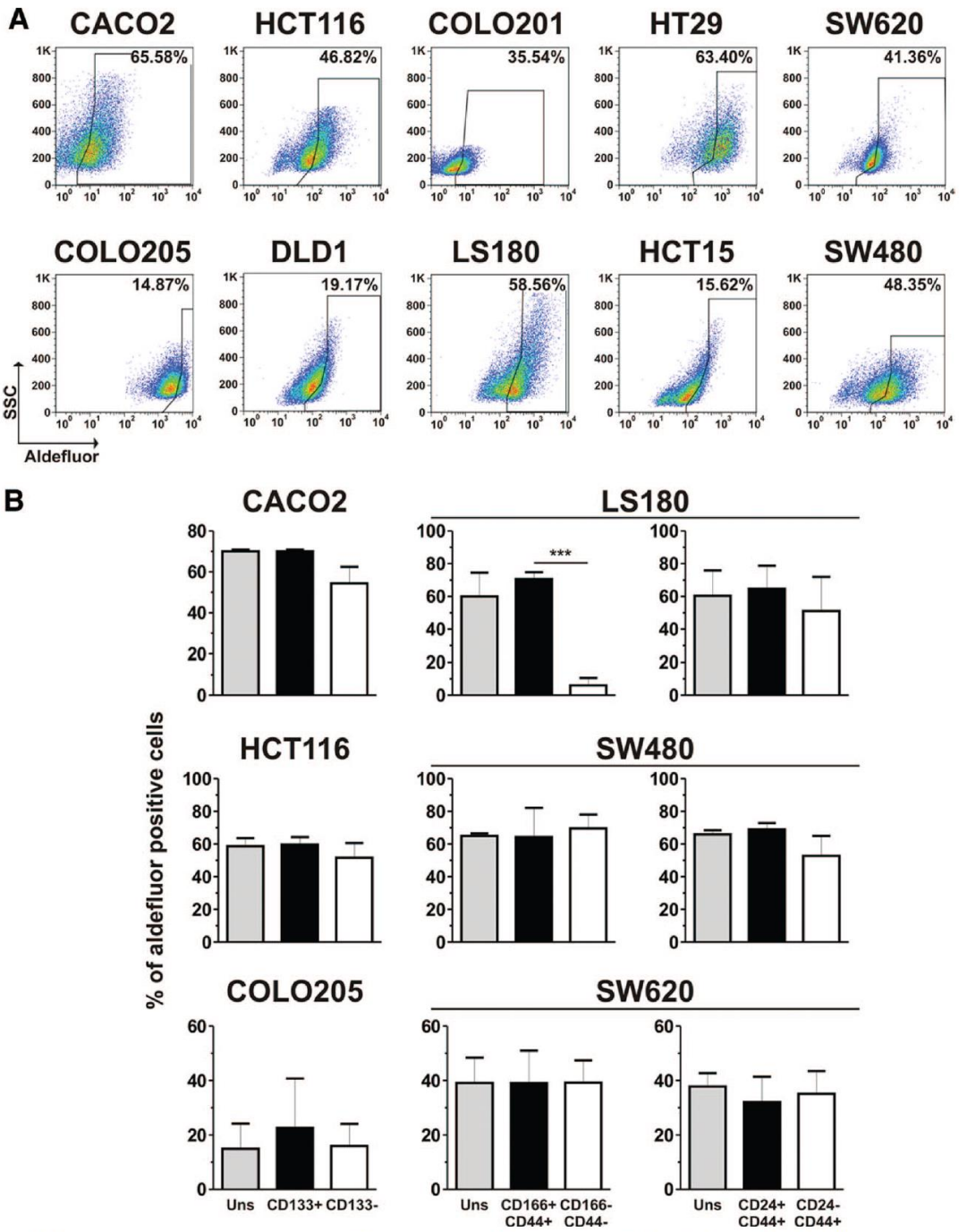

Figure 3. ALDH-1 activity on putative cancer stem cell populations in colorectal cancer (CRC) cell lines. **(A):** CRC cell lines were stained with the Aldefluor reagent system. Aldefluor+ cells were gated relative to samples stained in the presence of the Aldefluor inhibitor diethylaminobenzaldehyde (supplemental online Fig. 2A). **(B):** Aldefluor-stained CRC cells were counterstained with CD133-, CD166-, CD44-, and CD24-specific antibodies. Percentages of Aldefluor+ cells within unsorted cell lines; gated CD133+, CD166+CD44+, or CD24+CD44+ subsets; and their negative counterparts were assessed. Means ± SD from triplicates of two independent experiments are reported. ***, $p \leq .005$. Abbreviations: SSC, side scatter; Uns, unsorted.

Finally, CD24+CD44+ cells from the SW480 cell line displayed significantly higher survival in comparison with unsorted cells in response to 5-FU ($p < .01$) and with both unsorted and CD24−CD44+ cells in response to oxaliplatin ($p < .05$). Furthermore, they showed a trend toward higher resistance in response to irinotecan (Fig. 5E). CD24+CD44+ cells from the SW620 line, however, exhibited a comparable or higher sensitivity compared with unsorted or CD24−CD44+ cells to all drugs tested (Fig. 5F). Thus, putative CSC populations did not consistently show higher survival rate upon treatment with anti-CRC chemotherapeutic drugs.

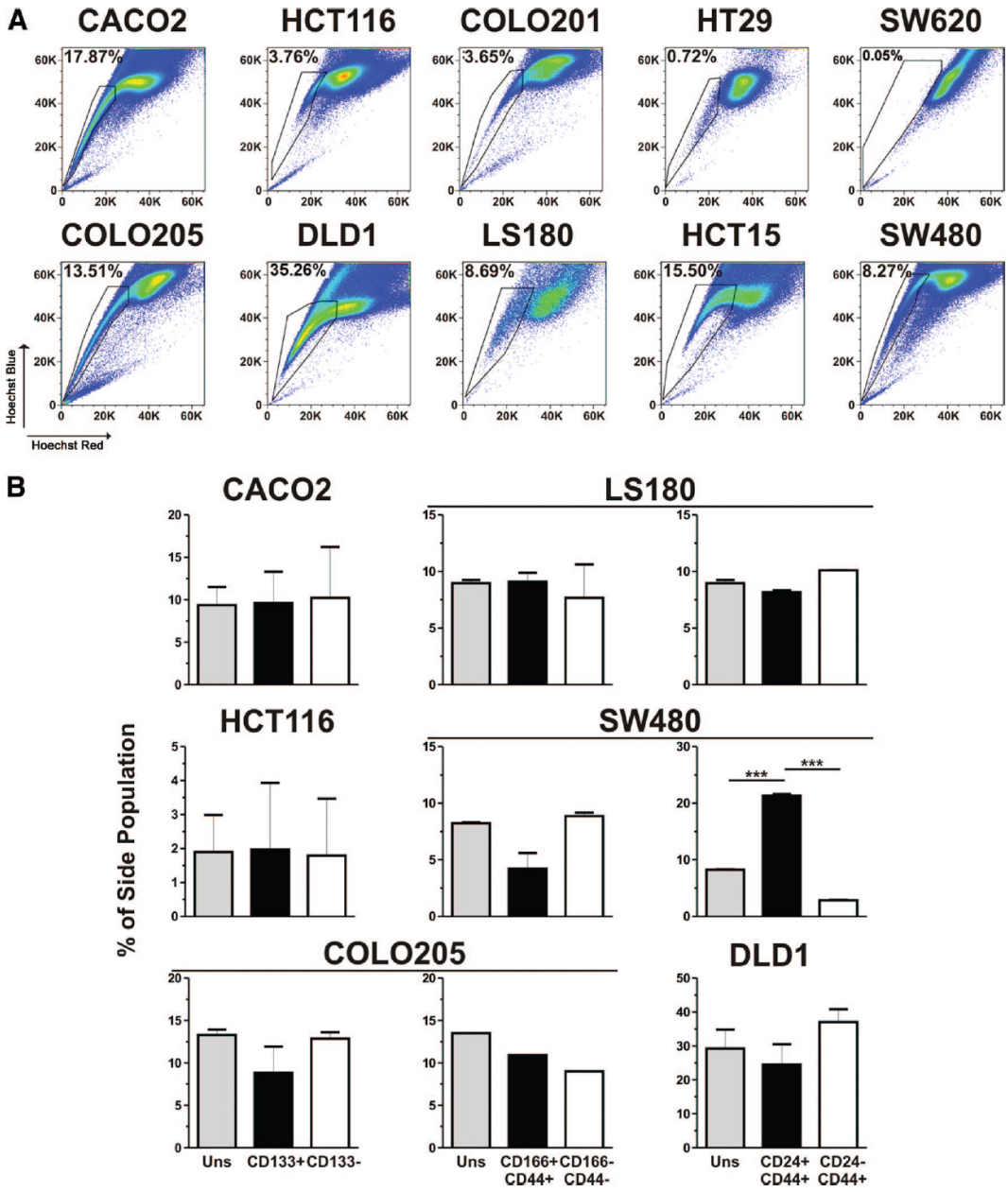

Figure 4. Side population phenotype versus cancer stem cell marker expression in colorectal cancer (CRC) cell lines. **(A):** CRC cell lines were stained with Hoechst 33342, and percentages of side population (SP) were evaluated in comparison with cells stained in the presence of verapamil (supplemental online Fig. 3A). **(B):** Hoechst-stained cells were counterstained with CD133-, CD166-, CD44-, and CD24-specific antibodies. Percentages of SP within unsorted cell lines; gated CD133+, CD166+CD44+, or CD24+CD44+ subsets; and their negative counterparts were assessed. Means ± SD from triplicates of two independent experiments are reported. ***, $p \leq .005$. Abbreviation: Uns, unsorted.

Tumor Initiating Capacity of CRC Cell Subsets Expressing Putative CSC Markers

Putative CSC subsets were finally evaluated for tumor formation capacity in immunodeficient mice. Titrated numbers of (a) CD133+ or CD133− cells, sorted from the CACO2, HCT116, and COLO205 cell lines; (b) CD44+CD166+ cells or their double-negative counterparts, sorted from the LS180, SW480, and COLO205 cell lines; and (c) CD24+CD44+ and CD24−CD44+ cells from LS180 cells were injected subcutaneously into NOD/SCID mice, and tumor development was monitored over time. No major differences in tumorigenicity between tumor cells expressing CSC markers and their negative counterparts or the unsorted parental cell lines were observed when cell lines were cultured in either serum-containing medium or in SF medium (Table 2). The growth kinetics of developing tumors from different cell subsets was also found to be comparable in most of cell line tested (supplemental online Fig. 5). Only CD166+CD44+ cells isolated from the LS180 displayed accelerated tumor development as compared with CD166−CD44− cells. Thus, CRC cells expressing putative CSC markers did not show preferential tumor initiating capacity in immunodeficient mice.

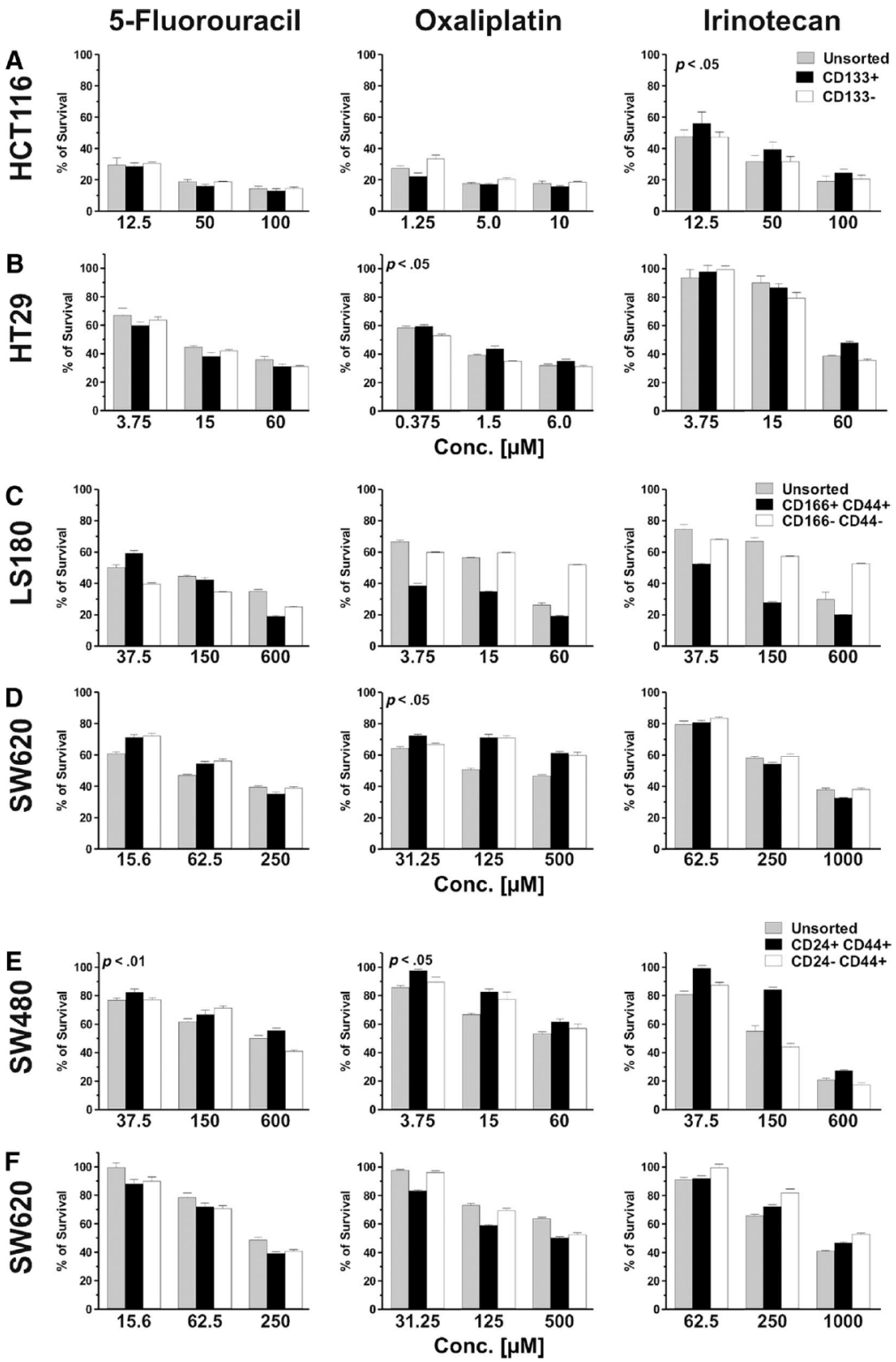

Figure 5. Drug sensitivity of colorectal cancer cell line-derived putative cancer stem cell (CSC) populations. CD133+, CD166+CD44+, and CD24+CD44+ or their negative counterparts were sorted from the indicated cell lines and cultured in the presence of the indicated concentrations of 5-fluorouracil, oxaliplatin, or irinotecan. After 72 hours, cell viability was evaluated by 3-(4,5-dimethylthiazol-2-yl)-2,5-diphenyltetrazolium (MTT) staining. Percentages (averages ± SD of quadruplicate cultures) of surviving cells are reported. Statistical evaluation was performed by two-tailed Student's *t* test. Only significantly increased percentages of survival ($p \leq .05$) of putative CSCs relative to negative counterparts or parental cells are indicated. Reported data refer to one representative experiment out of two performed with similar results. Abbreviation: Conc, concentration.

Table 2. Tumor formation capacity of putative of cancer stem cell (CSC) subsets in colorectal cancer cell lines

Cell lines	Subsets	Number of cells injected						Tumor incidence, total
		10^6	10^5	10^4	5×10^3	10^3	10^2	
CACO2								
10% FBS	Unsorted			3/3	2/3	2/3		7/9
	CD133+				6/6	6/8		12/14
	CD133−				5/5	6/8		11/13
HCT116								
10% FBS	Unsorted	2/3	2/3	3/3				7/9
	CD133+			3/3	2/3	4/6		9/12
	CD133−			2/3	1/3	5/6		7/12
SF medium	Unsorted				4/4			4/4
	CD133+				4/4	4/4		8/8
	CD133−				3/4	4/4		7/8
COLO205								
10% FBS	Unsorted	3/3	3/3	3/3				9/9
	CD133+			3/3	3/3	3/3		9/9
	CD133−			2/3	3/3	3/3		8/9
LS180								
10% FBS	Unsorted	6/6	6/6	8/8		3/3		23/23
	CD166+/CD44+			8/8	6/6	4/6		18/20
	CD166−/CD44−			8/8	5/6	4/6		17/20
SW480								
10% FBS	Unsorted		1/2	1/7		0/3	0/3	2/15
	CD166+/CD44+					2/7	0/7	2/14
	CD166−/CD44−				2/2	4/6	1/8	7/16
COLO205								
10% FBS	Unsorted					3/3	2/4	5/7
	CD166+/CD44+					4/4	4/4	8/8
	CD166−/CD44−					4/4	2/4	6/8
SF medium	Unsorted					3/3	4/4	7/7
	CD166+/CD44+					3/3	4/4	7/7
	CD166−/CD44−					4/4	2/4	6/8
LS180								
10% FBS	Unsorted					3/3	3/3	6/6
	CD24+/CD44+					3/3	3/3	6/6
	CD24−/CD44+					3/3	2/3	5/6
SF medium	Unsorted	n.t.	n.t.	n.t.	n.t.	n.t.	n.t.	
	CD24+/CD44+						4/4	4/4
	CD24−/CD44+						3/4	3/4

Titrated numbers of CSCs or parental tumor cells were injected subcutaneously in NOD/SCID mice, and tumor development was monitored over time.
Abbreviations: FBS, fetal bovine serum; n.t., not tested; SF, serum-free.

Discussion

Increasing evidence in favor of the existence, within primary tumors, of CSC populations capable of surviving conventional chemotherapies urges the development of novel CSC-targeted treatments. Screening of new anticancer compounds is conventionally conducted on established tumor cell lines, providing sufficient material for high-throughput studies [18, 26]. However, whether tumor cell lines might comprise CSC populations resembling those of primary tumors remains highly debated.

Here, we have evaluated the expression of surface molecules previously reported as CSC markers in human CRC, including CD133, CD166, CD44, and CD24, on a panel of CRC established cell lines, and we have analyzed their correlation with stem cell-like functional features. Whereas cell subsets expressing CSC markers were largely represented in all cell lines, no consistent correlation between expression of any of the putative CSC phenotypes and stem cell-like features was found. Cells expressing either CD133, CD166/CD44, or CD24/CD44 molecules did not preferentially exhibit CSC properties, such as spheroid formation ability, clonogenicity, high ALDH-1 activity, SP phenotype, tumorigenicity, and chemoresistance, as compared with their negative counterparts or parental cell lines. Thus, in human established CRC cell lines, CD133+, CD166+CD44+, and CD24+CD44+ phenotypes do not reliably identify CSC populations.

Recently, several groups have provided experimental evidence in favor of the existence of CSCs in human CRC. It was initially shown that tumor cells from primary CRC were not all endowed with comparable tumorigenicity, but only those expressing CD133 molecules exhibited cancer initiating capacity upon xenografting in immunodeficient mice [2, 6]. The existence of a hierarchical organization within CRC tissues has been subsequently confirmed by other groups, although the expression of CD44 and the coexpression of CD166/CD44 molecules, as well as ALDH-1 activity, have been proposed as alternative CSC phenotypes [8, 33, 37, 38].

In contrast, the existence of CSC populations, identifiable by specific phenotypes in established CRC cell lines, has not been convincingly demonstrated so far. The expression of putative CSC markers on CRC cells from established cell lines has been investigated in previous work, but contradictory findings have been reported. Expression of CD133 in several established CRC cell lines has been reported, and its presence has been shown to correlate with high clonogenicity and increased tumorigenicity, although in the latter case, CD133+ or CD133− cells from a single cell line (HT29) were tested in a limited number of recipients ($n = 5$ per subset) [23]. In another study, CD24+CD44+ cells from one cell line (SW1222), cultured in three-dimensional (3D) structures, were shown to be characterized by higher clonogenicity and tumorigenicity than CD24−CD44− cells [9]. This

finding, however, did not apply to other cell lines tested [9]. In addition, the relevance of CD44 expression, in the absence of CD24, was not fully evaluated. Kai et al. reported an association between CD44 expression and high clonogenicity in one CRC cell line [39]. However, no preferential tumorigenicity by CD44+ as compared with CD44− cells was observed [39].

More recently, expression of several CSC markers, including CD133, CD166, CD44, CD24, and ALDH-1, was extensively analyzed in the entire NCI60 panel, including seven CRC cell lines, but no correlation between these markers and clonogenicity and/or tumorigenicity was observed [40]. In this study, however, stem cell-like features of tumor cells have been evaluated in parental cell lines only. No analysis on sorted putative CSC subsets from individual cell lines in comparison with their negative counterparts was conducted. Importantly, the chemosensitivity of putative CSC populations was not tested.

Here, we have performed a systematic assessment of the major putative CSC phenotypes reported in human CRC, including the expression of CD133 and the coexpression of CD166 and CD44 or of CD24 and CD44, on a panel of 10 established cell lines, 6 of which were included in the NCI60 panel. In accordance with previous findings, we found that all putative CSC markers were expressed in CRC cell lines, although their distribution largely varied between different cell lines. On parental cell lines, none of the markers was found to correlate with spheroid formation ability. Furthermore, upon sorting of specific cell subsets, CD133+ and CD133− cells isolated from three different cell lines consistently exhibited comparable clonogenicity, tumorigenicity, and chemosensitivity. In contrast, CD166+CD44+ cells from the LS180 cell line showed higher clonogenicity and accelerated tumor development as compared with CD166−CD44− cells. This association however, was not present when CD166+CD44+ and CD166−CD44− cells from SW480 and SW620 were tested. Thus, the correlation between CD166/CD44 coexpression and high clonogenicity or tumorigenicity appears to be unique to the LS180 cell line. Furthermore, CD166/CD44 expression did not correlate with high chemoresistance, since CD166+CD44+ cells from the LS180 cell line displayed a comparable or higher sensitivity to the drugs tested compared with their negative counterparts.

Similarly, coexpression of CD24 and CD44 molecules was ineffective in discriminating tumor cells endowed with stemness-related properties. Indeed, CD24-expressing cells demonstrated neither higher clonogenicity nor higher tumorigenicity. Alternatively, upon evaluation of chemosensitivity, CD24+CD44+ cells from SW480, but not those from SW620, displayed a higher survival rate than their CD24−CD44+ counterparts.

Flow cytometry-based analysis of CSC markers in combination with additional putative CSC phenotypes, such as ALDH-1 activity and SP phenotype, did not reveal differences between CSC marker-expressing or nonexpressing cells. Notably, ALDH-1 activity was found in a majority of CRC cells, in contrast to what has been reported for primary CRCs, where ALDH-1 activity was found in a limited subset of cells [8, 33]. SPs were detected in all cell lines except SW620, but no consistent enrichment within the tumor cells expressing putative CSC markers was observed. This is in accordance with previous reports indicating that SPs in CRC cell lines are not enriched in CSCs [41, 42]. Within SW480 cells, however, SP phenotype was associated with CD24/CD44 expression. Interestingly, CD24+CD44+ SW480 cells displayed enhanced resistance to all drugs tested, suggesting that the expression of specific molecular pumps on these cells might contribute to surviving chemotherapy. The association between SP and CD24/CD44 expression was not confirmed, however, in the SW620 cell line, where no SP was detected despite the presence of a large fraction of CD24+CD44+ cells. Taken together, our results demonstrate that in contrast to human primary tumors, in CRC established cell lines, CD133, CD166/CD44, and CD24/CD44 expression correlates with CSC properties sporadically and in a cell line-specific manner but does not reliably identify CSC populations.

Several factors might account for the discrepancy observed between primary tumors and established CRC cell lines. One possibility is that CSCs potentially comprised within established cell lines express markers that differ from those expressed by CSCs in vivo. Indeed, the expression of surface molecules, and in particular of adhesion molecules such as CD44, CD166, and CD24, is tightly modulated by signals derived from the microenvironment, such as interactions with extracellular matrix components and/or surrounding cells [40, 43], which may be missing in conventional in vitro cultures.

Also, the absence of a three-dimensional architecture in conventional monolayers may, per se, account for different surface molecule expression profiles. Patterns of surface marker expression in tumor cell lines expanded in two dimensions have been shown to differ from those of corresponding cell lines grown in three dimensions [40].

Conversely, a variety of factors related to in vitro cultures, including high proliferation rates [44], occult infections [45], high cell density, and medium compositions [25] (M.G. Muraro, unpublished observations), may contribute to altering putative CSC marker expression levels. Serum-containing media, in particular, have been shown to inhibit expression of CSC markers, including CD133, on CRC cells [7]. Indeed, upon culture of cell lines in SF medium we observed modifications in the expression levels of CD133, CD44, and CD24 molecules (supplemental online Fig. 1). Also under these culture conditions, however, no consistent correlation between expression of CSC markers and stem cell-like properties was observed, indicating that the unreliability of the proposed CSC phenotypes in established cell lines is not merely related to the presence of serum in culture media.

The identification of more reliable markers would therefore be desirable for the detection of CSCs in cell lines. Recently, in a mouse model of intestinal adenomas, crypt stem cells, expressing the Wnt target gene *Lrg5*, have been shown to be uniquely endowed with tumor initiating capacity [46]. Consistently, in primary CRC and established cell lines, high Wnt signaling activity, revealed by a fluorescent-reporter assay, has been found to mark tumor cells with high clonogenic and tumorigenic capacities [43]. The use of this type of reporter assay might prove helpful in identifying CSC populations in cell lines for drug screenings.

Alternatively, because of adaptation to in vitro culture conditions, established cell lines may have lost the hierarchical structure typical of primary tumors. Some observations suggest that in defined CRC cell lines, all tumor cells appear to possess an equal capacity to generate xenografts in immunodeficient mice, thus conforming to a stochastic model rather than a CSC model [39, 47]. Importantly, it has recently been demonstrated that stemness of CRC cells is largely regulated by extrinsic factors derived by tumor-associated myofibroblasts [43]. Thus, monocultures of established cell lines may fail to reproduce the CSC

model observed in primary CRC because of the lack of cross-talk between cancer and stromal cells. The establishment of improved culture systems integrating 3D structures and stromal cell components is therefore required for the development of novel drug screening systems.

Conclusion

By performing a comprehensive analysis of putative CSC markers on established CRC cell lines, we demonstrated that in contrast to primary tumors, in cell lines the expression of CD133, CD166/CD44, and CD24/CD44 does not reliably identify CSC populations. Our findings reveal an inadequacy of conventional cultures of tumor cell lines for the screening of CSC-specific therapies and underline the urgency of developing novel platforms for anticancer drug discovery.

Acknowledgments

We thank Verena Jäggin, Emmanuel Traunecker, and Toni Krebs for excellent technical assistance with the flow cytometry-based analysis. We also thank Dr. B. Kvinlaug and C. Le Magnen for helpful discussion and critical revision of the manuscript and Dr. C. Mengus for advice regarding statistical analysis. This work was supported by Kommission für Technologie und Innovation (10761), the Swiss National Science Foundation (PMPD33-118653, PP00P3-133699, 31003A-122235, and 310030-127490), and Freiwillige Akademische Gesellschaft.

Author Contributions

M.G.M.: conception and design, collection and assembly of data, data analysis and interpretation, manuscript writing, final approval of manuscript; V.M., S.D., and J.H.: collection and assembly of data, data analysis and interpretation, final approval of manuscript; M.H.: conception and design, data analysis and interpretation, financial support, final approval of manuscript; G.C.S.: conception and design, data analysis and interpretation, obtaining funding, final approval of manuscript; G.I.: conception and design, collection and assembly of data, data analysis and interpretation, obtaining funding, manuscript writing, final approval of manuscript, study supervision.

Disclosure of Potential Conflicts of Interest

The authors indicate no potential conflicts of interest.

References

1 Polyak K, Hahn WC. Roots and stems: Stem cells in cancer. Nat Med 2006;12:296–300.
2 Reya T, Morrison SJ, Clarke MF et al. Stem cells, cancer, and cancer stem cells. Nature 2001;414:105–111.
3 Clevers H. The cancer stem cell: Premises, promises and challenges. Nat Med 2011;17:313–319.
4 Dalerba P, Cho RW, Clarke MF. Cancer stem cells: Models and concepts. Annu Rev Med 2007;58:267–284.
5 Gires O. Lessons from common markers of tumor-initiating cells in solid cancers. Cell Mol Life Sci 2011;68:4009–4022.
6 O'Brien CA, Pollett A, Gallinger S et al. A human colon cancer cell capable of initiating tumour growth in immunodeficient mice. Nature 2007;445:106–110.
7 Ricci-Vitiani L, Lombardi DG, Pilozzi E et al. Identification and expansion of human colon-cancer-initiating cells. Nature 2007;445:111–115.
8 Dalerba P, Dylla SJ, Park IK et al. Phenotypic characterization of human colorectal cancer stem cells. Proc Natl Acad Sci USA 2007;104:10158–10163.
9 Yeung TM, Gandhi SC, Wilding JL et al. Cancer stem cells from colorectal cancer-derived cell lines. Proc Natl Acad Sci USA 2010;107:3722–3727.
10 Visvader JE, Lindeman GJ. Cancer stem cells in solid tumours: Accumulating evidence and unresolved questions. Nat Rev Cancer 2008;8:755–768.
11 Zhang M, Behbod F, Atkinson RL et al. Identification of tumor-initiating cells in a p53-null mouse model of breast cancer. Cancer Res 2008;68:4674–4682.
12 Bao S, Wu Q, McLendon RE et al. Glioma stem cells promote radioresistance by preferential activation of the DNA damage response. Nature 2006;444:756–760.
13 Ginestier C, Hur MH, Charafe-Jauffret E et al. ALDH1 is a marker of normal and malignant human mammary stem cells and a predictor of poor clinical outcome. Cell Stem Cell 2007;1:555–567.
14 Bleau AM, Hambardzumyan D, Ozawa T et al. PTEN/PI3K/Akt pathway regulates the side population phenotype and ABCG2 activity in glioma tumor stem-like cells. Cell Stem Cell 2009;4:226–235.
15 Hirschmann-Jax C, Foster AE, Wulf GG et al. A distinct "side population" of cells with high drug efflux capacity in human tumor cells. Proc Natl Acad Sci USA 2004;101:14228–14233.
16 Patrawala L, Calhoun T, Schneider-Broussard R et al. Side population is enriched in tumorigenic, stem-like cancer cells, whereas ABCG2+ and ABCG2− cancer cells are similarly tumorigenic. Cancer Res 2005;65:6207–6219.
17 Shoemaker RH. The NCI60 human tumour cell line anticancer drug screen. Nat Rev Cancer 2006;6:813–823.
18 Zhou BB, Zhang H, Damelin M et al. Tumour-initiating cells: Challenges and opportunities for anticancer drug discovery. Nat Rev Drug Discov 2009;8:806–823.
19 Fillmore CM, Kuperwasser C. Human breast cancer cell lines contain stem-like cells that self-renew, give rise to phenotypically diverse progeny and survive chemotherapy. Breast Cancer Res 2008;10:R25.
20 Charafe-Jauffret E, Ginestier C, Iovino F et al. Breast cancer cell lines contain functional cancer stem cells with metastatic capacity and a distinct molecular signature. Cancer Res 2009;69:1302–1313.
21 Kondo T, Setoguchi T, Taga T. Persistence of a small subpopulation of cancer stem-like cells in the C6 glioma cell line. Proc Natl Acad Sci USA 2004;101:781–786.
22 Hermann PC, Huber SL, Herrler T et al. Distinct populations of cancer stem cells determine tumor growth and metastatic activity in human pancreatic cancer. Cell Stem Cell 2007;1:313–323.
23 Ieta K, Tanaka F, Haraguchi N et al. Biological and genetic characteristics of tumor-initiating cells in colon cancer. Ann Surg Oncol 2008;15:638–648.
24 Sandberg R, Ernberg I. Assessment of tumor characteristic gene expression in cell lines using a tissue similarity index (TSI). Proc Natl Acad Sci USA 2005;102:2052–2057.
25 van Staveren WC, Solis DY, Hebrant A et al. Human cancer cell lines: Experimental models for cancer cells in situ? For cancer stem cells? Biochim Biophys Acta 2009;1795:92–103.
26 Gupta PB, Onder TT, Jiang G et al. Identification of selective inhibitors of cancer stem cells by high-throughput screening. Cell 2009;138:645–659.
27 Kreso A, O'Brien CA. Colon cancer stem cells. Curr Protoc Stem Cell Biol 2008;Chapter 3:Unit 3.1.
28 Ghosh S, Spagnoli GC, Martin I et al. Three-dimensional culture of melanoma cells profoundly affects gene expression profile: A high density oligonucleotide array study. J Cell Physiol 2005;204:522–531.
29 Hu Y, Smyth GK. ELDA: Extreme limiting dilution analysis for comparing depleted and enriched populations in stem cell and other assays. J Immunol Methods 2009;347:70–78.
30 Goodell MA, Brose K, Paradis G et al. Isolation and functional properties of murine hematopoietic stem cells that are replicating in vivo. J Exp Med 1996;183:1797–1806.
31 Scudiero DA, Shoemaker RH, Paull KD et al. Evaluation of a soluble tetrazolium/

formazan assay for cell growth and drug sensitivity in culture using human and other tumor cell lines. Cancer Res 1988;48:4827–4833.

32 Reynolds BA, Rietze RL. Neural stem cells and neurospheres—re-evaluating the relationship. Nat Methods 2005;2:333–336.

33 Huang EH, Hynes MJ, Zhang T et al. Aldehyde dehydrogenase 1 is a marker for normal and malignant human colonic stem cells (SC) and tracks SC overpopulation during colon tumorigenesis. Cancer Res 2009;69:3382–3389.

34 Dylla SJ, Beviglia L, Park IK et al. Colorectal cancer stem cells are enriched in xenogeneic tumors following chemotherapy. PLoS One 2008;3:e2428.

35 Todaro M, Alea MP, Di Stefano AB et al. Colon cancer stem cells dictate tumor growth and resist cell death by production of interleukin-4. Cell Stem Cell 2007;1:389–402.

36 Li X, Lewis MT, Huang J et al. Intrinsic resistance of tumorigenic breast cancer cells to chemotherapy. J Natl Cancer Inst 2008;100:672–679.

37 Chu P, Clanton DJ, Snipas TS et al. Characterization of a subpopulation of colon cancer cells with stem cell-like properties. Int J Cancer 2009;124:1312–1321.

38 Du L, Wang H, He L et al. CD44 is of functional importance for colorectal cancer stem cells. Clin Cancer Res 2008;14:6751–6760.

39 Kai K, Nagano O, Sugihara E et al. Maintenance of HCT116 colon cancer cell line conforms to a stochastic model but not a cancer stem cell model. Cancer Sci 2009;100:2275–2282.

40 Stuelten C, Mertins S, Busch J et al. Complex display of putative tumor stem cell markers in the NCI60 tumor cell line panel. Stem Cells 2010;28:649–660.

41 Haraguchi N, Utsunomiya T, Inoue H et al. Characterization of a side population of cancer cells from human gastrointestinal system. Stem Cells 2006;24:506–513.

42 Burkert J, Otto WR, Wright NA. Side populations of gastrointestinal cancers are not enriched in stem cells. J Pathol 2008;214:564–573.

43 Vermeulen L, De Sousa E Melo, van der HM et al. Wnt activity defines colon cancer stem cells and is regulated by the microenvironment. Nat Cell Biol 2010;12:468–476.

44 Jaksch M, Munera J, Bajpai R et al. Cell cycle-dependent variation of a CD133 epitope in human embryonic stem cell, colon cancer, and melanoma cell lines. Cancer Res 2008;68:7882–7886.

45 Mariotti E, Gemei M, Mirabelli P et al. The percentage of CD133+ cells in human colorectal cancer cell lines is influenced by *Mycoplasma hyorhinis* infection 4. BMC Cancer 2010;10:120.

46 Barker N, Ridgway RA, van Es JH et al. Crypt stem cells as the cells-of-origin of intestinal cancer. Nature 2009;457:608–611.

47 Dittfeld C, Dietrich A, Peickert S et al. CD133 expression is not selective for tumor-initiating or radioresistant cell populations in the CRC cell line HCT-116. Radiother Oncol 2010;94:375–383.

See www.StemCellsTM.com for supporting information available online.

Supplementary Table 1: Characteristics of human CRC cell lines used in the study.

Name	CACO2	HCT116	COLO201	HT29	SW620	COLO205	DLD1	LS180	HCT15	SW480
ATCC #	HTB-37	CCL-247	CCL-224	HTB-38	CCL-227	CCL-222	CCL-221	CL-187	CCL-225	CCL-228
Morphology	Epithelial	Epithelial	Bipolar, slightly refractile, fibroblast-like cell	Epithelial	Epithelial	Epithelial	Epithelial	Epithelial	Epithelial	Epithelial
Growth Properties	Adherent	Adherent	Suspension, with some loosely adherent cells	Adherent	Adherent	Mixed, adherent and suspension	Adherent	Adherent	Adherent	Adherent
Age	72	Adult	70	44	51	70	Adult	58	Adult	50
Gender	Male	Male	Male	Female	Male	Male	Male	Female	Male	Male
Ethnicity	Caucasian	n.r.	Caucasian	Caucasian	Caucasian	Caucasian	Caucasian	Caucasian	Caucasian	Caucasian
Tumor Stage	n.r.	n.r.	Duke's type D	n.r.	Duke's type C	Duke's type D	Duke's type C	Duke's type B	Duke's type C	Duke's type B
Derived from metastatic site	n.r.	n.r.	Ascites	n.r.	Lymph node	Ascites	n.r.	n.r.	n.r.	n.r.
Tumorigenic	Yes, in nude mice	Yes, in nude mice	Yes, in nude mice	Yes, in nude mice	Yes, in nude mice	Yes, in nude mice	Yes, in nude mice	Yes, in nude mice	Yes, in nude mice	Yes, in nude mice
Oncogene	n.r.	n.r.	myc+; myb+; ras+; fos+; p53+; sis+; abl-; ros-; src-	myc+; myb+; ras+; fos+; p53+; sis+; abl-; ros-; src-	myc+; myb+; ras+; fos+; p53+; sis+; abl-; ros-; src-	n.r.	myc+; myb+; ras+; fos+; p53+; sis+; abl-; ros-; src-	n.r.	n.r.	myc+; myb+; ras+; fos+; p53+; sis+; abl-; ros-; src-
Antigen Expression	n.r.	n.r.	n.r.	HLA-A1, A3, B12, B17, Cw5; Blood type A; Rh+	HLA-A2, B8, B17; Blood type A; Rh+	n.r.	n.r.	HLA-A2, B13,B50; Blood type 0	n.r.	HLA-A2, B8, B17; Blood type A; Rh+
MMR Expression	n.r.	MLH1 Deficient	n.r.	Proficient	Proficient	n.r.	MSH6 Deficient	n.r.	MSH6 Deficient	Proficient
Growth Factor Receptors	STa; EGF	n.r.	n.r.	u-PAR; vit-D	n.r.	n.r.	n.r.	n.r.	n.r.	n.r.
CELLULAR PRODUCTS										
Mucin	n.r.	n.r.	n.r.	Yes	n.r.	n.r.	n.r.	Yes	n.r.	n.r.
Keratin	Yes	Yes	n.r.	n.r.	Yes	Yes	Yes	n.r.	Yes	Yes
CEA	n.r.	1ng/10^6c/10d	No	Yes	0.15ng/10^6/10d	1.5-4.1ng/10^6c/10d	0.5ng/10^6/10d	1916ng/10^6c/10d	5.4ng/10^6/10d	0.7ng/10^6/10d
NCI60 Panel	No	Yes	No	Yes	Yes	Yes	Yes	No	Yes	No

(n.r. = not reported)

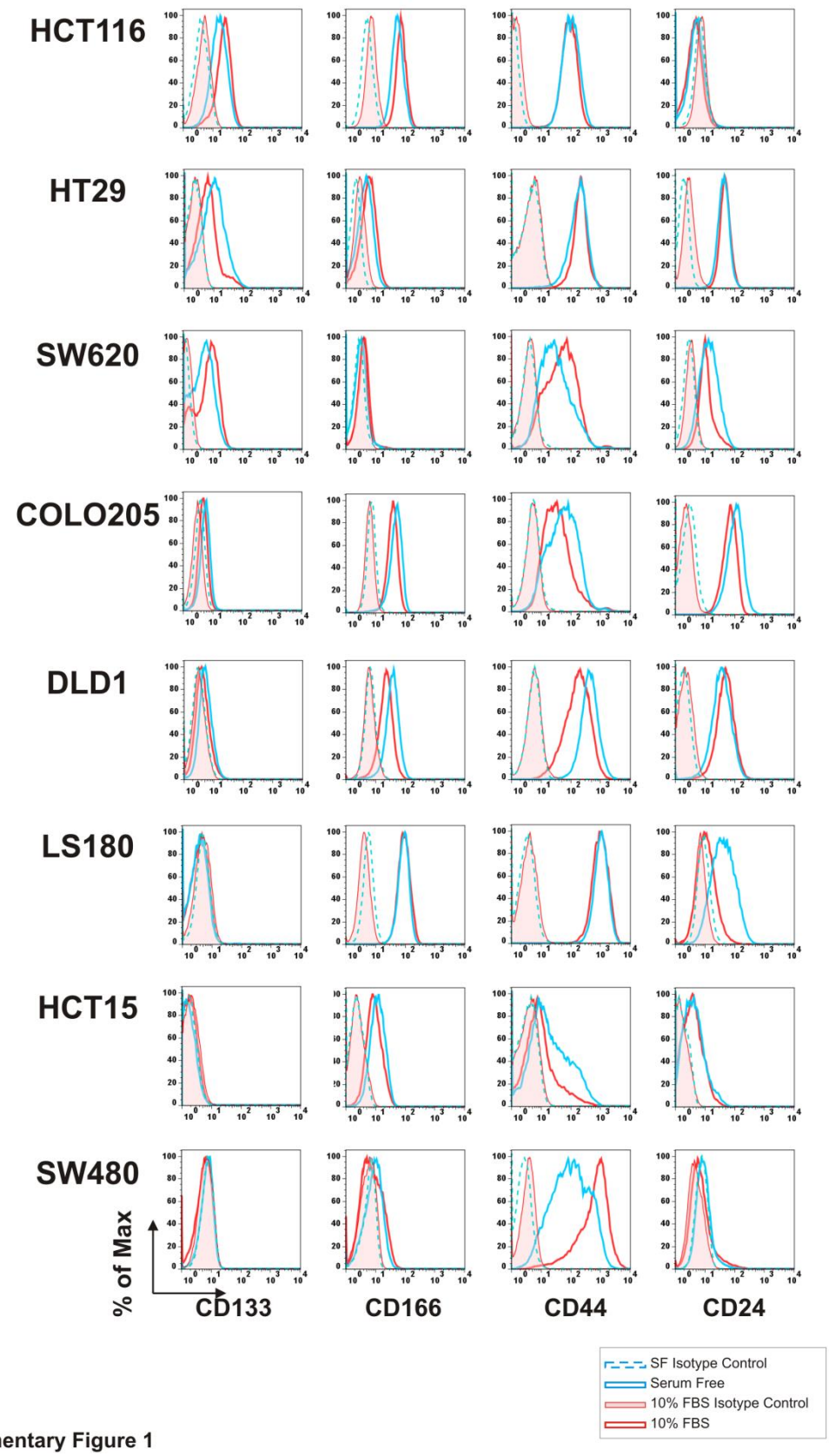

Supplementary Figure 1

Supplementary Figure 1 Phenotypic profiles of CRC cell lines cultured in the presence or absence of serum. CRC cell lines were cultured up to 10 days in serum containing or in SF medium and stained with APC-labeled anti-CD133, PE-labeled anti-CD166, APC-H7-labeled anti-CD44, and FITC-labeled anti-CD24 antibodies. Histograms represent the fluorescence intensity of the indicated marker in cells cultured in serum containing (solid red line) or in SF medium (solid blue line) overlaid to corresponding isotype controls (tinted red histogram and dashed blue line, respectively).

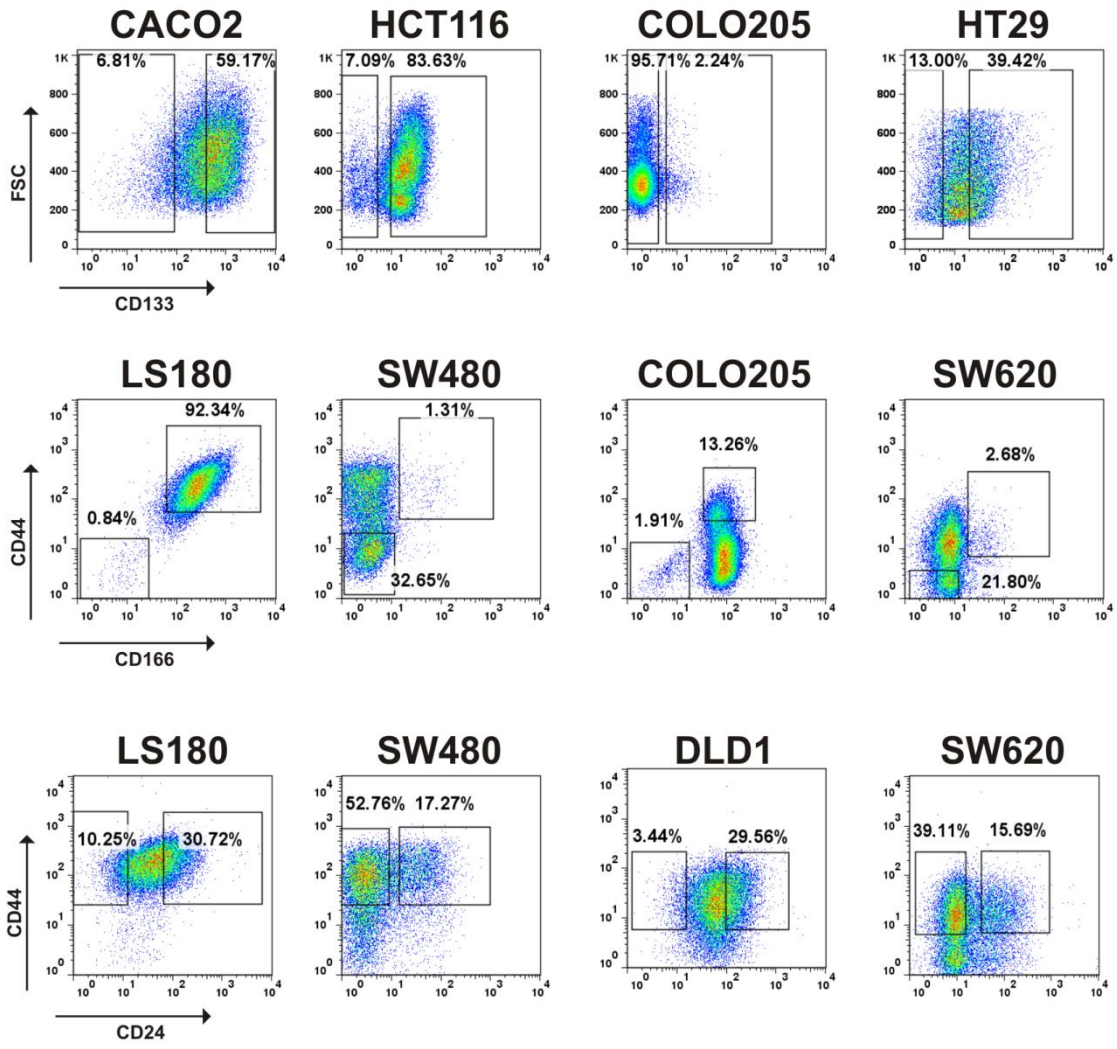

Supplementary Figure 2

Supplementary Figure 2 Definition of gates used for cell sorting
CD133+ and CD133- cells were sorted from CACO2, HCT116, COLO205, and HT29 cell lines following staining with PE-labeled anti-CD133 antibodies. CD166+CD44+ and CD166-CD44- cells were isolated from LS180, SW480, COLO205, and SW620 cell lines, following staining with PE-labeled anti-CD166 and APC-labeled anti-CD44 antibodies. CD24+CD44+ and CD24-CD44+ cells were sorted from LS180, SW480, DLD1, and SW620 cell lines following staining with PE-labeled anti-CD24 and APC-labeled anti-CD44 antibodies. Cell subsets were gated as depicted, after exclusion of dead cells, based on 7-AAD incorporation.

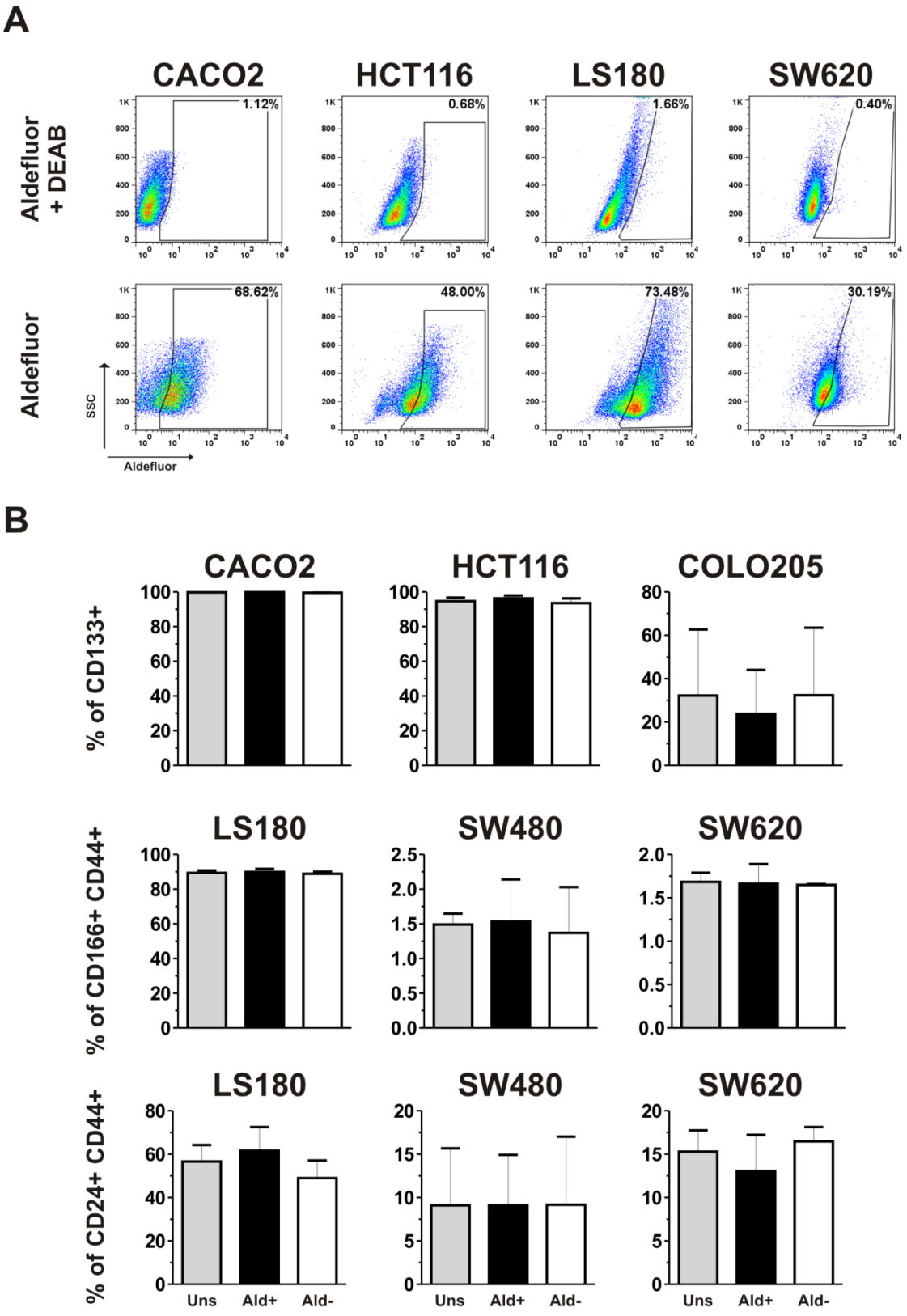

Supplementary Figure 3 ALDH-1 activity in CRC cell lines does not correlate with the expression of putative CSC markers. A. CRC cell lines were stained with the Aldefluor Kit assay. Representative dot plots illustrating ALDH-1 activity obtained upon staining of CRC cells in the absence, or presence of DEAB are shown. B. Aldefluor-stained CRC cells were counterstained with CD133-, CD166-, CD44-, and CD24-specific antibodies. Percentages of CD133+, CD166+CD44+, or CD24+CD44+ cells within unsorted (Uns), Aldefluor+ (Ald+) or Aldefluor- (Ald-) cells were assessed. Average frequencies ± SD from two experiments are reported.

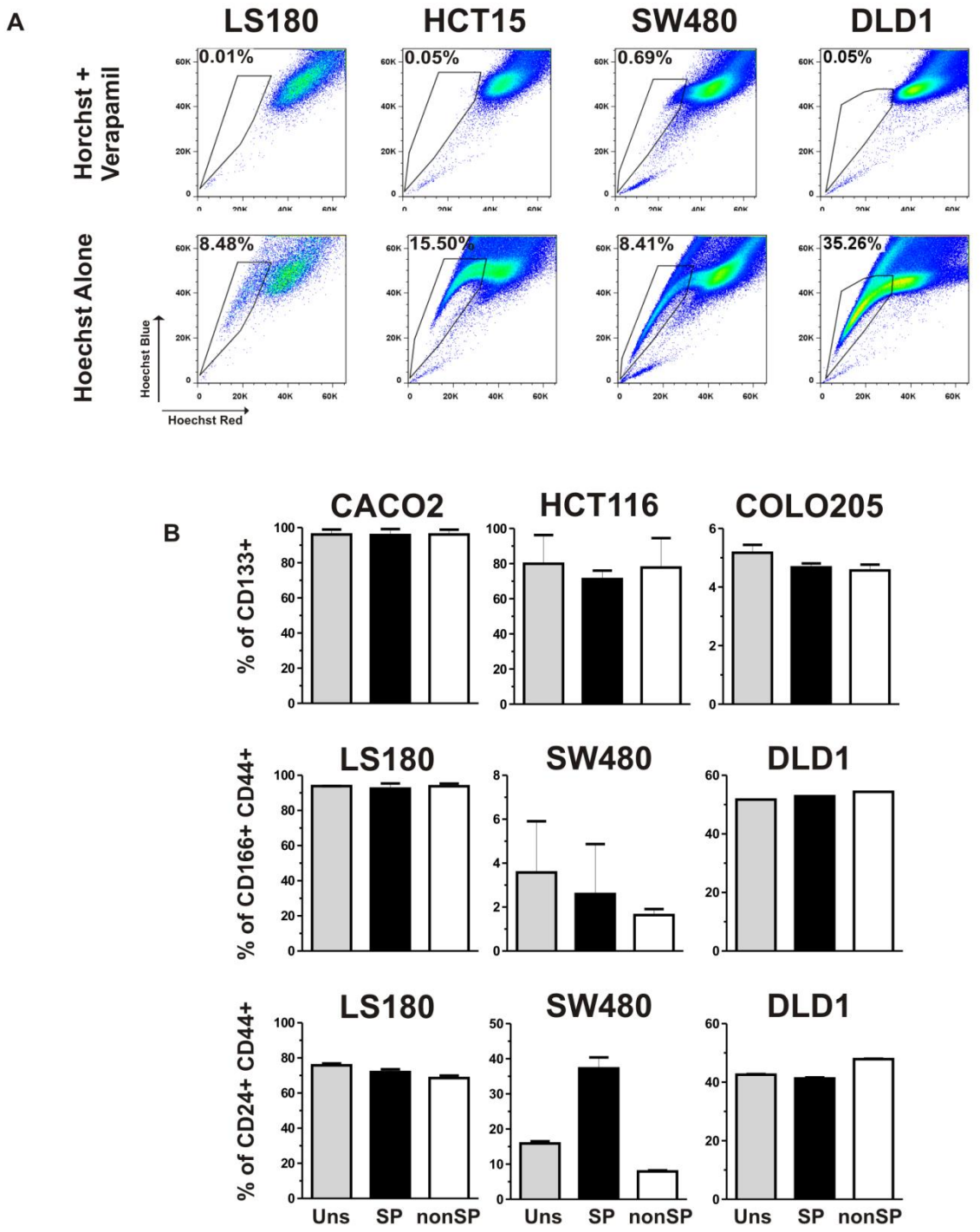

Supplementary Figure 4 SPs in CRC cells lines do not preferentially express CSC markers. A. CRC cell lines were stained with Hoechst 33342 and percentages of SP were gated in comparison to samples treated with Verapamil. B. Hoechst-stained cells were counterstained with CD133-, CD166-, CD44-, and CD24-specific antibodies. Frequencies of CD133+, CD166+CD44+ or CD24+CD44+ cells within unsorted (Uns), SP, or non-SP cells were assessed. Average frequencies ± SD from two experiments are reported.

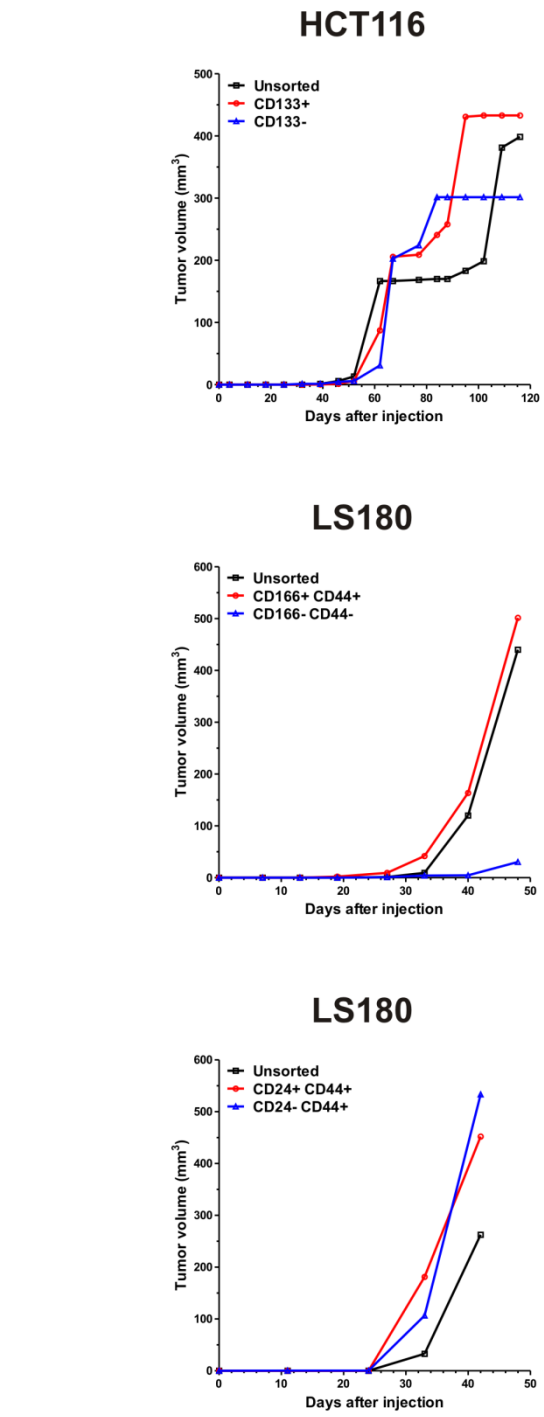

Supplementary Figure 5

Supplementary Figure 5 Tumor growth kinetics upon injection of putative CSCs in immunodeficient mice. NOD/SCID mice were injected subcutaneously with: CD133+, CD133-, or unsorted cells from the HCT116 cell line (104 cells/mouse); CD166+CD44+, CD166-CD44-, or unsorted cells from the LS180 cell line (104 cells/mouse); CD24+CD44+, CD24-CD44+, or unsorted cells from the LS180 cell line (103 cells/mouse). Tumor volume was assessed over time.

3.4 Differential gene expression patterns in 3D cultures of human colon cancer cells in the presence of hypoxic and/or necrotic cores

Silvio Däster[1], Nunzia Amatruda[1], Diego Calabrese, Paul Zajac, Giulio C. Spagnoli, Giandomenica Iezzi, Valentina Mele[2], Manuele G. Muraro[2]

Institute of Surgical Research and Hospital Management ICFS, University Hospital Basel, Basel, Switzerland

1 These authors contributed equally to this work.

2 Shared last authorship

Manuscript in preparation

Introduction

Pre-screening of novel potential anti-cancer agents is conventionally conducted on established cancer cell lines from the US National Cancer Institute (NCI) 60 panel, a collection of 60 tumor cell lines representing nine distinct human tumor types (89). These cells growing in two-dimensional (2D) monolayers are easy to propagate and amenable to high throughput studies. However, it is well known that these cells growing in 2D inadequately reflect the genetic make-up of the cancer cells in human disease, possibly because of missing features of the three-dimensional (3D) in vivo microenvironment that has a huge impact on cell proliferation, differentiation, migration, and intracellular signal transduction (68, 90-94). This might represent the background for the high attrition rates of compounds that are selected during pre-clinical studies. Therefore the pharmaceutical industry is highly interested in models

that increase the efficacy of pre-screening to reduce the high failure-rate in drug development. Although 3D in vitro models are known since more than thirty years (68), only recent work has highlighted the need for better 3D models that may bridge the gap between conventional 2D models and in vivo studies (95).

The multicellular tumor spheroid (MCTS) model is one of the best established 3D culture methods and it is currently being tested for drug screening purposes (96). MCTSs are cellular aggregates that resemble the microenvironmental condition of small avascular tumor regions and micrometastases (68). MCTS may be cultured exploiting the hanging-drop method described by Kelm et al (96) based on the capacity of cells to adhere to each other without artificial scaffolds.

Most solid tumors develop hypoxic regions which may determine dramatic changes in tumor cell gene expression (97). Tumors with hypoxic areas are known to display a more aggressive tumor phenotype and tumor cells in hypoxic areas are also more resistant to chemo- and radio-therapies due to direct and indirect effects of hypoxia (91, 98, 99). Furthermore, hypoxia seems also to be associated with the generation or expansion of tumor-initiating cells or cancer stem cells (CSC) (100). Therefore, MCTS may represent a good tool to study cancer stem cell biology and the best in the development of CSC-specific drugs.

Similar to in vivo tumors, with increasing size, hypoxia and apoptosis/necrosis occur within MCTS due to oxygen and nutrient gradients (101). The effects of these phenomena on gene expression profiles of human colorectal cancer (CRC) MCTS at different growth stages have not been elucidated so far.

This study presents a straightforward method to obtain human CRC-MCTSs of different sizes resembling specific growth stages characterized by the presence or absence of hypoxic and/or apoptotic/necrotic cores.

In order to obtain insights into similarities and differences between tumor cells growing in physically different microenviroments, here we analyzed gene expression profiles of CRC cells cultured in standard 2D conditions, as MCTS, or growing in a in-vivo environments as xenograft in immunodeficient mice.

The comparison of the gene expression profiles of MCTS at different stages with CRC cells cultured on monolayer or xenografts showed that the presence of both hypoxic and necrotic cores are essential to adequately mimic in vivo conditions.

Material and Methods

Cell cultures

Authenticated human established colorectal cancer cell lines HCT116 and HT-29 were purchased from American Type Culture Collection (ATCC, Manassas, VA). HCT116 cells were maintained in RPMI-1640 supplemented with 10% fetal bovine serum (FBS), GlutaMAX-I, Non Essential Amino Acids (NEAA), 100 mM sodium pyruvate, 10 mM HEPES (all from Gibco), and 50 µM 2-Mercaptoethanol (Sigma). HT-29 was maintained in McCoy's 5A (Sigma) supplemented with 10% FBS and GlutaMAX-I. Both media were also supplemented with kanamycin sulphate (Gibco). Cells were cultured at 37°C with 5% CO2. The absence of mycoplasma contamination in cells was verified by PCR testing prior to investigation.

Generation of MCTS

MCTS were formed by the hanging drop method as described by Kelm JM and collegues (96) using the 96-well GravityPlus plates (Insphero AG, Zurich, Switzerland), where each well consists of a hourglass-like structure open on both sides. The shape of the wells allows the creation of hanging-drops in the lower part and enables the change of the medium through the upper part, without modifying the MCTS structure. Briefly, cells were seeded as a single cell suspension of 40 µl per well by top-loading. Medium change was performed replacing twice half of the old medium with fresh medium, every three-four days. All steps were performed using an automatic multichannel pipette at a flow rate of 10 µl/s (Viaflo, Integra Biosciences, Zizers, Switzerland). After seeding the cell plates were cultured at 37°C with 5% CO2 for 3–4 days to allow cell assembly for gravity-enforced and the formation of the MCTS.

Growth kinetics analysis

MCTS growth kinetic was examined at different time-points using an inverted phase contrast microscope (Nikon Eclipse TS100, Nikon Co.) equipped with a digital camera (Nikon Digital Sight DS-2MBWc, Nikon Co.). Five pictures for each time-point were acquired and MCTSs diameters were measured (Image-Pro Plus v4.5.1, Media Cybernetics).

Xenograft cultures

In vivo experiments were approved by the Basel Cantonal Veterinary Office. NOD/SCID mice, initially obtained by Charles River Laboratories (Sulzfeld, Germany), were bred and maintained under specific pathogen free conditions in the animal

facility of the Basel University Hospital. Eight to ten week old mice were used for experiments. For both cell lines one hundred thousand cells were re-suspended in a 1:1 mixture of PBS and BD Matrigel Matrix Growth Factor Reduced (BD Biosciences) and inoculated subcutaneously into the flank of recipient mice. Tumor formation was monitored weekly by palpation and caliper measurements. Mice were sacrificed when tumors reached a maximum diameter of 10 mm. Samples from all mice were frozen in RNA Later (Sigma-Aldrich) and embedded in Optimal Cutting Temperature compound (OCT) (CellPath Ltd, UK) for subsequent gene expression evaluation and histological examination after cryocutting, respectively. The remaining tissues were enzymatically digested and the presence of tumor cells was assessed by flow cytometry upon staining with human EpCAM-specific antibodies (clone EBA-1, BD Bioscience).

Spheroid fixation, cryosection and H&E staining

After harvesting, MCTS were fixed in cold methanol for 10 minutes at -20°C, washed in PBS, and then transferred to molds, embedded in OCT, and stored at -80°C until sectioning. Serial frozen sections were cut at 10 µm with a cryostat, and mounted onto Superfrost Plus microscope glass slides (Menzel-Glaeser, Braunschweig, Germany). Sections were stored at -20°C until further use. Hematoxylin and eosin (H&E) staining of cryostat-sectioned slides was performed in an automatic staining workstation Tissue Stainer COT 20 (Medite GmbH, Burgdorf, Germany) with standard procedures.

Immunostaining

For immunofluorescence staining, sections were blocked with 2% goat serum diluted in PBS containing 0.3% Triton X-100 for one hour at room temperature (RT) and then incubated with either rabbit monoclonal anti-Ki67 (Abcam, 1:200), rabbit monoclonal anti-cleaved caspase 3 (Cell Signaling Technology, 1:200), or mouse monoclonal anti-EBP50 (BD Biosciences, 1:50) for one hour at 37° C. Slides were washed with PBS and then incubated for one hour at RT with goat anti-mouse or anti-rabbit Alexa Fluor 488- or 546-conjugated antibodies (Invitrogen, 1:800). During the last ten minutes of incubation DAPI (Invitrogen, 1:100) was added. Sections were analyzed either on a confocal laser scanning microscope (Zeiss LSM-710 system, Carl Zeiss Microimaging GmbH) or on a fluorescence microscope (Olympus BX61, Olympus Inc.).

To detect hypoxia, immunohistochemical staining with the monoclonal antibody hypoxia-inducible factor 1, variant alpha (HIF1α) (Abcam, 1:25) was performed. After adding the blocking solution (1% goat serum diluted in PBS) for 30 minutes to prevent unspecific binding, the sections were incubated with HIF1α antibody for 16 hours at 4° C in a dark wet chamber. Sections were washed with double distilled water and incubated for 30 minutes at RT with the secondary antibody conjugated to alkaline phosphatase (AP Histofine Simplestain M). The primary-secondary complex was then detected by enzymatic reaction by adding an appropriate chromogenic substrate (Histofine 415161F, New Fuchsin Substrate Kit) for 5 minutes at RT. After blocking the reaction by immersing the slides in tap water, nuclear staining was performed using hematoxylin staining. Sections were analyzed on a fluorescence microscope (Olympus BX61, Olympus Inc.).

Real-time RT-PCR

Total RNA isolation was performed using the Nucleospin RNA isolation kit (Macherey-Nagel GmbH & Co.) according to the manufacturer's protocol. RNA concentration and quality were evaluated using Nanodrop ND-1000 spectrophotometer (Thermo Scientific Inc.). Reverse transcription was performed using the M-MLV-RT enzyme kit (Invitrogen, Basel, Switzerland), following the manufacturer's recommendation, and cDNAs were then stored at -20°C for further use.

A TaqMan Custom Array micro fluidic card (Applied Biosystems Inc.) was designed to study a panel of 94 genes of interest (Supplementary Table 1). The cards were run on a 7900HT thermal cycler (Applied Biosystems Inc.) according to manufacturer's guideline. The comparative Ct method was used to quantify the relative gene expression levels, upon normalization against the expression of the 18S housekeeping gene as reference. Each sample was assessed in duplicate and experiments were repeated twice. Data were analyzed using Spotfire software (TIBCO Software, Somerville, Massachusetts, US) to generate the heat map and cluster plot analysis.

Results

MCTS formation and growth kinetics

As first stem, we tested the growth kinetics of MCTSs generated by different numbers of cells (100, 500, and 1000 cells per well), in order to identify the right starting condition to obtain small and compact MCTSs within 3 or 4 days. Optimal initial cell density was defined at 100 tumor cells per hanging drop both for HT29 and HCT116 (Figure 11 and data not shown).

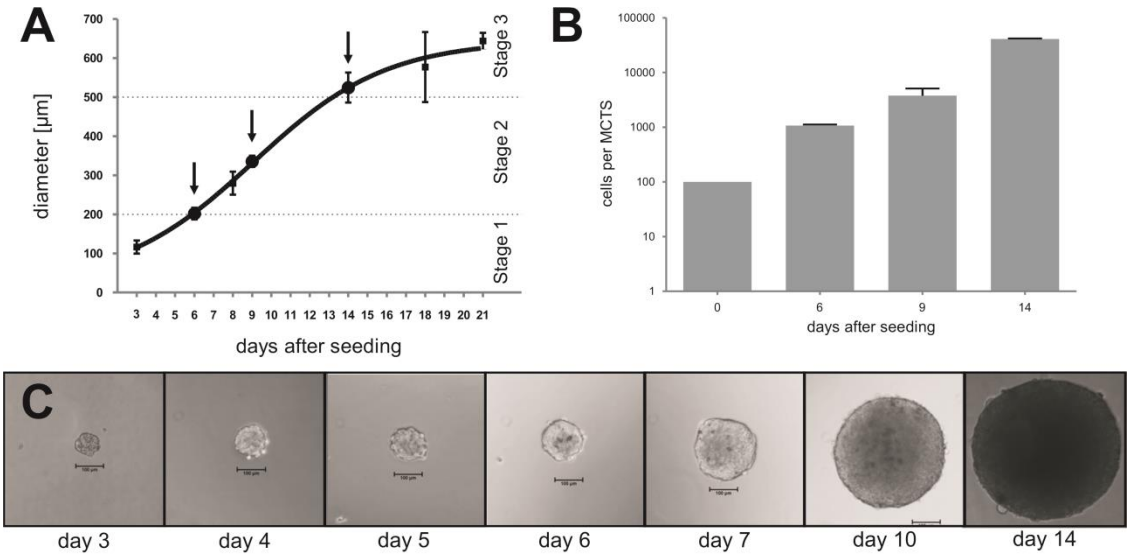

Figure 11 MCTS were generated from the HT29 CRC cell line by the hanging drop method. Cultures were performed in suspension using *InSphero GravityPlus* plates. To determine the optimal initial cell density, titrated tumor cell numbers per drop were seeded and MCTS growth kinetic was monitored. (A) MCTS growth over time. Optimal initial cell density was defined at 100 tumor cells per hanging drop. Day 6, 9, and 14 were defined as optimal timepoints for different MCTS stages. (B) MCTS proliferation; cell numbers obtained at different stages. (C) MCTS morphology over time. Scale bars represent 100 µm.

Definition of MCTS maturation stages

MCTSs were analyzed at different time-points aiming at the identification of three growth stages, characterized by presence of only normoxic cells (stage1), a hypoxic area in the inner part of the MCTS (stage2), and hypoxic and apoptotic/necrotic cores (stage3). In previous studies it has been reported that a hypoxic core begins to be formed in spheroids larger than 200 µm and that a necrotic core is detectable in MCTSs larger than 500 µm (101). Based on these findings we defined our time-points to obtain within 6-7 days a diameter size <200 µm for the stage 1, within 9-10 days a diameter of 300-350 µm for the stage 2 and within 14-15 days a diameter size >500 µm for the stage 3, respectively for HT29 and HCT116 cells (Figure 11A and data not shown). We confirmed the presence of a hypoxic area within the MCTSs stage 2 by the detection of hypoxia-inducible factor 1a (HIF1a) positive staining (Figure 12, E-L). The presence of apoptotic/necrotic cells was assessed by cleaved caspase3 (cC3) staining and ethidium homodimer incorporation (Figure 12, M-P and Supplementary Figure 1). We observed only few apoptotic/necrotic cells in the first two stages. Instead, in stage 3, we detected an apoptotic/necrotic core. By staining with Ki-67 MCTS we could show a highly compact and organized cell growth in outer layers at any maturation stage (Figure 12, Q-T).

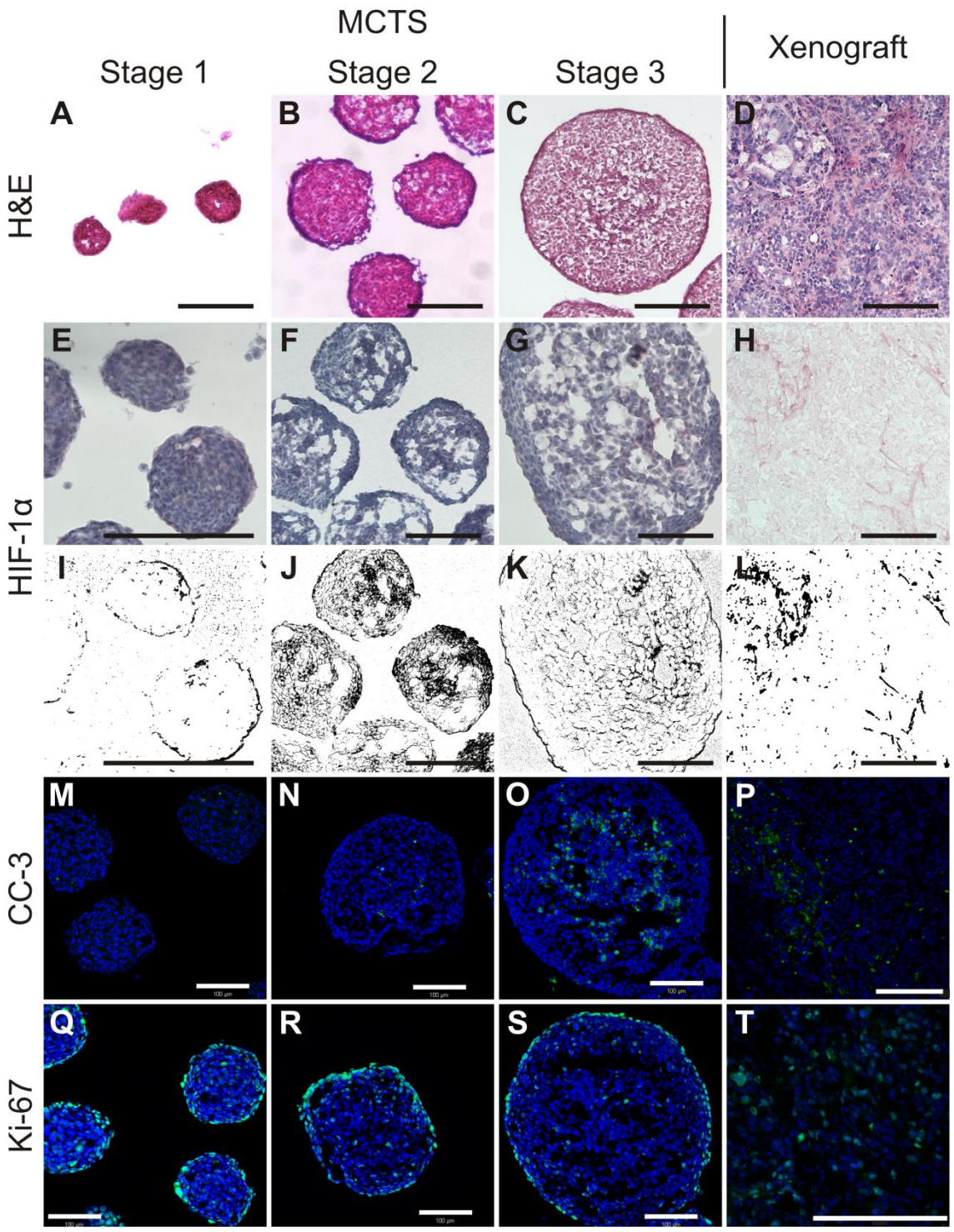

Figure 12 To detect hypoxic and necrotic inner cores and proliferating cells we performed immuno-fluorescence and immunohistochemistry on frozen sections with hypoxia-inducible factor 1 alpha (HIF-1α), cleaved caspase-3 (CC-3), and Ki-67 specific antibodies, respectively. Stage 1 (MCTS diameter size < 200 µm) was defined by the absence of hypoxia/necrosis (E, I, M), stage 2 (300-350 µm) was characterized by the presence of hypoxic, but not necrotic cores (F, J, N) and stage 3 (> 500 µm) was identified by the presence of both hypoxic and necrotic cores (G, K, O). At all maturation stages actively proliferating cells were mainly detected within the outer layers of MCTS (Q-S). Xenograft cultures of HT29 were obtained (HT29 cells were injected in NOD/SCID mice) and frozen sections were stained in the same manner as above (D, H, L, P, T) showing all features of stage 3 MCTS. Scale bars represent 100 µm.

Differential gene expression patterns

We then analyzed the gene expression profile of a panel of 94 genes related to tumor progression, metastatic behavior, and drug resistance in five different condition of growth namely: two-dimensional (2D) culture, stages 1, 2, and 3 of MCTS development (3D1, 3D2, and 3D3), and xenografted tumor cell (Xeno). For several genes we found a progressive up-regulation moving from 2D to 3D up tp xenograft. In particular this was conspicuously evident for P53, TRAIL, FAS, BAX, EpCAM, KRT20, CD133, CD44, and CD24 genes (Figure 13).

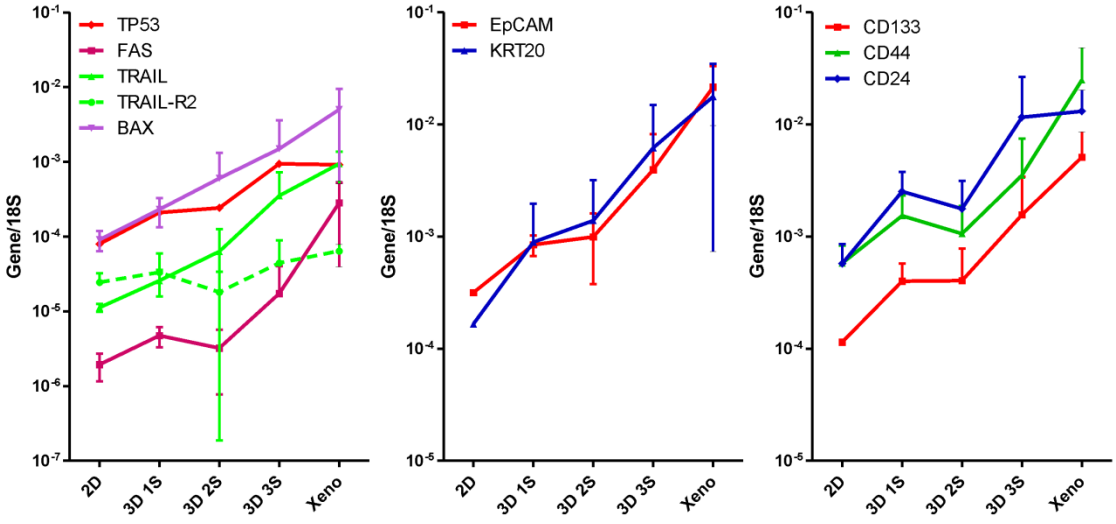

Figure 13 Cells obtained from 2D culture (2D), MCTS at first growth stage (3D 1S), second growth stage (3D 2S), third growth stage (3D 3S), and as xenograft (Xeno) were analysed using real-time quantitative PCR. Expression of each gene was normalized to that of 18S mRNA and is presented as $2^{-\Delta Ct}$. The relative mRNA expression levels are shown as means ± SD (n=2)

In order to highlight the difference between 2D- and 3D-culture we calculated the ratio between the gene expression found in 3D against that of the 2D. Comparing the three growth stages and the in-vivo condition, we observed a higher correlation between 3D stage-3 and the in-vivo condition. On the other hand the 3D stage-1 profile presented a remarkable similarity with the gene expression pattern detectable in cells cultured in 2D (Figure 14).

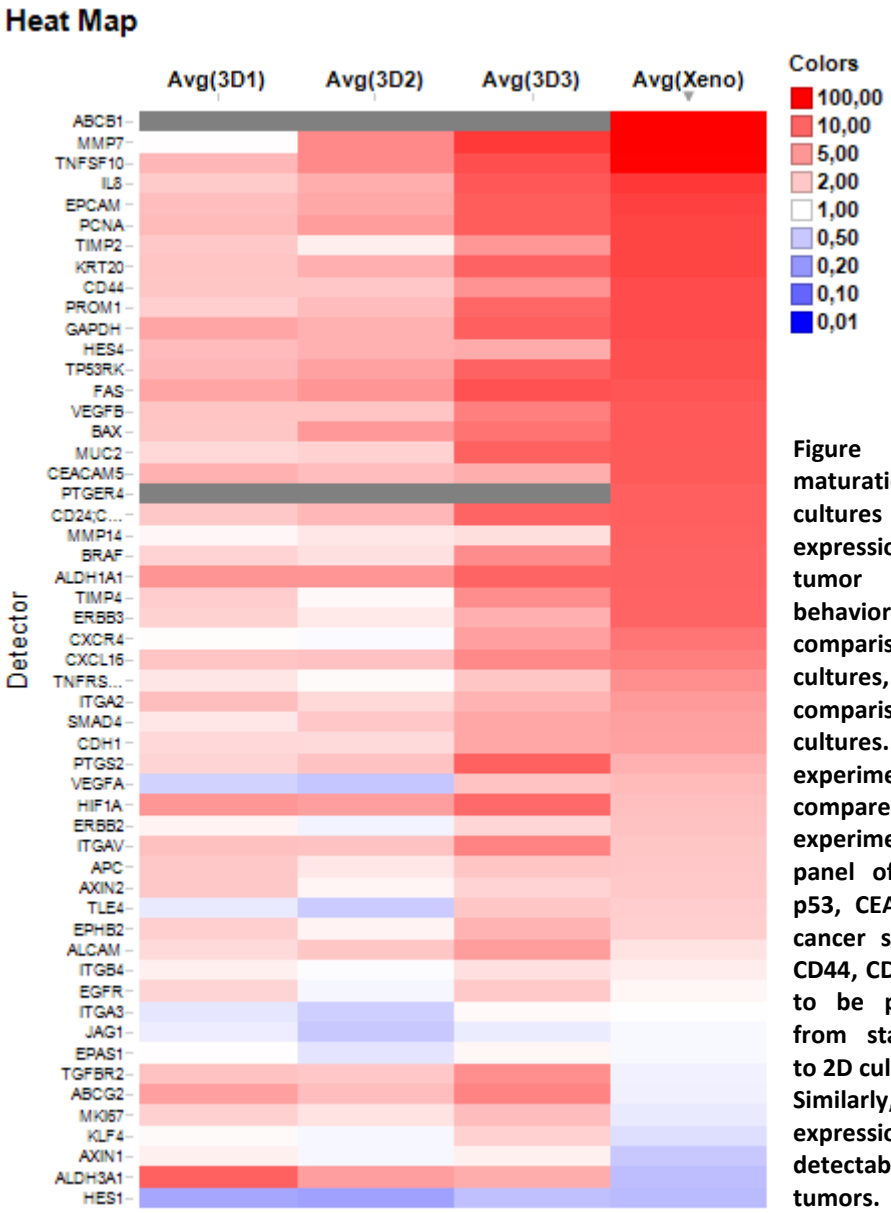

Figure 14 MCTS at different maturation stages and xenograft cultures were assessed for the expression of 94 genes related to tumor progression, metastatic behavior, and drug resistance in comparison to conventional 2D cultures, by real time PCR, in comparison to conventional 2D cultures. Heatmap (mean of two experiments, fold change as compared to 2D). In preliminary experiments, the expression of a panel of genes, including KRAS, p53, CEACAM5, and the putative cancer stem cell markers CD133, CD44, CD166, and CD24 was found to be progressively upregulated from stage 1 MCTS, as compared to 2D cultures.

Similarly, upregulated gene expression patterns were also detectable in "in vivo" xenografted tumors.

Discussion

Two-dimensional monolayer cultures are traditionally used to investigate cancer biology and develop novel treatments but they inadequately reproduce the pathophysiology of solid tumors (91, 102). Indeed 2D-culture of cell lines is simple, convenient, and amenable of high-throughput studies. However, it lacks the 3D structural architecture usually preserved in organ cultures (103). On the other hand, organ cultures may also be problematic, due to poor standardization and poor ability to grow in vitro.

Solid tumors often display hypoxic and necrotic areas. Furthermore, the presence of cells expressing stem cell characteristics, slow proliferation and barriers to drug diffusion contribute to drug resistance. These characteristics are not adequately reflected by monolayer cell cultures (102). Unlike monolayer culture, 3D-culture models capture the complexity of solid tumors and they might thus represent excellent tools for the development of novel in vitro assays and models of neoplastic cell culture with high potential clinical relevance. Indeed, cells cultured in 3D conditions have been shown to be endowed with specific characteristics, including resistance to apoptosis, and chemo- and radio-therapy, features closely matching those of ‘‘in vivo’’ tumors (68, 93, 97). On the other hand, MCTS 3D culture systems can easily be manipulated and exposed to specific treatments, at difference with in vivo xenografts (105).

Our experiments were performed using a 96-well GravityPlus plates from InSphero AG allowing easy handling of the hanging-drops cell culture technic and the possibility to make medium changes when needed (performed every 3 to 4 days) without perturbing the spheroid formation and growth. Thus, it was possible to

perform long-term MCTS culture. We could show that HT29 MCTS volume increased as a function of time in culture (Figure 7a) displaying the typical pattern of a Gompertz growth curve, a mathematical description of tumor and also spheroid growth kinetics characterized by an initial exponential increase in diameter followed by a growth deceleration phase (105-107).

HT29 cells generate, after six and nine days of culture, MCTSs with a diameter around 200 µm and 300 µm, respectively. By staining for HIF-1a, we demonstrated that a formation of a hypoxia areas occurs in MCTS with a size over 200 µm, similar to tumors in vivo, as also reported by Hirshhauser et al. (101).

The characterization of the third growth stage has been performed by testing the expression of cleaved caspase 3 (cC3) that is well known to be associated to apoptotic and necrotic events (108, 109). Apart for sporadic positive signals, both first and second growth stages were negative for cC3 (Figure 12, M and N, respectively). Instead, MCTS with a diameter >500 µm showed an apoptotic/necrotic core characterized by a cC3-positivity localized in the inner core of the spheroid structure (Figure 8, O). To confirm the cC3 staining data, we performed a two-color fluorescence cell viability assay that is based on the simultaneous determination of live and dead cells measuring intracellular esterase activity and plasma membrane integrity. We stained entire MCTSs showing live green-colored cells and eventually dead red-colored cells. Only in the third stage of growth a distinct accumulation of red signal in the spheroids central core was visible (Supplementary Figure 1).

Due to cell proliferation, the MCTSs increase in diameter over the time, generating concentration gradients of nutrients, oxygen, and catabolites. These transport phenomena have also been described in avascular tumors where the

formation of necrotic areas occurs (91, 92). By staining with Ki-67, we observed that in the first stage proliferating cells are numerous and spread within the MCTS whereas in the second stage they are mainly localized in the outer layer of the spheroid. Instead, in the third stage is possible to detect proliferating cells only in a compact ring localized in the outer MCTS layer. The inner core of the MSCTs is characterized by the presence of live quiescent cells or dying cells.

It has been reported that proliferation and functional features as well as the microenvironmental conditions inherent with the 3D cell-to-cell and cell-to-matrix interactions can affect gene and protein expression, and distribution and penetration of soluble factors including potentially therapeutic compounds (101). A number of comparative studies show that numerous genes are differentially expressed in cells cultured as MCTS versus monolayers (110-113). However, most of them were conducted on spheroids with a size of 300/350 μm and then possibly characterized by only the presence of hypoxia. To the best of our knowledge, no comparative study focusing the attention on the gene expression profiles of different spheroid maturation stages has been reported so far.

In this study we compared gene expression profiles of HT29 cells cultured as MCTS at three different stages with cells culture in 2D monolayers or engrafted in vivo upon xenografting in mice. We observed that the presence of both necrotic and hypoxic cores significantly impacts on gene expression profiles, resulting in patterns closely, resembling the in vivo situation as simulated by the xenograft. On the other side, MCTS with diameters <200 μm showed a gene expression profiles analogous to monolayer culture.

Hypoxic microenvironment has been shown to induce increased expression of p53 in solid tumors (92, 114). It has been observed that CRC cells respond to hypoxia by activating p53 and the apoptotic pathway through the HIF response element (HRE). HRE, in turn, activates the transcription initiation of *fas* gene causing the up-regulation of Fas/CD95 death receptor. Our data demonstrate an increasing expression of p53 and Fas through the three stages of MCTS maturation, especially evident at the third stage of maturation, as also confirmed by the parallel up-regulation of other apoptotic markers including TRAIL and BAX.

The analysis of the expression of genes encoding putative cancer stem cell markers CD44, CD166, CD133, and CD24 is also consistent with a trend of increasing expression in the three stages of maturation.

In neuroblastoma cells has been demonstrated that hypoxia leads to an inhibition of cell differentiation, resulting in maintenance of a stem-like phenotype (51, 115). Moreover, upon increasing hypoxia an increased expression of genes involved in tumor progression namely KRAS, BRAF and SMAD4 was also detectable.

In conclusion, we have shown that culture of CRC cells from established cell lines offers the opportunity to investigate in standardized conditions different MCTS stages possibly providing an improved model of “in vivo” tumor growth.

Data obtained from spheroids at different stages indicate that hypoxia and necrosis significantly influence the expression of genes important for tumor progression, such as BRAF, KRAS and p53, and encoding putative cancer stem cells markers, CD44, CD166, CD24 and CD133. Importantly, the establishment of innovative culture systems might be essential not only for a more accurate study of tumor progression, but also for the screening of new cancer drugs.

Supplementary Table 1 Gene list for the RT-PCR 384 low-density plate

Gene Symbol	Gene name	Assay ID	Context Sequence
TP53RK	TP53 regulating kinase	Hs00369266_m1	TCGCCGCGCTGGAATATCTGCCCCA
CD44	CD44 molecule (Indian blood group)	Hs01075861_m1	TCGAAGAAGGTGTGGGCAGAAGAAA
18S	Eukaryotic 18S rRNA	Hs99999901_s1	CCATTGGAGGGCAAGTCTGGTGCCA
GAPDH	glyceraldehyde-3-phosphate dehydrogenase	Hs99999905_m1	GGGCGCCTGGTCACCAGGGCTGCTT
ALCAM	activated leukocyte cell adhesion molecule	Hs00233455_m1	TAGTCAAGGTGTTCAAGCAACCATC
CD24;CD24P4	CD24 molecule;CD24 molecule pseudogene 4	Hs02379687_s1	GCGGCTGGTGGTGCCCTGCAGTCAA
EPCAM	epithelial cell adhesion molecule	Hs00158980_m1	GCTCAGGAAGAATGTGTCTGTGAAA
LGR5	leucine-rich repeat-containing G protein-coupled receptor 5	Hs00173664_m1	GCCTTCAATCCCTGCGTCTGGATGC
EPHB2	EPH receptor B2	Hs01031827_m1	CCTCTCCTCTGGCATCAACCTGCCG
ALDH1A1	aldehyde dehydrogenase 1 family, member A1	Hs00946916_m1	GCCGACTTGGACAATGCTGTTGAAT
ALDH3A1	aldehyde dehydrogenase 3 family, member A1	Hs00964880_m1	AAGTCACTGAAAGAGTTCTACGGGG
SSPN	sarcospan (Kras oncogene-associated gene)	Hs01025520_m1	TATTCAATTTTCTATGAAACTGTTA
ABCG5	ATP-binding cassette, sub-family G (WHITE), member 5	Hs00223686_m1	GTGCTACTGGACGCTGGGCTTACAT
ABCB1	ATP-binding cassette, sub-family B (MDR/TAP), member 1	Hs01067802_m1	ATCGAGTCACTGCCTAATAAATATA
ABCG2	ATP-binding cassette, sub-family G (WHITE), member 2	Hs01053790_m1	GGAGGCAAATCTTCGTTATTAGATG
NANOG	Nanog homeobox	Hs02387400_g1	GCCTCACACGGAGACTGTCTCTCCT
POU5F1;POU5F1P3	POU class 5 homeobox 1;POU class 5 homeobox 1 pseudogene 3	Hs01895061_u1	AGCTGGAGCAAAACCCGGAGGAGTC
BRAF	v-raf murine sarcoma viral oncogene homolog B1	Hs00269944_m1	ATTCCGGAGGAGGTGTGGAATATCA
TGFBR2	transforming growth factor, beta receptor II (70/80kDa)	Hs00234253_m1	GCTCAACCACCAGGGCATCCAGATG
SMAD4	SMAD family member 4	Hs00929647_m1	CCATTGAGAGAGCAAGGTTGCACAT
PINK1	PTEN induced putative kinase 1	Hs00260868_m1	AGGAGATCCAGGCAATTTTTACCCA
APC	adenomatous polyposis coli	Hs01568269_m1	TAAAAAGGAATCAACCCTCAAAAGC
CEACAM5	carcinoembryonic antigen-related cell adhesion molecule 5	Hs00944025_m1	CACAGTCTCTGCGGAGCTGCCCAAG
PROM1	prominin 1	Hs01009250_m1	TTATCGACCCCTTGAATTTGTTTTG
SOX2OT	SOX2 overlapping transcript (non-protein coding)	Hs00415716_m1	TCTTTCTATTCCAGGGATTGCAGTG
TNFRSF10B	tumor necrosis factor receptor superfamily, member 10b	Hs00366278_m1	TCCCACTGAGACTCTGAGACAGTGC
TNFSF10	tumor necrosis factor (ligand) superfamily, member 10	Hs00921974_m1	AGCTGAAGCAGATGCAGGACAAGTA
BAK1	BCL2-antagonist/killer 1	Hs00940249_m1	AAGATTGCCACCAGGCCAGCAGCAA
BAX	BCL2-associated X protein	Hs00180269_m1	CTGGTGCTCAAGGCCCTGTGCACCA
ITGA2	integrin, alpha 2 (CD49B, alpha 2 subunit of VLA-2 receptor)	Hs00158127_m1	CTCAGTCAAGGCATTTTAAATTGTT
ITGA3	integrin, alpha 3 (antigen CD49C, alpha 3 subunit of VLA-3 receptor)	Hs01076873_m1	AGCACCTTCATCGAGGATTACAGAG
ITGA5	integrin, alpha 5 (fibronectin receptor, alpha polypeptide)	Hs01547673_m1	GGAAGTGTTTGGGGAGCAGAACCAT
ITGA9	integrin, alpha 9	Hs00979865_m1	ATACTGAAAAAGGACAGTTCGTCTG
ITGAV	integrin, alpha V (vitronectin receptor, alpha polypeptide, antigen CD51)	Hs00233808_m1	TTCACACTTTGGGTTGTGGAGTTGC
ITGB4	integrin, beta 4	Hs00236216_m1	GCTGCAAGGCCTGCCTGGCACTTCT
KLF4	Kruppel-like factor 4 (gut)	Hs00358836_m1	CCCGAATAACCGCTGGCGGGAGGAG
CDH1	cadherin 1, type 1, E-cadherin (epithelial)	Hs01023894_m1	CGCGTCCTGGGCAGAGTGAATTTTG
CDH2	cadherin 2, type 1, N-cadherin (neuronal)	Hs00983056_m1	ATCCTGCTTATCCTTGTGCTGATGT
TWIST1	twist homolog 1 (Drosophila)	Hs00361186_m1	CGGAGACCTAGATGTCATTGTTTCC
SNAI2	snail homolog 2 (Drosophila)	Hs00950344_m1	TTAGAACTCACACGGGGGAGAAGCC
SNAI1	snail homolog 1 (Drosophila)	Hs00195591_m1	GACTCTAATCCAGAGTTTACCTTCC
KRT20	keratin 20	Hs00300643_m1	TCCCATCTCAGCATGAAAGAGTCTT
MUC2	mucin 2, oligomeric mucus/gel-forming	Hs00159374_m1	ACCTGCAAGTCCTGCGTGTGTACCA
MKI67	antigen identified by monoclonal antibody Ki-67	Hs01032443_m1	CCTGAAGAAAATCATCAAGGAACAG
PCNA	proliferating cell nuclear antigen	Hs00696862_m1	TCTTCCCTTACGCAAGTCTCAGCCG
BMF	Bcl2 modifying factor	Hs00372937_m1	GACTCTTTTATGGCAATGCTGGCTA
BIRC5	baculoviral IAP repeat-containing 5	Hs00978503_m1	AACAAAATTGAGAGAGCTCTGTTAG
FAS	Fas (TNF receptor superfamily, member 6)	Hs00531110_m1	TCTGGACCCTCCTACCTCTGGTTCT
ZEB1	zinc finger E-box binding homeobox 1	Hs00232783_m1	TGATGAAAATGGAACACCAGATGCA
VEGFA	vascular endothelial growth factor A	Hs00900055_m1	ACATCACCATGCAGATTATGCGGAT
VEGFB	vascular endothelial growth factor B	Hs00173634_m1	CCAGTGTGAATGCAGACCTAAAAAA
VEGFC	vascular endothelial growth factor C	Hs01099203_m1	AGCTACCTCAGCAAGACGTTATTTG
HIF1A	hypoxia inducible factor 1, alpha subunit (basic helix-loop-helix transcription factor)	Hs00936371_m1	CAAGAAAAAGATAAGTTCTGAACGT

EPAS1	endothelial PAS domain protein 1	Hs01026149_m1	TCACCAGAACTTGTGCACCAAGGGT
EGF	epidermal growth factor	Hs01099999_m1	TGGACAAGTATGCATGCAACTGTGT
IGF1	insulin-like growth factor 1 (somatomedin C)	Hs01547656_m1	TTATTTCAACAAGCCCACAGGGTAT
IGF2	insulin-like growth factor 2 (somatomedin A)	Hs00171254_m1	CGGCTTCCAGACACCAATGGGAATC
IL8	interleukin 8	Hs00174103_m1	GTGTGAAGGTGCAGTTTTGCCAAGG
IL6	interleukin 6 (interferon, beta 2)	Hs00985639_m1	TCAGCCCTGAGAAAGGAGACATGTA
MMP1	matrix metallopeptidase 1 (interstitial collagenase)	Hs00899658_m1	AAGTCCGGTTTTTCAAAGGGAATAA
FLT1	fms-related tyrosine kinase 1 (vascular endothelial growth factor/vascular permeability factor receptor)	Hs00176573_m1	GACTTAAACTGGGCAAATCACTTGG
KDR	kinase insert domain receptor (a type III receptor tyrosine kinase)	Hs00911700_m1	ACACAGCAGGAATCAGTCAGTATCT
FLT4	fms-related tyrosine kinase 4	Hs01047677_m1	TGGCCGCCAGGTATTACAACTGGGT
EGFR	epidermal growth factor receptor	Hs01076078_m1	GAGGAAAAGAAAGTTTGCCAAGGCA
ERBB2	v-erb-b2 erythroblastic leukemia viral oncogene homolog 2, neuro/glioblastoma derived oncogene homolog (avian)	Hs01001580_m1	CTGTTTTGGACCGGAGGCTGACCAG
MMP2	matrix metallopeptidase 2 (gelatinase A, 72kDa gelatinase, 72kDa type IV collagenase)	Hs01548727_m1	ACCAGATCACATACAGGATCATTGG
MMP7	matrix metallopeptidase 7 (matrilysin, uterine)	Hs01042796_m1	GTAGCAGTCTAGGGATTAACTTCCT
MMP9	matrix metallopeptidase 9 (gelatinase B, 92kDa gelatinase, 92kDa type IV collagenase)	Hs00234579_m1	AGTACCGAGAGAAAGCCTATTTCTG
MMP14	matrix metallopeptidase 14 (membrane-inserted)	Hs00237119_m1	GCCCCGAAGCCTGGCTACAGCAATA
TIMP2	TIMP metallopeptidase inhibitor 2	Hs00234278_m1	TCTCATTGCAGGAAAGGCCGAGGGG
TIMP3	TIMP metallopeptidase inhibitor 3	Hs00165949_m1	CTCCGACATCGTGATCCGGGCCAAG
TIMP4	TIMP metallopeptidase inhibitor 4	Hs00162784_m1	GTATCTCTTGACTGGTCAGGTCCTC
ERBB3	v-erb-b2 erythroblastic leukemia viral oncogene homolog 3 (avian)	Hs00176538_m1	AACTCTCAGGCAGTGTGTCCTGGGA
CXCL16	chemokine (C-X-C motif) ligand 16	Hs00222859_m1	GATCTCAAAGAATGTGGACATGCTT
CX3CL1	chemokine (C-X3-C motif) ligand 1	Hs00171086_m1	GCTGGCTGGACAGCACCACGGTGTG
PTGS2	prostaglandin-endoperoxide synthase 2 (prostaglandin G/H synthase and cyclooxygenase)	Hs00153133_m1	CTGGGCCATGGGGTGGACTTAAATC
PTGER2	prostaglandin E receptor 2 (subtype EP2), 53kDa	Hs00168754_m1	GCTCCTTGCCTTTCACGATTTTTGC
PTGER4	prostaglandin E receptor 4 (subtype EP4)	Hs00168761_m1	TCCATCCCGCTCGTGGTGCGAGTAT
IDO1	indoleamine 2,3-dioxygenase 1	Hs00984148_m1	TTCTGCAATCAAAGTAATTCCTACT
LEF1	lymphoid enhancer-binding factor 1	Hs00212390_m1	GGACACGAGGTGGCCAGACAAGCAC
AXIN1	axin 1	Hs00394718_m1	CGGACAGCAGCGTGGATGGGATCCC
AXIN2	axin 2	Hs00610344_m1	CCTCATTTCCCGAGAACCCACCGCC
TLE4	transducin-like enhancer of split 4 (E(sp1) homolog, Drosophila)	Hs00419101_m1	TCAATACCACAGTCTGAAGCTGGAA
ERBB4	v-erb-a erythroblastic leukemia viral oncogene homolog 4 (avian)	Hs00955525_m1	TGCCAGACTTTGACAAGGACGGTGT
NOTCH1	notch 1	Hs01062011_m1	CGCGGGCCTGATGGCTTCACCCCGC
JAG1	jagged 1	Hs00164982_m1	TGACACCGTTCAACCTGACAGTATT
HES1	hairy and enhancer of split 1, (Drosophila)	Hs00172878_m1	CGCAGATGACGGCTGCGCTGAGCAC
HES4	hairy and enhancer of split 4 (Drosophila)	Hs00368353_g1	CAGGTGACGGCCGCGCTCAGCGCCG
HES6	hairy and enhancer of split 6 (Drosophila)	Hs00936587_g1	CCGGGCGCGCGAGCGCGAGCAGCTG
FCGR1A;FCGR1C	Fc fragment of IgG, high affinity Ia, receptor (CD64);Fc fragment of IgG, high affinity Ic, receptor (CD64)	Hs02340031_m1	CAAGTGCTTGGCCTCCAGTTACCAA
CXCL12	chemokine (C-X-C motif) ligand 12	Hs00171022_m1	CTTCAGATTGTAGCCCGGCTGAAGA
CCL5	chemokine (C-C motif) ligand 5	Hs00174575_m1	CCAACCCAGCAGTCGTCTTTGTCAC
CXCL10	chemokine (C-X-C motif) ligand 10	Hs00171042_m1	TGGCATTCAAGGAGTACCTCTCTCT
CXCL9	chemokine (C-X-C motif) ligand 9	Hs00171065_m1	GTGCAAGGAACCCCAGTAGTGAGAA
CXCR4	chemokine (C-X-C motif) receptor 4	Hs00237052_m1	CATGGAGGGGATCAGTATATACACT

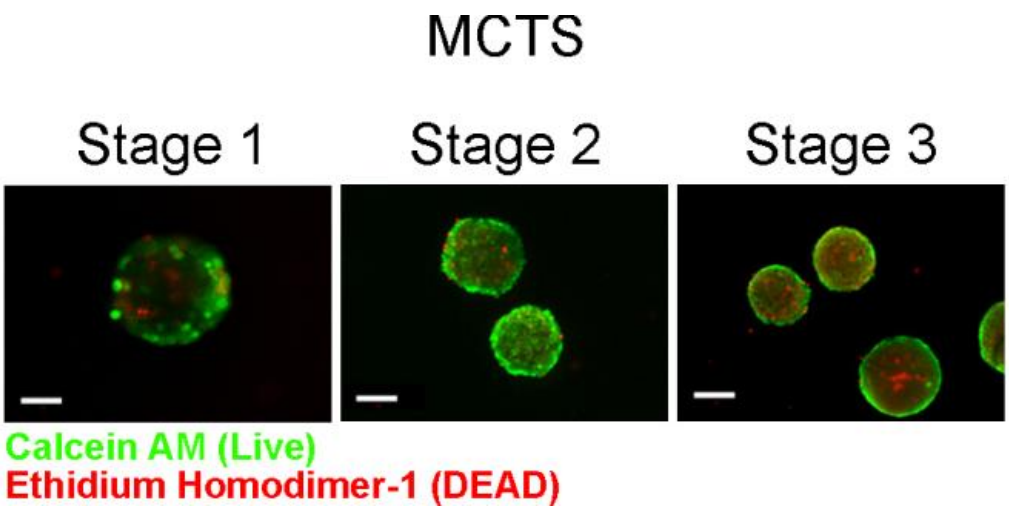

Supplementary Figure 1 Live and Dead staining on HT29 MCTSs (size bar: Stage 1 100x; Stage2 200x; Stage 3 400x)

-4-

CONCLUSIONS

&

OUTLOOK

In an increasing number of cancers, CSCs have been defined on the basis of the self-renewal and tumor initiation capacity by functional assays. It has been also suggested that CSC populations might be responsible for chemo- and radio-therapy resistance within tumors and ultimately for the post-therapeutic tumor recurrence. The development of more effective cancer therapies may thus require targeting this important cell population.

In the past five years, CD133, CD44 and CD166 have been proposed as putative CSC markers in CRC. These findings have opened the field for an extensive validation of the markers and their use for the development of specific anti-CSC therapy.

However, the phenotypic characterization of CRC-SC is still debated. We, therefore, attempted to extend the knowledge on CSC markers in order to validate their clinical relevance, and to evaluate the possibility to isolate putative CSCs from established CRC cell lines in order to assess their potential suitability for drug screening purposes.

Our studies lead to a number of important conclusions. First, increased expression of CD133, CD166, and CD44 putative CSC markers does not appear to be associated with unfavorable prognosis, as established by analyzing a substantial number of clinically annotated CRC. Rather, a loss of expression of CD166 and CD44, and in particular the loss of both markers, appears to be associated with an aggressive tumor phenotype.

CSCs are also called cancer initiating cells for their capacity to recapitulate tumors in mouse model as xenograft. The evaluation of this specific feature represents the gold standard used to identify the CSC phenotype. We assessed the tumor initiating capacity of primary cells isolated from CRC specimens hypothesizing that the presence of high percentages of CSCs within the samples might be correlated with a higher ability to engraft in immunodeficient mice. We did not observe a relation between tumorigenic capacity and the expression of putative CSC markers. We showed, instead, cells expressing these markers are not a small subpopulation within a tumor but they could represent substantial percentages of cells within the epithelial compartment.

We also investigated the usefulness of CRC cell lines for the development of novel CSC-targeted treatments. However, whether tumor cell lines comprise CSC-populations remains highly debated. We first assessed the surface expression of CD133, CD166, CD44, and CD24 on ten established human CRC cell lines. These results showed that the expression of CSC markers is highly heterogeneous and not restricted to small cell subsets raising the question of whether the cell lines consist of only CSC and about the validity of CSC markers for in vitro studies using cell lines. Furthermore, we have analyzed their correlation with stem cell-like functional features, but no consistent results was found confirming stemness property associated with expression of those markers.

These results obviously question the validity of putative surface CRC-SC markers. Taken together these data might suggest that their expression and CSC functional features might be associated with some degree of plasticity, potentially

related to tumor microenvironmental characteristics being lost in conventionally cultured tumor cell lines and in primary tumor derived cell suspensions.

Based on this background we have investigated the possibility to perform 3D culture of CRC cell lines to assess whether these systems might provide useful insights for the interpretation of our data. Our findings clearly document the plasticity of gene expression profiles of cultured CRC cells depending on their three-dimensional architectures. Most importantly we demonstrate that major gene expression modulation events only occur when culture in MCTS is associated with ischemia and necrosis. Indeed, as compared to 2D gene expression profile, 3D culture per se appeared not to be sufficient to change the gene expression profile of the cell lines investigated. However, with the increase of MCTS diameter a gradient of nutrient, oxygen, and catabolites occurs altering gene expression profiles in ways matching those detectable in xenografts. We also showed that the gene expression of putative CSC markers increases with the MCTS size. Future studies are warranted to assess whether this ischemia/necrosis related plasticity is also associated with improved tumor transplantation ability.

Reference List:

(1) Hanahan D, Weinberg RA. Hallmarks of cancer: the next generation. Cell 2011;144:646-74.

(2) Ferlay J, Shin HR, Bray F, Forman D, Mathers C, Parkin DM. Estimates of worldwide burden of cancer in 2008: GLOBOCAN 2008. Int J Cancer 2010;127:2893-917.

(3) Ferlay J, Parkin DM, Steliarova-Foucher E. Estimates of cancer incidence and mortality in Europe in 2008. Eur J Cancer 2010;46:765-81.

(4) Jemal A, Bray F, Center MM, Ferlay J, Ward E, Forman D. Global cancer statistics. CA Cancer J Clin 2011;61:69-90.

(5) Greene FL, American Joint Committee on Cancer, American Cancer Society. Ajcc Cancer Staging Manual. Springer-Verlag; 2002.

(6) Mejia A, Schulz S, Hyslop T, Weinberg DS, Waldman SA. Molecular staging individualizing cancer management. J Surg Oncol 2012;105:468-74.

(7) Fearon ER, Vogelstein B. A genetic model for colorectal tumorigenesis. Cell 1990;61:759-67.

(8) Reya T, Morrison SJ, Clarke MF, Weissman IL. Stem cells, cancer, and cancer stem cells. Nature 2001;414:105-11.

(9) Human gastrointestinal tract. 22-5-2012.
Ref Type: Online Source

(10) Humphries A, Wright NA. Colonic crypt organization and tumorigenesis. Nat Rev Cancer 2008;8:415-24.

(11) Catalano V, Di FS, Iovino F, Dieli F, Stassi G, Todaro M. CD133 as a target for colon cancer. Expert Opin Ther Targets 2012;16:259-67.

(12) Ricci-Vitiani L, Fabrizi E, Palio E, De MR. Colon cancer stem cells. J Mol Med (Berl) 2009;87:1097-104.

(13) Hannan LM, Jacobs EJ, Thun MJ. The association between cigarette smoking and risk of colorectal cancer in a large prospective cohort from the United States. Cancer Epidemiol Biomarkers Prev 2009;18:3362-7.

(14) Campos FG, Logullo Waitzberg AG, Kiss DR, Waitzberg DL, Habr-Gama A, Gama-Rodrigues J. Diet and colorectal cancer: current evidence for etiology and prevention. Nutr Hosp 2005;20:18-25.

(15) Doyle VC. Nutrition and colorectal cancer risk: a literature review. Gastroenterol Nurs 2007;30:178-82.

(16) Harriss DJ, Atkinson G, Batterham A, George K, Cable NT, Reilly T, et al. Lifestyle factors and colorectal cancer risk (2): a systematic review and meta-analysis of associations with leisure-time physical

activity. Colorectal Dis 2009;11:689-701.

(17) Lashner BA, Epstein SS. Industrial risk factors for colorectal cancer. Int J Health Serv 1990;20:459-83.

(18) Dyson JK, Rutter MD. Colorectal cancer in inflammatory bowel disease: what is the real magnitude of the risk? World J Gastroenterol 2012;18:3839-48.

(19) Hamilton SR. Colorectal carcinoma in patients with Crohn's disease. Gastroenterology 1985;89:398-407.

(20) Brenner H, Chang-Claude J, Jansen L, Seiler CM, Hoffmeister M. Role of colonoscopy and polyp characteristics in colorectal cancer after colonoscopic polyp detection: a population-based case-control study. Ann Intern Med 2012;157:225-32.

(21) Brenner H, Chang-Claude J, Rickert A, Seiler CM, Hoffmeister M. Risk of colorectal cancer after detection and removal of adenomas at colonoscopy: population-based case-control study. J Clin Oncol 2012;30:2969-76.

(22) Mlecnik B, Bindea G, Pages F, Galon J. Tumor immunosurveillance in human cancers. Cancer Metastasis Rev 2011;30:5-12.

(23) Weichert W, Knosel T, Bellach J, Dietel M, Kristiansen G. ALCAM/CD166 is overexpressed in colorectal carcinoma and correlates with shortened patient survival. J Clin Pathol 2004;57:1160-4.

(24) DUKES CE, BUSSEY HJ. The spread of rectal cancer and its effect on prognosis. Br J Cancer 1958;12:309-20.

(25) Greene FL, Sobin LH. A worldwide approach to the TNM staging system: collaborative efforts of the AJCC and UICC. J Surg Oncol 2009;99:269-72.

(26) Yasuda K, Nirei T, Sunami E, Nagawa H, Kitayama J. Density of CD4(+) and CD8(+) T lymphocytes in biopsy samples can be a predictor of pathological response to chemoradiotherapy (CRT) for rectal cancer. Radiat Oncol 2011;6:49.

(27) Sconocchia G, Zlobec I, Lugli A, Calabrese D, Iezzi G, Karamitopoulou E, et al. Tumor infiltration by FcgammaRIII (CD16)+ myeloid cells is associated with improved survival in patients with colorectal carcinoma. Int J Cancer 2011;128:2663-72.

(28) Boon T, Cerottini JC, Van den Eynde B, van der Bruggen P, Van PA. Tumor antigens recognized by T lymphocytes. Annu Rev Immunol 1994;12:337-65.

(29) Galon J, Costes A, Sanchez-Cabo F, Kirilovsky A, Mlecnik B, Lagorce-Pages C, et al. Type, density, and location of immune cells within human colorectal

tumors predict clinical outcome. Science 2006;313:1960-4.

(30) Catenacci DV, Kozloff M, Kindler HL, Polite B. Personalized colon cancer care in 2010. Semin Oncol 2011;38:284-308.

(31) Park CY, Tseng D, Weissman IL. Cancer stem cell-directed therapies: recent data from the laboratory and clinic. Mol Ther 2009;17:219-30.

(32) Dalerba P, Cho RW, Clarke MF. Cancer stem cells: models and concepts. Annu Rev Med 2007;58:267-84.

(33) Bonnet D, Dick JE. Human acute myeloid leukemia is organized as a hierarchy that originates from a primitive hematopoietic cell. Nat Med 1997;3:730-7.

(34) Vermeulen L, de Sousa E Melo, Richel DJ, Medema JP. The developing cancer stem-cell model: clinical challenges and opportunities. Lancet Oncol 2012;13:e83-e89.

(35) Barker N, Ridgway RA, van Es JH, van de Wetering M, Begthel H, van den Born M, et al. Crypt stem cells as the cells-of-origin of intestinal cancer. Nature 2009;457:608-11.

(36) Schepers AG, Snippert HJ, Stange DE, van den Born M, van Es JH, van de Wetering M, et al. Lineage tracing reveals Lgr5+ stem cell activity in mouse intestinal adenomas. Science 2012;337:730-5.

(37) O'Brien CA, Pollett A, Gallinger S, Dick JE. A human colon cancer cell capable of initiating tumour growth in immunodeficient mice. Nature 2007;445:106-10.

(38) Ricci-Vitiani L, Lombardi DG, Pilozzi E, Biffoni M, Todaro M, Peschle C, et al. Identification and expansion of human colon-cancer-initiating cells. Nature 2007;445:111-5.

(39) Dalerba P, Dylla SJ, Park IK, Liu R, Wang X, Cho RW, et al. Phenotypic characterization of human colorectal cancer stem cells. Proc Natl Acad Sci U S A 2007;104:10158-63.

(40) Huang EH, Hynes MJ, Zhang T, Ginestier C, Dontu G, Appelman H, et al. Aldehyde dehydrogenase 1 is a marker for normal and malignant human colonic stem cells (SC) and tracks SC overpopulation during colon tumorigenesis. Cancer Res 2009;69:3382-9.

(41) Barker N, van Es JH, Kuipers J, Kujala P, van den Born M, Cozijnsen M, et al. Identification of stem cells in small intestine and colon by marker gene Lgr5. Nature 2007;449:1003-7.

(42) Zhu L, Gibson P, Currle DS, Tong Y, Richardson RJ, Bayazitov IT, et al. Prominin 1 marks intestinal stem cells that are susceptible to neoplastic transformation. Nature 2009;457:603-7.

(43) Todaro M, Francipane MG, Medema JP, Stassi G. Colon cancer stem cells: promise of targeted therapy. Gastroenterology 2010;138:2151-62.

(44) Miraglia S, Godfrey W, Yin AH, Atkins K, Warnke R, Holden JT, et al. A novel five-transmembrane hematopoietic stem cell antigen: isolation, characterization, and molecular cloning. Blood 1997;90:5013-21.

(45) Gires O. Lessons from common markers of tumor-initiating cells in solid cancers. Cell Mol Life Sci 2011;68:4009-22.

(46) Shmelkov SV, Butler JM, Hooper AT, Hormigo A, Kushner J, Milde T, et al. CD133 expression is not restricted to stem cells, and both CD133+ and CD133- metastatic colon cancer cells initiate tumors. J Clin Invest 2008;118:2111-20.

(47) Tachezy M, Zander H, Gebauer F, Marx A, Kaifi JT, Izbicki JR, et al. Activated leukocyte cell adhesion molecule (CD166)-Its prognostic power for colorectal cancer patients. J Surg Res 2012.

(48) Lugli A, Iezzi G, Hostettler I, Muraro MG, Mele V, Tornillo L, et al. Prognostic impact of the expression of putative cancer stem cell markers CD133, CD166, CD44s, EpCAM, and ALDH1 in colorectal cancer. Br J Cancer 2010;103:382-90.

(49) Horst D, Kriegl L, Engel J, Kirchner T, Jung A. Prognostic significance of the cancer stem cell markers CD133, CD44, and CD166 in colorectal cancer. Cancer Invest 2009;27:844-50.

(50) Baumann P, Cremers N, Kroese F, Orend G, Chiquet-Ehrismann R, Uede T, et al. CD24 expression causes the acquisition of multiple cellular properties associated with tumor growth and metastasis. Cancer Res 2005;65:10783-93.

(51) Yeung TM, Gandhi SC, Wilding JL, Muschel R, Bodmer WF. Cancer stem cells from colorectal cancer-derived cell lines. Proc Natl Acad Sci U S A 2010;107:3722-7.

(52) Barker N, Clevers H. Leucine-rich repeat-containing G-protein-coupled receptors as markers of adult stem cells. Gastroenterology 2010;138:1681-96.

(53) Vermeulen L, Todaro M, de Sousa MF, Sprick MR, Kemper K, Perez AM, et al. Single-cell cloning of colon cancer stem cells reveals a multi-lineage differentiation capacity. Proc Natl Acad Sci U S A 2008;105:13427-32.

(54) Kemper K, Prasetyanti PR, de LW, Rodermond H, Clevers H, Medema JP. Monoclonal Antibodies Against Lgr5 Identify Human Colorectal Cancer Stem Cells. Stem Cells 2012.

(55) Vaiopoulos AG, Kostakis ID, Koutsilieris M, Papavassiliou AG. Colorectal cancer stem cells. Stem Cells 2012;30:363-71.

(56) Iinuma H, Watanabe T, Mimori K, Adachi M, Hayashi N, Tamura J, et al. Clinical significance of circulating tumor cells, including cancer stem-like cells, in peripheral blood for recurrence and prognosis in patients with Dukes' stage B and C colorectal

cancer. J Clin Oncol 2011;29:1547-55.

(57) Saigusa S, Tanaka K, Toiyama Y, Yokoe T, Okugawa Y, Ioue Y, et al. Correlation of CD133, OCT4, and SOX2 in rectal cancer and their association with distant recurrence after chemoradiotherapy. Ann Surg Oncol 2009;16:3488-98.

(58) Dylla SJ, Beviglia L, Park IK, Chartier C, Raval J, Ngan L, et al. Colorectal cancer stem cells are enriched in xenogeneic tumors following chemotherapy. PLoS One 2008;3:e2428.

(59) Zhang M, Behbod F, Atkinson RL, Landis MD, Kittrell F, Edwards D, et al. Identification of tumor-initiating cells in a p53-null mouse model of breast cancer. Cancer Res 2008;68:4674-82.

(60) Bao S, Wu Q, McLendon RE, Hao Y, Shi Q, Hjelmeland AB, et al. Glioma stem cells promote radioresistance by preferential activation of the DNA damage response. Nature 2006;444:756-60.

(61) Ginestier C, Hur MH, Charafe-Jauffret E, Monville F, Dutcher J, Brown M, et al. ALDH1 is a marker of normal and malignant human mammary stem cells and a predictor of poor clinical outcome. Cell Stem Cell 2007;1:555-67.

(62) Bleau AM, Hambardzumyan D, Ozawa T, Fomchenko EI, Huse JT, Brennan CW, et al. PTEN/PI3K/Akt pathway regulates the side population phenotype and ABCG2 activity in glioma tumor stem-like cells. Cell Stem Cell 2009;4:226-35.

(63) Hirschmann-Jax C, Foster AE, Wulf GG, Nuchtern JG, Jax TW, Gobel U, et al. A distinct "side population" of cells with high drug efflux capacity in human tumor cells. Proc Natl Acad Sci U S A 2004;101:14228-33.

(64) Patrawala L, Calhoun T, Schneider-Broussard R, Zhou J, Claypool K, Tang DG. Side population is enriched in tumorigenic, stem-like cancer cells, whereas ABCG2+ and ABCG2- cancer cells are similarly tumorigenic. Cancer Res 2005;65:6207-19.

(65) Todaro M, Alea MP, Di Stefano AB, Cammareri P, Vermeulen L, Iovino F, et al. Colon cancer stem cells dictate tumor growth and resist cell death by production of interleukin-4. Cell Stem Cell 2007;1:389-402.

(66) Abraham BK, Fritz P, McClellan M, Hauptvogel P, Athelogou M, Brauch H. Prevalence of CD44+/CD24-/low cells in breast cancer may not be associated with clinical outcome but may favor distant metastasis. Clin Cancer Res 2005;11:1154-9.

(67) Vermeulen L, de Sousa E Melo, van der Heijden M, Cameron K, de Jong JH, Borovski T, et al. Wnt activity defines colon cancer stem cells and is regulated by the microenvironment. Nat Cell Biol 2010;12:468-76.

(68) Sutherland RM. Cell and environment interactions in tumor microregions: the multicell spheroid model. Science 1988;240:177-84.

(69) Weinberg RA. Coevolution in the tumor microenvironment. Nat Genet 2008;40:494-5.

(70) Visvader JE, Lindeman GJ. Cancer stem cells in solid tumours: accumulating evidence and unresolved questions. Nat Rev Cancer 2008;8:755-68.

(71) Choi D, Lee HW, Hur KY, Kim JJ, Park GS, Jang SH, et al. Cancer stem cell markers CD133 and CD24 correlate with invasiveness and differentiation in colorectal adenocarcinoma. World J Gastroenterol 2009;15:2258-64.

(72) Horst D, Kriegl L, Engel J, Kirchner T, Jung A. CD133 expression is an independent prognostic marker for low survival in colorectal cancer. Br J Cancer 2008;99:1285-9.

(73) Kojima M, Ishii G, Atsumi N, Fujii S, Saito N, Ochiai A. Immunohistochemical detection of CD133 expression in colorectal cancer: a clinicopathological study. Cancer Sci 2008;99:1578-83.

(74) Li CY, Li BX, Liang Y, Peng RQ, Ding Y, Xu DZ, et al. Higher percentage of CD133+ cells is associated with poor prognosis in colon carcinoma patients with stage IIIB. J Transl Med 2009;7:56.

(75) Herrlich P, Pals S, Ponta H. CD44 in colon cancer. Eur J Cancer 1995;31A:1110-2.

(76) Mulder JW, Kruyt PM, Sewnath M, Oosting J, Seldenrijk CA, Weidema WF, et al. Colorectal cancer prognosis and expression of exon-v6-containing CD44 proteins. Lancet 1994;344:1470-2.

(77) Weg-Remers S, Anders M, von LB, Riecken EO, Schuder G, Feifel G, et al. Decreased expression of CD44 splicing variants in advanced colorectal carcinomas. Eur J Cancer 1998;34:1607-11.

(78) Jass JR, Love SB, Northover JM. A new prognostic classification of rectal cancer. Lancet 1987;1:1303-6.

(79) Zlobec I, Gunthert U, Tornillo L, Iezzi G, Baumhoer D, Terracciano L, et al. Systematic assessment of the prognostic impact of membranous CD44v6 protein expression in colorectal cancer. Histopathology 2009;55:564-75.

(80) Zlobec I, Lugli A, Baker K, Roth S, Minoo P, Hayashi S, et al. Role of APAF-1, E-cadherin and peritumoral lymphocytic infiltration in tumour budding in colorectal cancer. J Pathol 2007;212:260-8.

(81) Zlobec I, Steele R, Terracciano L, Jass JR, Lugli A. Selecting immunohistochemical cut-off scores for novel biomarkers of progression and survival in colorectal cancer. J Clin Pathol 2007;60:1112-6.

(82) Albini A, Benelli R. The chemoinvasion assay: a method to assess tumor and endothelial cell invasion and its modulation. Nat Protoc 2007;2:504-11.

(83) Ngan CY, Yamamoto H, Seshimo I, Ezumi K, Terayama M, Hemmi H, et al. A multivariate analysis of adhesion molecules expression in assessment of colorectal cancer. J Surg Oncol 2007;95:652-62.

(84) Patel BB, Yu Y, Du J, Levi E, Phillip PA, Majumdar AP. Age-related increase in colorectal cancer stem cells in macroscopically normal mucosa of patients with adenomas: a risk factor for colon cancer. Biochem Biophys Res Commun 2009;378:344-7.

(85) Kristiansen G, Pilarsky C, Wissmann C, Stephan C, Weissbach L, Loy V, et al. ALCAM/CD166 is up-regulated in low-grade prostate cancer and progressively lost in high-grade lesions. Prostate 2003;54:34-43.

(86) Mezzanzanica D, Fabbi M, Bagnoli M, Staurengo S, Losa M, Balladore E, et al. Subcellular localization of activated leukocyte cell adhesion molecule is a molecular predictor of survival in ovarian carcinoma patients. Clin Cancer Res 2008;14:1726-33.

(87) Baiocchi M, Biffoni M, Ricci-Vitiani L, Pilozzi E, De MR. New models for cancer research: human cancer stem cell xenografts. Curr Opin Pharmacol 2010;10:380-4.

(88) Jin K, Teng L, Shen Y, He K, Xu Z, Li G. Patient-derived human tumour tissue xenografts in immunodeficient mice: a systematic review. Clin Transl Oncol 2010;12:473-80.

(89) Shoemaker RH. The NCI60 human tumour cell line anticancer drug screen. Nat Rev Cancer 2006;6:813-23.

(90) Yamada KM, Cukierman E. Modeling tissue morphogenesis and cancer in 3D. Cell 2007;130:601-10.

(91) Desoize B, Jardillier J. Multicellular resistance: a paradigm for clinical resistance? Crit Rev Oncol Hematol 2000;36:193-207.

(92) Hauptmann S, Gebauer-Hartung P, Leclere A, Denkert C, Pest S, Klosterhalfen B, et al. Induction of apoptosis in the centre of multicellular tumour spheroids of colorectal adenocarcinomas--involvement of CD95 pathway and differentiation. Apoptosis 1998;3:267-79.

(93) Weaver VM, Lelievre S, Lakins JN, Chrenek MA, Jones JC, Giancotti F, et al. beta4 integrin-dependent formation of polarized three-dimensional architecture confers resistance to apoptosis in normal and malignant mammary epithelium. Cancer Cell 2002;2:205-16.

(94) Bissell MJ, Radisky DC, Rizki A, Weaver VM, Petersen OW. The organizing principle: microenvironmental influences in the normal and malignant

breast. Differentiation 2002;70:537-46.

(95) Pampaloni F, Reynaud EG, Stelzer EH. The third dimension bridges the gap between cell culture and live tissue. Nat Rev Mol Cell Biol 2007;8:839-45.

(96) Kelm JM, Timmins NE, Brown CJ, Fussenegger M, Nielsen LK. Method for generation of homogeneous multicellular tumor spheroids applicable to a wide variety of cell types. Biotechnol Bioeng 2003;83:173-80.

(97) Ghosh S, Spagnoli GC, Martin I, Ploegert S, Demougin P, Heberer M, et al. Three-dimensional culture of melanoma cells profoundly affects gene expression profile: a high density oligonucleotide array study. J Cell Physiol 2005;204:522-31.

(98) Ravizza R, Molteni R, Gariboldi MB, Marras E, Perletti G, Monti E. Effect of HIF-1 modulation on the response of two- and three-dimensional cultures of human colon cancer cells to 5-fluorouracil. Eur J Cancer 2009;45:890-8.

(99) Shannon AM, Bouchier-Hayes DJ, Condron CM, Toomey D. Tumour hypoxia, chemotherapeutic resistance and hypoxia-related therapies. Cancer Treat Rev 2003;29:297-307.

(100) Keith B, Simon MC. Hypoxia-inducible factors, stem cells, and cancer. Cell 2007;129:465-72.

(101) Hirschhaeuser F, Menne H, Dittfeld C, West J, Mueller-Klieser W, Kunz-Schughart LA. Multicellular tumor spheroids: an underestimated tool is catching up again. J Biotechnol 2010;148:3-15.

(102) Karlsson H, Fryknas M, Larsson R, Nygren P. Loss of cancer drug activity in colon cancer HCT-116 cells during spheroid formation in a new 3-D spheroid cell culture system. Exp Cell Res 2012;318:1577-85.

(103) Kim JB. Three-dimensional tissue culture models in cancer biology. Semin Cancer Biol 2005;15:365-77.

(104) LAIRD AK. DYNAMICS OF TUMOR GROWTH. Br J Cancer 1964;13:490-502.

(105) Friedrich J, Eder W, Castaneda J, Doss M, Huber E, Ebner R, et al. A reliable tool to determine cell viability in complex 3-d culture: the acid phosphatase assay. J Biomol Screen 2007;12:925-37.

(106) LAIRD AK. DYNAMICS OF TUMOR GROWTH. Br J Cancer 1964;13:490-502.

(107) Marusic M, Bajzer Z, Vuk-Pavlovic S, Freyer JP. Tumor growth in vivo and as multicellular spheroids compared by mathematical models. Bull Math Biol 1994;56:617-31.

(108) Dursun B, He Z, Somerset H, Oh DJ, Faubel S, Edelstein CL. Caspases and calpain are independent mediators of cisplatin-induced endothelial

cell necrosis. Am J Physiol Renal Physiol 2006;291:F578-F587.

(109) Denecker G, Vercammen D, Declercq W, Vandenabeele P. Apoptotic and necrotic cell death induced by death domain receptors. Cell Mol Life Sci 2001;58:356-70.

(110) Timmins NE, Maguire TL, Grimmond SM, Nielsen LK. Identification of three gene candidates for multicellular resistance in colon carcinoma. Cytotechnology 2004;46:9-18.

(111) Kim H, Phung Y, Ho M. Changes in global gene expression associated with 3D structure of tumors: an ex vivo matrix-free mesothelioma spheroid model. PLoS One 2012;7:e39556.

(112) Kenny PA, Lee GY, Myers CA, Neve RM, Semeiks JR, Spellman PT, et al. The morphologies of breast cancer cell lines in three-dimensional assays correlate with their profiles of gene expression. Mol Oncol 2007;1:84-96.

(113) Chang TT, Hughes-Fulford M. Monolayer and spheroid culture of human liver hepatocellular carcinoma cell line cells demonstrate distinct global gene expression patterns and functional phenotypes. Tissue Eng Part A 2009;15:559-67.

(114) Liu T, Laurell C, Selivanova G, Lundeberg J, Nilsson P, Wiman KG. Hypoxia induces p53-dependent transactivation and Fas/CD95-dependent apoptosis. Cell Death Differ 2007;14:411-21.

(115) Jogi A, Ora I, Nilsson H, Lindeheim A, Makino Y, Poellinger L, et al. Hypoxia alters gene expression in human neuroblastoma cells toward an immature and neural crest-like phenotype. Proc Natl Acad Sci U S A 2002;99:7021-6.

(116) Barker N, van de Wetering M, Clevers H. The intestinal stem cell. Genes Dev 2008;22:1856-64.

(117) Weaver VM, Petersen OW, Wang F, Larabell CA, Briand P, Damsky C, et al. Reversion of the malignant phenotype of human breast cells in three-dimensional culture and in vivo by integrin blocking antibodies. J Cell Biol 1997;137:231-45.